TOWARDS THE DEVELOPMENT OF A BIOLOGICALLY FUNCTIONAL TISSUE ENGINEERED VASCULAR GRAFT

by

Diana Catalina Ardila-Montoya

Chemical Engineer, Universidad de los Andes, Colombia, 2009

Master of Science in Chemical Engineering, Universidad de los Andes, Colombia, 2012

Master of Science in Biomedical Engineering, University of Arizona, 2016

Submitted to the Graduate Faculty of

the Swanson School of Engineering in partial fulfillment

of the requirements for the degree of

Doctor of Philosophy in Bioengineering

University of Pittsburgh

2018

UNIVERSITY OF PITTSBURGH

SWANSON SCHOOL OF ENGINEERING

This dissertation was presented

by

Diana Catalina Ardila-Montoya

It was defended on

September 26, 2018

and approved by

William Wagner, Ph.D., Director, McGowan Institute for Regenerative Medicine

Bryan Brown, Ph.D., Assistant Professor, Department of Bioengineering

Thomas Doetschman, Ph.D., Professor, Department of Cellular and Molecular Medicine, The

University of Arizona

Dissertation Director: Jonathan Vande Geest, PhD, Bioengineering, University of Pittsburgh

TOWARDS THE DEVELOPMENT OF A BIOLOGICALLY FUNCTIONAL TISSUE

ENGINEERED VASCULAR GRAFT

Diana Catalina Ardila Montoya, PhD

University of Pittsburgh, 2018

Coronary artery disease (CAD) is the leading cause of death worldwide [1], and it is predicted that 23 million deaths will be attributed to CAD by 2030. Treatment of CAD has required over 400,000 coronary artery bypass graft (CABG) surgeries every year [2], representing a cost to the country of nearly $439 billion in direct and indirect expenses annually [3]. As autologous veins are often unavailable for in CABG surgeries [4, 5], and commercially available synthetic grafts have shown limited efficacy when used in small diameter vessels [5-7], a readily available tissue engineered vascular graft (TEVG) for use in CABG surgeries would provide drastic improvements in patient care. Despite significant recent progress [7, 8], the development of a biologically functional TEVG that is biocompatible, biofunctional, and anti-thrombogenic has remained elusive [9, 10]. The primary goal of this dissertation is to fabricate a TEVG that supports and modulates the growth and collagen production of vascular smooth muscle cells (VSMCs) and promotes the formation of a functional endothelium. For this purpose, an initial assessment of biocompatibility was performed by culturing SMCs in gelatin/fibrinogen electrospun scaffolds, using exogenous TGFβ2 to modulate cell response. It was demonstrated that that TGFβ2 had a differential effect on cell proliferation, migration, and collagen deposition of SMCs growing in our biopolymer materials. In order to provide additional biofunctionality to the TEVG, a tubular scaffold able to release TGFβ2 was fabricated. The combination of gelatin and PCL at different

ratios allowed elution tunability. The released TGFβ2 was bioactive and was able to modulate SMCs growth in vitro and in 3D culture. To evaluate anti-thrombogenicity and perform an additional assessment of biocompatibility, human derived endothelial cells (hCB-ECs) were cultured in surface modified gelatin/fibrinogen/PCL electrospun scaffolds. hCB-ECs growing in the scaffolds showed similar or superior behavior to human umbilical vein ECs (HUVEC) in terms of platelet deposition and activation, producing eNOS, and responding to a proinflammatory stimulus. Our data suggests that a biofunctional biopolymer based TEVG can be fabricated that can control SMC response and promote the formation of a functional endothelium

TABLE OF CONTENTS

LIST OF TABLES

LIST OF FIGURES

AKNOWLEDGEMENTS

I would like to extend my sincere gratitude to my advisor, and chairman of my committee Dr. Jonathan Vande Geest for believe in me from the very first moment. Thank you for offering me be part of the Soft Tissue Biomechanics Laboratory (STBL) at the University of Arizona, first as a research engineer, and then for encourage me to pursuit a PhD, and give me the opportunity to continue learning from you at STBL. You have been a great mentor and an incredible support, reasons why I followed you 2.000 miles away from Tucson to continue working towards my degree at the University of Pittsburgh under your mentorship.

I would like to also thank my dissertation committee, Dr. William Wagner, Dr. Tom Doetschman, and Dr. Bryan Brown for their time, willingness and knowledge.

To all my lab mates at STBL, thank you for the help and support. Reza, Ehab and Hirut, you have been like a family to me these pasts years. Thanks for your constant help, encouragement, and specially for your friendship. I will miss you guys very much. To the brilliant people that had contributed to this work: Darren Hasket, Dom Muli, Kenny Furdella, Andrea Acuña, Corina MacIsaac, David Maestas, Jamie Hernandez, Josh Uhlorn, Victoria Lundine, and Hannah Smith; thank you, without you some of the work would not have been possible. To all my friends from the University of Arizona, Jun Chai, Bruce Chen, Bharani Malladi, Avinash Ayyalasomayajula, Nathalie Risso, Alvaro Viñas, Sean Phillips, Savannah Rodgers, Rafael Gil, Alexandrea Soto, you all have a special place in my heart. I look forward to see you again!

I would like to thank the Cardiovascular Biomedical Engineering training grant at the University of Arizona, and the Cellular Approaches to Tissue Engineering and Regeneration (CATER) training grant at the University of Pittsburgh for the financial support through my

graduate studies. I am grateful for the skillset I have gained being part of these two prestigious training grants.

To my family, specially my parents Adolfo and Carmenza, and my two sisters Paula and Liliana for always giving me your unconditional love and support. It has been very hard to be far from you. You mean everything to me, thanks for always encourage me to be the best version of myself and to always dream big.

Thank you, Mila and Martina, you two are angels on earth. You have been my loyal friends and companions. I love coming home every day and see your wiggling tails at full speed. Thanks for all the love, the wet kisses and for making every day so fun!

Finally, I would like to thank my husband Pablo and my baby boy Santiago. Pablo, you have been my rock. Thank you for your love and for all you do for our family. I can't imagine doing this without you by my side. You and our Santi are my whole world, and my principal motivation to be better every day. Santi, I hope you had enjoyed all the classes, seminars, conferences and meetings we went together for almost 10 months! I know you will like math as you kept kicking and kicking during my statistics class. All this hard work is for you. I hope one day you will be proud of your mama.

1.0   CHAPTER 1: INTRODUCTION

Coronary heart disease (CHD) resulting from atherosclerosis remains the leading cause of death in the United States [11]. CHD alone caused approximately 1 of 7 deaths in 2013, and 660,000 hospitalizations as a result of myocardial infarctions [12]. It is documented that this condition costs more than any other diagnostic group, resulting in more than $439 billion in direct and indirect expenses from 2011 to 2012 [12]. Once a coronary artery is compromised, vascular bypass is an option to restore blood flow to tissues distal to the restriction or blockage [6]. According to the American Heart Association there are nearly 400,000 artery bypass graft surgery procedures performed annually in the United States [13], in many cases involving the replacement of a coronary artery with an autologous vessels such as the saphenous vein or internal mammary artery [4, 13]. Nevertheless, autologous grafts are not always available due to preexisting vascular conditions, or their use in a prior bypass operation [5]. The commercial alternatives to autologous grafts are vessels made of synthetic materials such as expanded polytetrafluoroethylene (ePTFE) and woven or knitted Dacron. These grafts have been implemented with some success in medium and large diameter vessel replacement, but their efficacy is severely limited when used in small diameter vessels where low blood flow makes the synthetic graft difficult to cellularize and more prone to thrombus formation, calcification and intimal hyperplasia (IH) [5-7].

Therefore, there is an urgent need for small diameter graft alternatives to the autologous vessels that are able to support cell growth and match the mechanical properties of a native coronary artery while reducing the risk of acute thrombus formation and restenosis [9, 10].

Recently, tissue engineering has gained attention as an alternative approach for developing small diameter vascular grafts from biocompatible natural or synthetic polymers. Tissue engineering can be defined as a triad of scaffolds, cells, and signals which function synergistically to enable new functional tissue growth either in vitro or in vivo, and its principal goal is to fabricate new, physiological, and viable tissue substitutes that can be integrated into the patient to successfully restore function [14-16]. To enable injured tissue to regenerate, tissue engineered scaffolds must mimic native tissue, which is mainly comprised of cells supported by an extracellular matrix (ECM) and signaling molecules such as growth factors and cytokines [17, 18]. Tissue engineered scaffolds must promote cell-biomaterial interactions, cell growth, and ECM deposition [14-16, 18]. Additionally, they should permit nutrient transport and gas exchange to allow cell proliferation while minimizing inflammation and toxicity. In addition, scaffold degradability rate needs to be comparable to that of tissue regeneration [14-16, 18].

Biopolymers are widely used to fabricate tissue engineered grafts due to their mechanical properties, biocompatibility, biodegradability, and chemical versatility [16]. Synthetic biodegradable polymer used in tissue engineering can mimic the mechanical properties of native tissue [19, 20] and can give the strength to the scaffold. However, these polymers differ from native biopolymers in the ECM, and therefore have different binding sites, making cell attachment and migration difficult [21]. Additionally, synthetic polymers are often hydrophobic, which limits the absorption of culture medium, and consequently, cell proliferation becomes slow and poor [22, 23]. Recently, naturally derived biopolymers have received increased attention in tissue

engineering applications. They are mainly comprised of proteins derived from the ECM of a specific tissue, which has been shown to provide better physiological support for cell attachment and growth [21]. In contrast to synthetic biopolymers, natural biopolymers are mainly hydrophilic, facilitating the absorption and diffusion of nutrients, while also providing specific interaction sites with cells, enhancing cell adhesion and proliferation [20, 21, 24-26]. In vascular tissue engineering natural polymers such as collagen, gelatin, elastin, and hyaluron have been the basis to build scaffolds with good biocompatibility. However, these natural polymers have shown lack of good biomechanical properties and have to be reinforces with synthetic polymers such as polycaprolactone.

For a tissue engineered vascular graft to be successful, it has to meet different requirements such as: Biocompatibility, nonthrombogenicity, maintenance of a functional endothelium, compliance matching, and post-implantation function and durability [27]. The focus of this thesis is the fabrication of a tissue engineered vascular graft that is biocompatible, bioactive and antithrombogenic by using of natural and synthetic polymers, signaling factors to modulate smooth muscle cells infiltration, migration and collagen production, and surface modification of biomaterials to promote the formation of a healthy monolayer of endothelial cells.

1.1   CORONARY ARTERIES

Blood vessels form a complex network of capillaries, veins and arteries which principal function is to transport blood to and from the heart, organ, and tissues in the body. Depending on the location on the body, blood vessels vary in size, structural organization, biomechanical properties, biochemistry and cellular composition. Arteries are thick wall vessels that transport

high pressure oxygenated blood to the organs and tissues. Similar to all other tissues in the body, the heart muscle needs oxygen-rich blood to function, and oxygen-depleted blood must be unloaded. The coronary arteries are the first blood vessels that branch off from the ascending aorta extending to the heart walls to supply blood to the atria, ventricles, and septum of the heart. The two main coronary arteries are the right and the left main coronary arteries [28]. A representation of the coronary artery branches is presented in Figure 1 [29]
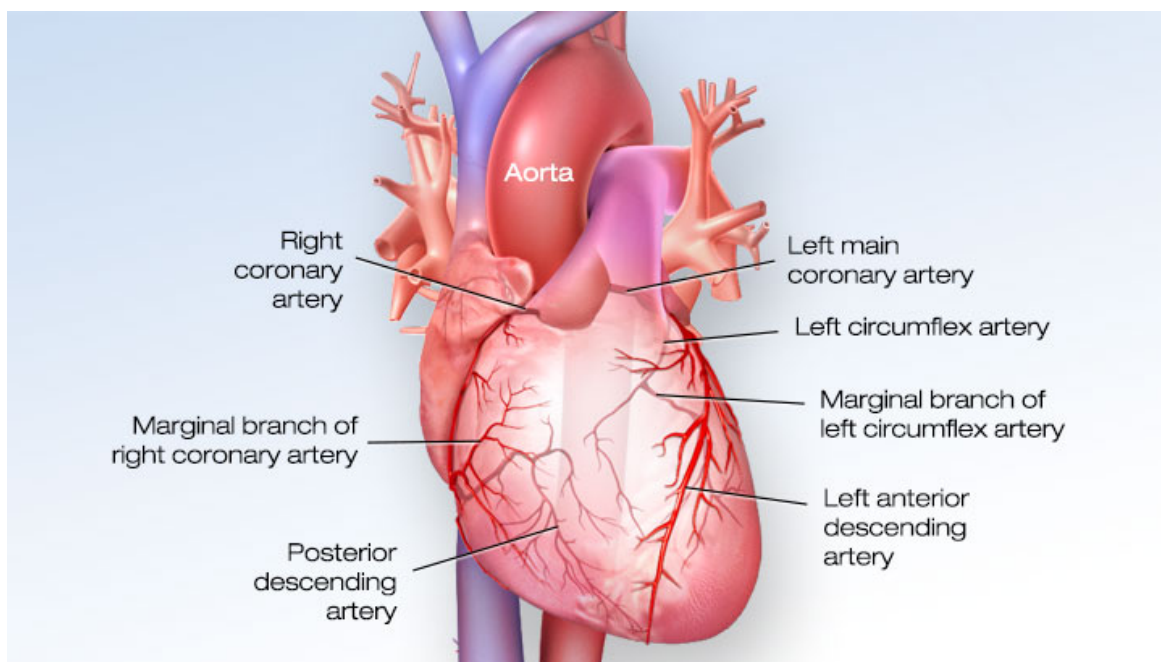
Figure 1 Representation of the coronary arteries

The right coronary artery supplies blood to the right ventricle, the right atrium, and the sinoatrial and atrioventricular nodes, which regulate the heart pacing. The right coronary artery divides into smaller branches, including the right posterior descending artery and the acute

marginal artery [28, 30]. The left main supplies blood to the left side of the heart muscle, in other words, supplies blood to the left ventricle and left atrium. The left main coronary divides into branches: the left anterior descending artery, which supplies blood to the front of the left side of the heart; and the circumflex artery, which encircles the heart muscle supplying blood to the outer and back sides of the heart [28, 30].

The basic organization of the coronary arterial wall is similar to all arteries in that three concentric layers can be distinguished as shown in Figure 2 [31] :

1. The inner layer or tunica intima

2. The middle layer or the tunica media

3. The outer layer or tunica adventitia.
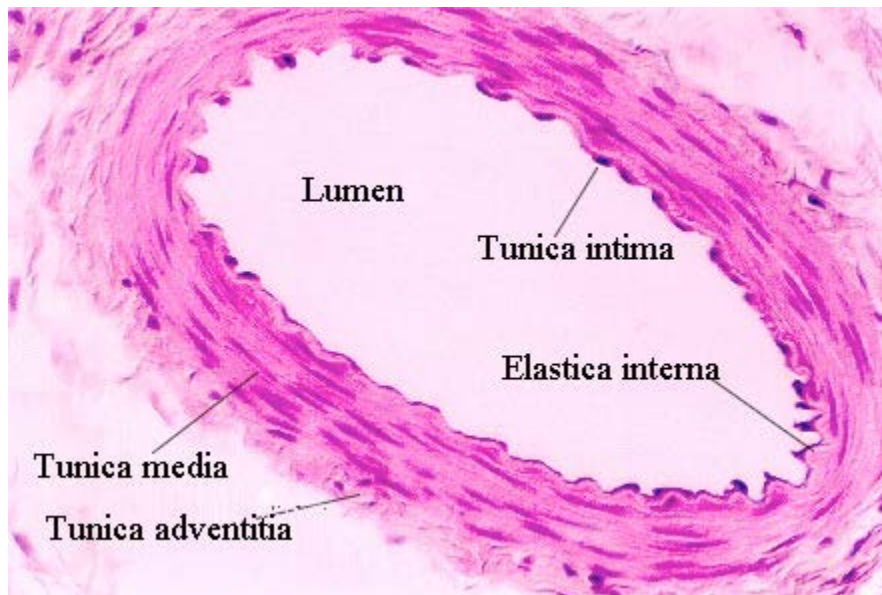
Figure 2 Coronary artery cross-sectional histological view stained with H&E

The intima consists of a lining layer of endothelial cells and a sub-endothelial layer containing connective tissue. The endothelial cells are oriented longitudinally relative to the artery

and are attached by occluding junctions and gap (communicating) junctions. Endothelial cells play a wide variety of critical roles in the control of vascular function. They participate in all aspects of the vascular homeostasis but also to physiological or pathological processes like thrombosis, inflammation, or vascular wall remodeling [32, 33].

The medial layer consists of multiple layers (about 40) of smooth muscle cells and connective tissue (collagen, elastin and proteoglycans) [32]. Smooth muscle cells are essential for the good performance of the coronary arteries. By contraction and relaxation, they alter the luminal diameter which enables blood vessels to maintain an appropriate blood pressure and transmural flow. Smooth muscle cells also synthesize large amounts of extracellular matrix components including collagen [34].

The adventitia consists of fibrous tissue (collagen, elastic fibers) that is surrounded by vasa vasorum, nerves and lymphatic vessels. The orientation of the collagen and the relatively "loose" consistency of the adventitia permit continual changes in the coronary diameter [32].

1.2   CORONARY ARTERY DISEASE

Coronary artery disease (CAD) is the most common type of heart disease, and is the leading cause of death in the United States in both men and women [35]. "From 2011 to 2012, the estimated annual costs for CAD and stroke were $316.6 billion, including $193.1 billion in direct costs (hospital services, physicians and other professionals, prescribed medications, home health care, and other medical durables) and $123.5 billion in indirect costs from lost future productivity (cardiovascular and stroke premature deaths)" [12]. CAD costs more than any other diagnostic group, being the most expensive condition treated [11, 12].

CAD happens when a cholesterol plaque (atherosclerosis) builds up on the inner walls of the coronary arteries making these vessels, which supply blood to the heart, hardened and narrowed. As this plaque grows, less blood can flow to the heart muscle restricting the oxygen needed for the heart function as is shown in Figure 3 [36]. This can lead to chest pain or a heart attack. Most heart attacks happen when a blood clot suddenly cuts off the hearts' blood supply, causing permanent heart damage [35].

Figure 3 Representation of a plaque buildup in the CAD

The risk factors for CAD are [37, 38]:

- Male sex

- Family history of CAD.

- Tobacco use

- Hyperlipidemia

- Hypertension

- Diabetes mellitus

- Obesity

- Sedentary lifestyle

- Left ventricular hypertrophy

Nowadays the principal treatments for an occlude coronary artery are balloon angioplasty, stenting or bypass grafting in order to restore the blood flow. Angioplasty and stenting are the standard of care when the patient has a simple cholesterol blockade. However, in the case the blockage is calcified, or if the patient has more than one blockage or the blockage is very long, or if the artery blocked is the left main coronary artery, or if the patient had a previous angioplasty or stent placement that wasn't successful, or if the patient had stent placement but the artery has narrowed again (restenosis) the bypass grafts becomes the best option to restore the blood flow.

The bypass surgery creates a new path for blood flow, using a graft that is connected from the aorta to a site just distal to the blockage [39, 40] which is represented in Figure 4 [41] . This allows blood to bypass the stenosed vessel. Sometimes people need more than one bypass.
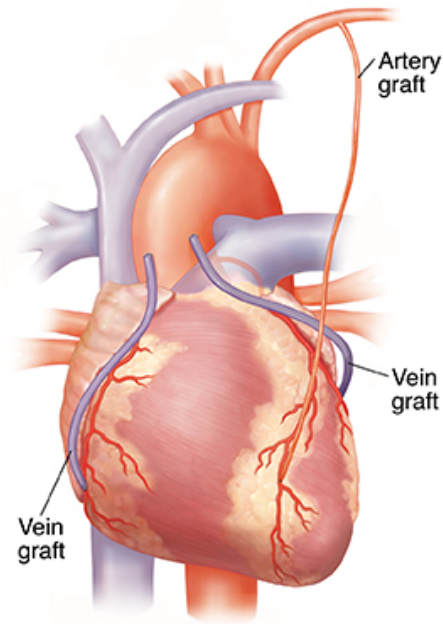
Figure 4 Illustration of bypass grafting

Coronary artery bypassing is usually performed with autologous harvest vessels such as the saphenous vein, the mammary artery or the internal thoracic artery [4, 13]. Nevertheless, the availability of autologous grafts is very limited due to preexisting vascular conditions, or their use in a prior bypass operation. Also the saphenous vein from elderly patients often suffers from thrombus, aneurysm formation or arthrosclerosis in high pressure arterial sites [5]. Previously allografts have previously been used, however they come with the risk of immune-rejection and disease transmission. Therefore, their use in clinical applications have been discontinued.

The commercial alternatives to autologous grafts are vessels made of synthetic materials such as expanded polytetrafluoroethylene (ePTFE) and woven or knitted Dacron. These grafts have been implemented with long-termsuccess in medium and large diameter vessel replacement (<6mm). This success, however, has not being replicated with small diameter grafts where low blood flow makes the synthetic graft difficult to cellularize and more prone to thrombus formation,

calcification and intimal hyperplasia (IH), making the synthetic grafts not suitable for coronary artery bypassing [5-7]. Therefore, there is an urgent need for small diameter graft alternatives that are able to support cell growth and match the mechanical properties of a native coronary artery while reducing the risk of acute thrombus formation and restenosis, and possess the long-term durability and growth potential of native vasculature [9, 10].

1.3   TISSUE ENGINEERED VASCULAR GRAFTS

The failure or loss of tissue is one of the most common and costly problems in medicine today [14, 15, 18]. The main treatments for these disorders are tissue transplants and surgical reconstruction [14-16]. The principal limiting factors for these transplants include donor availability, immunocompatibility of the donated tissue with the host body, and the suitability of the alternative tissue availability, especially in the case of auto-transplant [14, 17]. Surgical reconstructions are limited by the amount of viable and healthy tissue surrounding the wound, and many times requires a graft transplantation [14, 16]. Tissue engineering is an advancing interdisciplinary field that applies an engineering approach combined with life science knowledge towards the development of scaffolds that replace, restore, and improve diseased tissue [16, 17]. The goal of tissue engineering is to fabricate new, physiological, and viable tissue substitutes that can be integrated into the patient to successfully restore function [14-16]. To enable injured tissue to regenerate, tissue engineered scaffolds must mimic native tissue, which is mainly comprised of cells supported by an extracellular matrix (ECM) and signaling molecules such as growth factors and cytokines [17, 18]. Tissue engineered scaffolds must promote cell-biomaterial interactions, cell growth, and ECM deposition [14-16, 18]. Additionally, they should permit nutrient transport

and gas exchange to allow cell proliferation while minimizing inflammation and toxicity. In addition, scaffold degradability rate needs to be comparable to that of tissue regeneration [14-16, 18]. The tissue engineering principle has been applied to create tissue engineered vascular grafts (TEVGs) where patient's autologous cells or a patient's stem-cell-derived cells are used, in combination with a scaffold that supports cell growth [8]. A functional TEVG should display biocompatibility, anti-thrombogenicity, lack of immune response, contractility, in response to active cytokines, appropriate mechanical properties, and it can also be further functionalized by the integration of signaling factors.

1.3.1   Biomaterials

Most scaffolds employed in TEVGs are constructed from biodegradable polymers which can be synthetic or natural. Synthetic polymers have been widely used for the fabrication of TEVGs, with the principal advantage of providing good mechanical properties that can be tuned. These polymers are degraded by hydrolytic cleavage of ester linkages, and the rate of degradation can be modulated by multiple factors, including molecular weight, surface-area-to-volume ratio, and crystallinity The most common synthetic polymers used in the fabrication of TEVGs are: PCL, PGA, PLA, PEG, PU, PHA, PHO, PDS, PGS, PEUU, P4HB, and different copolymers [8]. However synthetic TEVGs have the disadvantage of However, these polymers differ from native biopolymers in the ECM, and therefore lack of the cellular binding sites, making cell attachment and migration difficult [21]. Additionally, synthetic polymers are often hydrophobic, which limits the absorption of culture medium, and consequently, cell proliferation becomes slow and poor [22, 42].

11

Recently, naturally derived biopolymers have received increased attention in tissue engineering applications. Natural polymers can be classified as proteins (silk, collagen, gelatin, fibrinogen, elastin, keratin, actin, and myosin), polysaccharides (cellulose, amylose, dextran, chitin, and glycosaminoglycans), or polynucleotides (DNA, RNA) [20] . The most common used for vascular tissue engineering are mainly comprised of proteins derived from the ECM, which has been shown to provide better physiological support for cell attachment and growth [21, 43]. In contrast to synthetic biopolymers, natural biopolymers are mainly hydrophilic, facilitating the absorption and diffusion of nutrients, while also providing specific interaction sites with cells, thus enhancing cell adhesion and proliferation [25, 26].

Hybrid scaffolds are fabricated using a combination of both synthetic and natural polymers. These hybrid scaffolds may be considered as new smart biomaterials that incorporate the strength, tunability, and manufacturing control of synthetic materials with the improved biocompatibility and biochemical cues that come from natural polymer components. Hybrid scaffolds exploit the advantages of both types of polymers and may provide good mechanical properties while enhancing the biocompatibility and cellular recruitment. However, some of the limitations associated with using polymer scaffolds to generate a TEVG are likely to remain a factor, particularly the requirement for long periods of *in vitro* culture to generate robust constructs [44].

1.3.2   Methods of fabrications

Electrospinning is one of the most common methods to fabricate TEVGs. It is a highly versatile method to process solutions or melts, mainly of polymers, into continuous fibers with diameters ranging from a few micrometers to a few nanometers. This method can be applied to

synthetic and natural polymers, polymer alloys, and polymers loaded with chromophores, nanoparticles, or active agents, as well as to metals and ceramics [45].

The typical electrospinning experiment in the laboratory is presented in Figure 5 [46], and it consists in a polymer solution that is fed through a thin nozzle or needle tip using a syringe pump. The nozzle simultaneously serves as an electrode, to which a high electric field is applied. The substrate on which the electrospun fibers are collected is typically brought into contact with the counter electrode that is grounded to create a differential potential [46]. First, the syringe pump forces the polymer solution to form a pendant polymer droplet held by surface tension at the needle tip. Then an electric field is applied to the system, which induces a repulsion force that opposes the surface tension of the polymer solution. The polymer droplet at the needle tip becomes elongated and deforms into a conical shape (Taylor cone). When the electric field reaches a critical value, a charged polymer jet is ejected from the apex of the Taylor cone, and directed to the collector [46]. The polymer jet is accelerated and stretched due to both external and internal electrostatic forces originating from the charged ions within the polymer jet [45, 46]. On the way to the collector, the solvent evaporates and solid fibers with diameters ranging from micrometers to nanometers are deposited on the substrate collected as an interconnected web [45, 46].
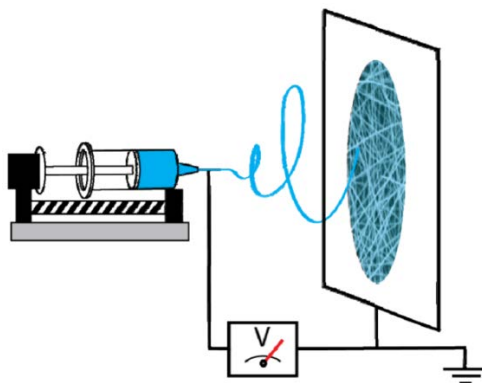
Figure 5 representation of the electrospinning setup

An important characteristic of electrospinning is the ability to make fibers with diameters in the range of nanometers to a few microns. Consequently these fibers have a large surface area per unit mass so that nanowoven fabrics of these nanofibers collected on a screen can be used for example, for filtration of submicron particles in separation industries and biomedical applications, such as wound dressing in medical industry, tissue engineering scaffolds and artificial blood vessels [47].

Thermally induced phase separation (TIPS) is another popular technique to fabricate porous scaffolds for vascular tissue engineering. TIPS is based on changes in thermal energy to induce the de-mixing of a homogeneous polymer solution into a two or multi-phase system. When the phase separation occurs, the homogenous solution separates in a polymer-rich phase and apolymer-poor phase. This usually occurs by either exposure of the solution to another immiscible solvent or cooling the solution until a liquid–liquid phase separation or solid–liquid de-mixing is present. After that, the solvent is extracted by liofilization and depending upon the system and phase separation conditions, different morphologies and characteristics of the materials can be obtained [48, 49].

Another common method is particulate leaching, where particulates such as salt, sugar, or wax serve as placeholders for pore formation in the actual scaffold, before being leached by evaporation or crosslinking [8] .

Freeze drying is a different TEVG fabrication method where a polymer is first dissolved in a solvent, and the solution is frozen and the solvent is allowed to sublime during the drying process. Pore size can be controlled by changing conditions, such as freezing rate and solute concentration [8].

Other techniques to produce scaffolds for TEVGs include, decellularized native tissue, self-assembly, melt molding, membrane lamination, solvent casting micro-tissue aggregation, and bio-printing [8, 50].

1.3.3   Cells

Cells are a key component for tissue engineering as they are involved in the scaffold remodeling and production of new ECM. These cells can be derived from primary tissue or cell lines [26]. For tissue engineering purposes, cells should be highly proliferative, easy to harvest, and have the necessary specialized functions to replace the injured tissue [14, 26]. The field of TEVG is generally focused on the study of SMCs and ECs, as these cell types are present in the media and intima layers of native arteries respectively. The source for SMCs and ECs used in TEVG are generally adult blood vessels, stem cells, and stem cells derived vascular cells [51].

SMCs comprise the main part of the artery wall, and are important for the maintenance of vessel architecture by the production of ECM, and thus the preservation of mechanical properties. SMCs are also responsible for the modulation of vascular tone in response to a variety of mechanical and biochemical stimuli. It is well know that SMCs can modulate from a mature or contractile phenotype, which is exhibited in mature tissue, to a proliferative or synthetic phenotype, found in new born arteries or under conditions such as injury or atherogenesis [34, 52] . In the contractile phenotype these cells have a low rate of proliferation, produce small amounts of ECM, and due to their contractile function, are less able to migrate [34, 52, 53]. In contrast, when SMCs are in a synthetic phenotype they are highly proliferative, are able to migrate and synthesize ECM [34, 52]. However, mature SMCs display extraordinary plasticity over the course of their life and may switch phenotype in response to local environment changes. These local

environment changes may result in SMCs changing from a contractile phenotype to a more synthetic phenotype [34, 52]. Figure 6 shows the phenotype plasticity of SMCs [53].
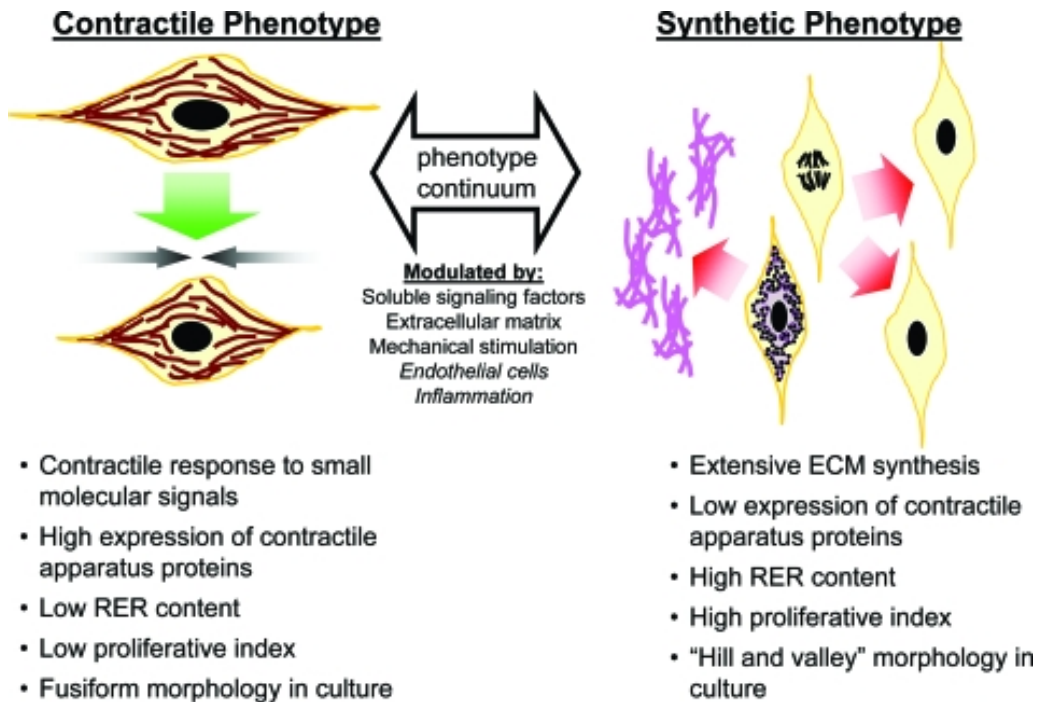
Figure 6 SMCs phenotype plasticity

Therefore, it is crucial that the fabricated TEVG scaffolds are able to promote SMCs attachment and migration. Also, the ability to control the response of SMCs may be very advantageous as it could allow in vitro maturation of vascular grafts through inducing highly proliferative SMCs to populate the scaffold wall followed by a switch to ECM producing and low proliferative SMCs that are able to remodel the TEVG scaffold.

For vascular tissue engineering the study of the intima layer is also crucial as the endothelial cells are involved in reducing the thrombus formation and maintaining the vessel patency. Endothelial cells play a wide variety of critical roles in the control of vascular function. They participate in all aspects of the vascular homeostasis, but additionally are critical in

physiological or pathological processes like regulation of vascular tone, inflammation, and prevention of both thrombosis and intima hyperplasia [32, 33, 54].

Therefore, a correct establishment of a healthy endothelium is crucial for the long term success of a TEVG. Figure 7 is a representation of the normal function of the endothelium [55]
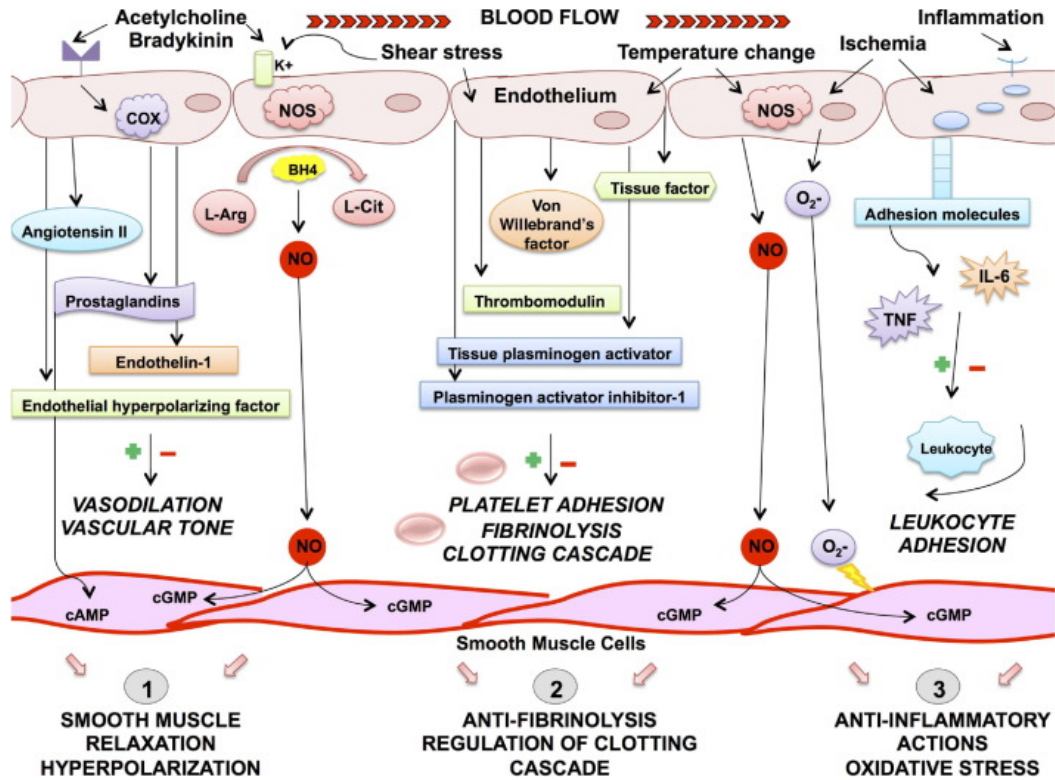
Figure 7 Functions of the endothelium

The crosstalk between endothelial cells and smooth muscle cells are very important to reduce the risk of intimal hyperplasia by reducing SMC proliferation. Additionally, ECs produce nitric oxide which is the signaling factor for SMCs contraction or relaxation depending on its concentration. Therefore the communication amongst the two cell types is also important for the regulation of vascular tone [55].

1.3.4 Release of growth factors from vascular grafts

The gene expression of cells in engineered tissues can be regulated by the addition of various exogenous signaling molecules including platelet derived growth factor (PDGF), fibroblast growth factor (FGF), activin A, angiotensin II (AngII), insulin growth factor (IGF), transforming growth factor (TGFβ), among others [21]. Each of them has a particular effect on the cell phenotype and can be impregnated in the scaffold, which allows for selective improvement of cell function [21].

However, this is feasible only in vitro but not in in vivo applications, when it is desirable to have a sustained release of bioactive growth factor from the scaffold. Then it is necessary to integrate the signaling factor into the scaffold during the fabrication process.

Different methods have been used to load growth factors in polymeric matrixes for tissue engineering. Some researchers have used physical encapsulation [49, 56], which is a simple method to incorporate growth factors in a polymeric matrix by mixing them with the polymeric solution before processing. Physical encapsulation allows for the retention of both the desired biomechanical properties of the scaffolds and the bioactivity of the growth factors simultaneously [56]. Other authors have utilized the absorption of growth factors into the processed matrix surface [49, 56], in which the already fabricated TEVG is put in contact with the growth factors in solution to allow for their absorption on the graft surface. This method has gained attention because it is easy to performed; however, it has the disadvantage of low retention of the growth factors and poor controlled delivery [49]. Another method utilized by research groups is the incorporation of growth factors containing microspheres with the polymeric solution [49], where the studied molecules are first immobilized in polymeric microspheres and then mixed with the biomaterials before processing. This method uses solvents such as methylene chloride, which negatively affect

the bioactivity of the encapsulated molecules [49, 57]. Covalent immobilization has also been used by researchers [58], in which the biomolecules are chemically bound to the biomaterial. With this approach, it is possible to improve the stability and persistence of the growth factors, while offering the possibility of controlling the local and sustained delivery. One disadvantage of this method is that the growth factor can be bound in different configurations introducing problems with homogeneity, reproducibility, and the possible loss in bioactivity [58]. ECM-inspired immobilization using heparin has also been used by research groups [56]. The use of heparin has been thoroughly investigated for the immobilization of growth factors into matrices, especially in studies that demonstrate the endothelialization of TEVGs [49, 59]. Heparin has been shown to increase the hydrophilicity of the scaffold, and thus accelerate the initial burst release [49, 59]. However, different authors have shown that that heparin can also inhibit SMCs growth [60-63].

In the case of vascular tissue engineering, the release of growth factors has been used principally to promote endothelialization of the scaffolds. Different authors have used BFGF, VEGF, EGF combined with heparin immobilization to improve antithrombogenicity and endothelialization [49, 64, 65]. Additional to endothelialization promoting growth factors, other authors have used a wide variety of small-molecule drugs, and other bioactive molecules have been released from tissue engineered scaffolds. These drugs are often added to either promote aspects of tissue growth or modulate the inflammatory response. Some of these molecules are: Ascorbic acid, pentha-galloyl glucose, carbon monoxide, nitric oxide, and S-nitrosothiols. However relatively few molecules have been delivered to encourage graft remodeling through the modulation of SMCs response [66]. The delivery of corticosteroids, NSAIDs, and adenoviruses to deliver IL-4, IL-1, IL-10 TNF-α or to block leukocyte specific integrins, have been used to reduce immune and inflammatory response which have been associated with the switch of SMCs to an

activated phenotype and thus with the appearance of intimal hyperplasia and stenosis [66]. However, these molecules do not act directly on the SMCs but rather the modulation of the cell response is a consequence of the reduction on inflammation. Recently Strobel et al, 2017 incorporated gelatin microspheres loaded with TGFβ1 to a SMC self-assembled ring [67]. The study concluded that with the inclusion of TGFβ1 releasing microspheres, the SMC expressed contractile proteins and reduced ring thickness [67]. However little is known about the concentration of this growth factor in the media and the release profile form the microspheres.

1.4 HYPOTHESES AND SPECIFIC AIMS

The number one killer of men and women in the United States is heart disease, with coronary artery disease being the cause of 1 of 7 deaths every year, and 660.000 hospitalized myocardial infarction [1]. This condition has required over 400,000 coronary artery bypass graft (CABG) surgeries annually [2]. Treatment of coronary artery disease also has a significant impact on national health care as it costs the country nearly $439 billion in direct and indirect expenses yearly [3]. As autologous veins are often unavailable for use as a vascular substitute [4, 5], and commercially available synthetic grafts have shown limited efficacy when used in small diameter vessels as a coronary artery [5-7], a readily available tissue engineered vascular graft (TEVG) for use in CABG surgeries would provide drastic improvements in patient care. Despite significant recent progress [7, 8], the development of a biologically functional TEVG has remained elusive. A biologically functional TEVG has to be biocompatible, biofunctional and anti-thrombogenic [9, 10]. The primary goal of this dissertation is to investigate the fabrication of a TEVG that supports

20

and modulates the growth and collagen production of vascular smooth muscle cells (VSMCs), and promotes the formation of a healthy endothelial cell (EC) monolayer in the electrospun scaffolds.

Hypothesis 1: TGFβ2 can be used to modulate SMCs proliferation, migration and collagen production in electrospun scaffolds

Specific Aim 1: Determine how different concentrations of exogenous TGFβ2 can modulate SMCs growth and migration as well as soluble collagen deposition in electrospun constructs.

Rationale: TGFβ2 as a growth and differentiation factor essential for cardiovascular development through modulation of cell proliferation, stimulation of matrix deposition and remodeling of resultant tissues, will differentially modulate VSMCs phenotype.

Hypothesis 2: A biodegradable electrospun scaffold can be developed to control the release of bioactive TGFβ2

Specific Aim 2: control the TGFβ2 elution from electrospun scaffolds by combining natural polymers such as with the synthetic biopolymer PCL, in order to systematically modulate VSMCs response.

Rationale: To use the degradation times of gelatin and PCL as a way to control the amount of TGFβ2 *released directly from the electrospun graft.*

Hypothesis 3: Surface modification of gelatin/fibrinogen/PCL scaffolds will improve attachment and function of human cord blood derived endothelial cells

Specific Aim 3: Assess the attachment, coverage, antithrombogenicity, eNOs production, and response to proinflammatory cytokines of human cord blood derived endothelial cells (hCB-ECs), growing on gelatin and PCL electrospun scaffolds that are surface modified by thermoforming and coating with ECM related proteins.

Rationale: Endothelial cells obtained from cord blood have shown great proliferation potential as well as adhesion while showing overlapping markers with vascular endothelial cells, which need a smooth surface and ECM-integrin binding sites for the attachment and formation of an endothelium.

The above aims will serve as a first step towards our long-term goal of producing a functional TEVG for CABG surgeries.

2.0   CHAPTER 2: SPECIFIC AIM 1 DIFFERENTIAL EFFECT OF TGFβ2 ON THE GROWTH, INFILTRATION AND COLLAGEN PRODUCTION OF SMCS SEEDED ON ELECTROSPUN SCAFFOLDS

In this aim, I studied the fabrication of biopolymer-based planar scaffolds created through the electrospinning of gelatin and fibrinogen at different ratios, and their suitability of support growth and infiltration of SMCs. The scaffolds that promoted higher proliferation and migration were seeded once more with SMCs, and exogenous TGFβ2 was added to the culture media at different concentrations to assess its effect on SMC proliferation, migration, and collagen production. This aim evaluated the suitability of a biomaterial for vascular tissue engineering applications and also provided insight into the use of different concentrations of exogenous TGFβ2, ranging from 0.1 ng/ml up to 10ng/ml, as a signaling control factor to modulate different functions of SMCs growing in the supporting material.

This Aim is based on the publication **"Ardila D.C.,** Tamimi E., Danford F., Haskette D., Kellar R., Doetschman T., Vande Geest J., (2015). "TGFβ2 Differentially Modulates Smooth Muscle Cell Proliferation and Migration in Electrospun Gelatin-Fibrinogen Constructs". Biomaterials 37:164-73. doi: 10.1016"

2.1   INTRODUCTION

The development of a functional tissue engineering vascular graft (TEVG) is one of the urgent necessities in the effort to treat coronary heart disease [1-7]. A TEVG has to support the growth and induce matrix deposition of vascular smooth muscle cells (SMC) similar to the media layer of a coronary artery [8, 68, 69]. SMC are essential for the formation of a vascular media layer responsible for the modulation of vascular tone and ECM remodeling [70]. Therefore, the control of SMC recruitment, infiltration and proliferation is an important aspect of TEVG development and design. Tissue engineering is an advancing interdisciplinary field that applies an engineering approach towards the development of scaffolds that replace, restore, and improve diseased tissue [16, 17]. To enable injured tissue to regenerate, scaffolds must mimic native tissue, which is mainly comprised of cells supported by an extracellular matrix (ECM) and signaling molecules such as growth factors and cytokines [17, 18]. These scaffolds must promote cell-biomaterial interactions, cell growth, and ECM deposition [14-16, 18]. Biopolymers are widely used to fabricate tissue engineered grafts due to their mechanical properties, biocompatibility, biodegradability, and chemical versatility [16]. Recently, naturally derived biopolymers have received increased attention in tissue engineering applications. They are mainly comprised of proteins derived from the ECM of a specific tissue, which has been shown to provide better physiological support for cell attachment and growth [21]. Natural biopolymers are mainly hydrophilic, facilitating the absorption and diffusion of nutrients, while also providing specific interaction sites with cells, enhancing cell adhesion and proliferation [20, 21, 24-26].

Multiple techniques have been applied to fabricate scaffolds suitable for tissue replacement. Among these techniques, electrospinning has been extensively used to create fibrous scaffolds, showing promising results for tissue engineering applications [20, 71]. Electrospinning

produces non-woven meshes containing fibers ranging in diameter from tens of microns to tens of nanometers, generating matrices that mimic the natural ECM microstructure

The gene expression of cells in engineered tissues can be regulated by various signaling molecules such as growth factors. More specifically, it has been demonstrated that the growth, migration and matrix deposition of SMC can be stimulated by different growth factors such as platelet-derived growth factors (PDGFs) [72, 73], fibroblast growth factor (FGF) [73, 74], Activin A [73, 75] and transforming growth factor beta (TGFβ) [74, 76-78]. TGFβ2 is a pleiotropic cytokine that regulates different cellular processes such as cell cycle, cell differentiation, cell growth, cell death, and ECM deposition and organization [78-80]. This growth factor has received particular interest in the study of cardiovascular development and disease, since its signaling pathway is implicated in ECM remodeling of vascular and cardiac tissue [81-83]. For instance it was found that TGFβ2 is important for pharyngeal arch artery remodeling [84], ECM remodeling in heart valvulogenesis [82], and it was demonstrated to be a key player for vascular remodeling during embryogenesis [85].

In this study, non-synthetic biopolymer-based planar scaffolds were created through the electrospinning of gelatin and fibrinogen at different mass ratios [86]. The scaffolds were seeded with porcine aortic smooth muscle cells (PAOSMCs), and cell proliferation and scaffold infiltration were assessed to determine the most suitable substrate for SMC attachment, growth, and migration. The experimental ratios between gelatin and fibrinogen were selected based on the study of Balasubramanian et al, 2013 [86], where authors demonstrated that a scaffold composed of 80% gelatin-20% fibrinogen supported cardiac myocyte culture better than purely fibrinogen scaffolds. Additionally, the author's findings suggested that the addition of gelatin in a higher proportion to the polymeric solution, can enhance the mechanical properties of the scaffold [86].

However, the authors did not test cell behavior in 100% gelatin scaffolds. In this study, we compared cell proliferation and migration in scaffolds with compositional percentages of 100% gelatin; 80% gelatin-20% fibrinogen; and 50% gelatin-50% fibrinogen. TGFβ2 is was added to the culture medium at different concentrations to assess its effect on SMC proliferation, migration, and collagen production in the tissue engineered scaffolds.

2.2   MATERIALS AND METHODS

2.2.1   Smooth muscle cells isolation

Smooth muscle cells (SMCs) were isolated from porcine aorta using the explant method reported in Gallicchio et al, 2001; and Gotlieb & Boden, 1984 [87, 88]. Briefly, aortas were obtained from the University of Arizona meat science lab 10-20 minutes post-mortem. Explants were prepared under sterile conditions. Initially, removal of any excess fat, the adventitia, and the intima layers was performed. The media layer was cut into small pieces, and the explants were placed in 60 mm petri dishes containing 5 ml of Dulbecco's Modified Eagle Medium (DMEM) from Gibco® (Life technologies™, USA) supplemented with 10% Fetal Bovine Serum (FBS) from GemCell™, 100U/ml of penicillin, 100 µg/ml of streptomycin, 5 µg/ml of amphotericin B (Fungizone), and 25 mM HEPES from Gibco® (Life technologies™, USA). The culture medium was changed every other day and cultures were maintained in a humidified environment at 37°C and 5% CO_2. Cell outgrowth from the explants was observed after two weeks. Cell identity was confirmed by immunocytochemistry (ICC) on cells cultured onto glass coverslips after the second passage, using double immunostaining by primary monoclonal antibodies mouse anti-alpha

26

smooth muscle actin (ab7817; Abcam, USA) and rabbit anti-calponin (ab46794; Abcam, USA). Primary antibodies were conjugated with secondary antibodies Alexa Fluor® 488 goat anti mouse (Life Technologies™, USA) and goat anti-rabbit Cy5 (ab97077; Abcam, USA). Cell nuclei were counterstained using VECTSHIELD® mounting media containing 4',6-diamidino-2-phenylindole (DAPI) from Vector Laboratories, USA. For all other experiments performed, cells from passages 4-6 were used.

2.2.2   Scaffold fabrication

Gelatin-Fibrinogen flat sheet scaffolds were created by electrospinning. Gelatin extracted from porcine skin and fraction I bovine fibrinogen (Sigma-Aldrich, USA) were mixed at three different percentages: 100% gelatin (100 G), 80% gelatin-20% fibrinogen (80:20 G:F) and 50% gelatin-50% fibrinogen (50:50 G:F) [86]. The polymeric blends were dissolved in 1,1,1,3,3,3-Hexafluoro-2-propanol (HFP) (Sigma-Aldrich, USA) to create a 10% (w/v) solution under constant stirring. The solutions were loaded into a 5 ml BD syringe with a 23-gauge stainless steel dispensing blunt tip needle (CML supply, USA) attached. The syringe was then loaded onto a NE-1000 single syringe pump (New era pump systems inc., USA) set to a pumping rate of 100 μl/min. The distance from the needle tip to the target was 8 cm. The polymeric solutions were electrospun at a high voltage of 15 kV, onto glass coverslips attached to a metallic target to create fine fibers. The resultant flat sheets were crosslinked in 25% glutaraldehyde (Sigma-Aldrich, USA) in vapor phase for 24 h. The glutaraldehyde was then removed in a convection oven for 24h at 42°C. Additionally, membranes were rinsed with deionized water to remove any crosslinker residues and uncrosslinked gelatin.

2.2.3 Cell culture

Membranes were sterilized with 70% ethanol solution for 4 h, rinsed with sterile PBS (Gibco®, Life technologiesTM, USA), placed under UV light for 2h, and conditioned in culture medium for 30 min. After conditioning, the flat sheets were transferred to 6-well plates containing 3 ml of culture medium per well; having one scaffold per well. Each flat sheet was positioned so that it laid flat, covering the bottom of the well. Scaffolds were seeded by dispensing a solution of detached SMCs over the flat sheets at a concentration of 1x106 cells/ml into each well. Cultures were maintained at 37°C and 5% CO2 in a humidified atmosphere. Culture medium was changed every other day. After 2 and 7 days of culture, proliferation and infiltration were evaluated. All the experiments had 6 replicates (n=6).

2.2.4 Evaluation of cell proliferation

To quantify cell proliferation, a proliferation assay was performed on every flat sheet. A sample with a surface area of approximately 35 mm^2 was cut from each scaffold and then placed in a well of a 96-well plate containing 100µl of culture medium. Viable cell number was determined by the bioreduction of 3-(4,5-Dimethyl-thiazol-2yl)-5-(3-carboxymethoxyphenyl)-2-(4-sulfophenyl)-2H-tetrazolium contained in the CellTiter 96® AQueous One Solution Cell Proliferation Assay (Promega, USA) following the manufacturer's instruction. Absorbance was read at 490 nm in a Synergy H1 plate reader from BioTek®. Statistical significance was assessed using one way ANOVA.

2.2.5   Imaging of cell infiltration

The Advanced Intravital Microscope (AIM) for multiphoton imaging at the University of Arizona's BIO5 institute was used to observe the total cell migration along the scaffold depth [89, 90]. The AIM is an Olympus BX51 upright laser-scanning microscope coupled to a Coherent 120-fs tunable pulsed Titanium-Sapphire laser (Santa Clara, CA). For this study an Olympus XLUMPLFL 20x water immersion objective with a numerical aperture of 0.9 was used. Incident light was focused on the sample and the backscattered signal was collected over a 400x400 μm field of view at 5 μm steps, imaging through the flat sheet to a depth of approximately 150 μm. For cell imaging, the sheets were treated for 24h with VECTASHIELD® mounting medium with DAPI (Vector Laboratories, USA) to stain cell nuclei. The laser was centered at λ=700 nm to excite DAPI, and 2-photon excited fluorescence (2PEF) was split with a 505 nm dichroic mirror and collected through a 460/80 bandpass filter. The fibers were imaged colocalized using the autofluorescence signal from gelatin and fibrinogen by the excitation of NADPH 2PEF, centering the laser at λ=920 nm. 2PEF was split with a 580 nm dichroic mirror and collected through a 550/88 bandpass filter. The optics were chosen to maximize discrimination between NADPH and DAPI fluorescence. Two representative regions of the scaffold were imaged and infiltration was estimated by image analysis. The colocalized image stacks from DAPI and autofluorescence were merged to visualize the 3D cell location in the flat sheet. Infiltration was calculated as the average percentage of cell migration through the flat sheet (from the surface to the bottom) relative to the flat sheet thickness.

2.2.6 Scaffold porosity and fiber thickness

The scaffold characterization was performed on the 2PEF image volume described above to ensure that just fibers were being evaluated. Porosity was calculated by creating a maximum intensity projection (MIP) of the image volume, manually thresholding the resulting MIP, binarizing the image volume based on the chosen threshold value, selecting a smaller representative image volume (to avoid underestimation due to the surface of the sheet not being perfectly flat and loss of signal through the depth), and then dividing the total number of black pixels in the user defined image volume divided by the total number of pixels. The fiber thickness was calculated by manually measuring the diameter of 20 randomly selected fibers per scaffold via freehand lines superimposed over slices from the thresholded image volume in ImageJ. The above described process was performed by 3 separate individuals to minimize any user bias and capture a representative population of fiber diameters [91].

2.2.7 Addition of exogenous TGFβ2

Flat sheets composed of 80:20 G:F were seeded with PAOSMCs at a concentration of 1×10^6 cell/ml in 6-well plates, as previously described. Exogenous TGFβ2 (R&D Systems, USA) was added to the culture medium at different concentrations (0.05, 0.1, 0.5, 1, 3, 5, and 10 ng/ml). The absence of TGFβ2 in one of the cultures was considered as a control. The cultures were maintained in a humidified atmosphere at 37 °C and 5% CO_2. Culture medium was changed every alternate day, adding every time the predetermined concentration of exogenous TGFβ2.

After 7 days, cell proliferation and infiltration were assessed. Additionally, collagen production was analyzed. All the experiments had 6 replicates. Statistical significance was evaluated using one way ANOVA.

2.2.8 Analysis of collagen content

Collagen concentration was examined in the culture medium as well as in the flat sheets, using a soluble collagen assay (QuickZyme Biosciences, USA). To determine the collagen concentration dissolved in culture media at day 6 of culture, the membranes were rinsed with sterile PBS and placed in new 6-well plates containing fresh medium. Exogenous TGFβ2 was added to the predetermined concentration. After 24h, the medium was aspirated and centrifuged at 3000xg to remove cell debris. The assay was carried out according to the manufacturer's instructions. Absorbance was read at 540 nm in a Synergy H1 plate reader from Biotek®. In addition to running a collagen assay for the cell media, an assay was also performed for the flat sheets using a sample with a surface area of approximately 1.8 cm^2. The samples were rinsed with sterile PBS, homogenized in a collagen solubilization buffer (0.5M acetic acid, 5mM EDTA, and 0.05g pepsin/100g tissue) using the TissueRuptor® (Quiagen, Germany) and incubated under constant stirring. After 24h, the collagen dissolved in the buffer was analyzed using a QuickZyme soluble collagen assay, following the manufacturer's guidance. Absorbance was read at 540 nm in a Synergy H1 plate reader from Biotek®.

2.3   RESULTS

2.3.1   Scaffold characterization

The results from the three independent analysts were averaged to calculate the porosity and fiber diameter for each scaffold. For 100 G, the averaged porosity was 70.6% ± 14% and the fiber diameter 3.57 μm ± 1.66 μm. The results for the porosity in 80:20 G:F were 45.4% ± 1.5 % and 3.82 μm ± 2.04 μm for the fiber diameter. In the 50:50 G:F the porosity was calculated as 62.3% ± 5.0% and the fiber diameter as 4.48 μm ± 1.56 μm.

2.3.2   Cell culture, proliferation and infiltration in electrospun scaffolds with different compositions of gelatin and fibrinogen

Identity of the isolated SMCs was confirmed by ICC. The cells expressed both alpha-smooth muscle actin and calponin (Figure 8). These markers are specific to SMCs expressing a contractile phenotype [92-96]. The cells also presented an elongated morphology typical of contractile SMCs [34]. These cells were seeded onto electrospun flat sheet-like scaffolds composed of gelatin and fibrinogen blended at different percentages. Results showed a significant increase ($p<0.05$) in cell count from 2 to 7 days in all three types of scaffolds (Figure 9). After 2 and 7 days of cell seeding, SMCs showed more proliferation in 80:20 G:F scaffolds than in 50:50 G:F and 100 G. A significant effect on cell number ($p<0.05$) was identified after 2 days in culture comparing 80:20 G:F with 50:50 G:F ($1.79 \times 10^5 \pm 2.46 \times 10^4$ vs. $1.2 \times 10^5 \pm 1.12 \times 10^4$). Also cell number count was higher in 80:20 G:F compared with 100 G, with no significant difference identified ($1.79 \times 10^5 \pm 2.46 \times 10^4$ vs. $1.43 \times 10^5 \pm 2.73 \times 10^4$). After 7 days in culture a significant

increase in cell number was found for 80:20 G:F compared with 50:50 G:F ($5.28 \times 10^5 \pm 4.6 \times 10^4$ vs. $5.04 \times 10^5 \pm 4.60 \times 10^4$, p<0.05), and in 80:20 G:F compared 100 G ($5.28 \times 10^5 \pm 4.6 \times 10^4$ vs. $3.81 \times 10^5 \pm 7.1 \times 10^4$, p<0.05).

In Figure 9, it can also be observed that 2 days post seeding, the 100 G sheets have on average more cells attached than 50:50 G:F sheets. In contrast, at 7 days 100 G scaffolds showed the lowest cell proliferation of all scaffolds.
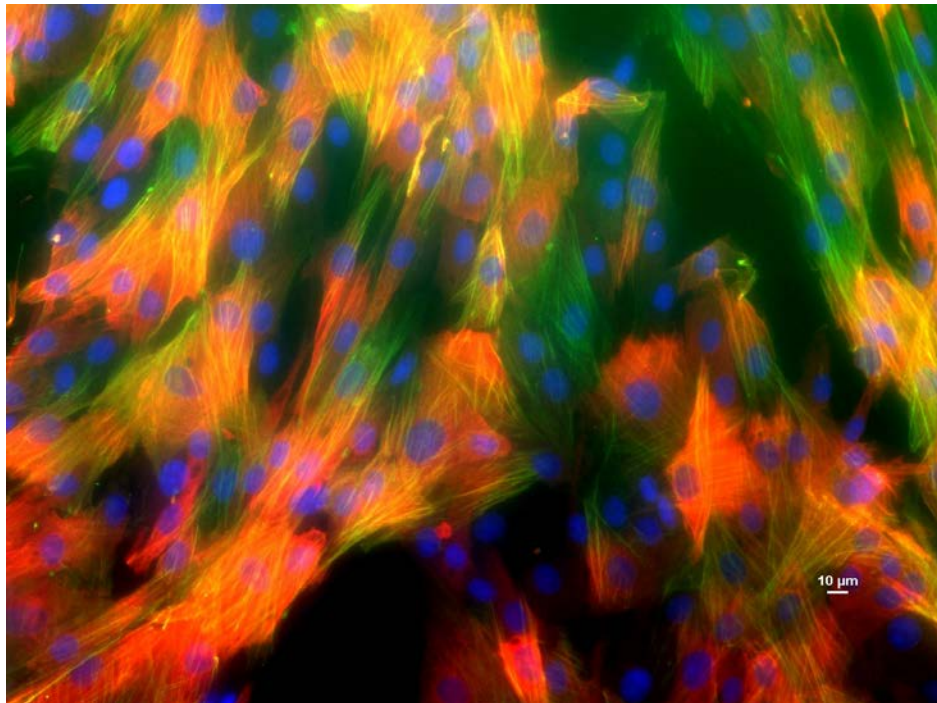
Figure 8 Immunostaining of alpha smooth muscle actin (green) and calponin (red) in PAOSMCs. Cell nuclei were counterstained with DAPI (blue). Image taken at a magnification of 20x

Migration results (Figure 10A) showed a significant increase (p<0.05) in cell movement through the scaffold depth from 2 to 7 days after cell seeding in all three experimental materials, being greater the percentage of scaffold infiltration after 7 days in culture.
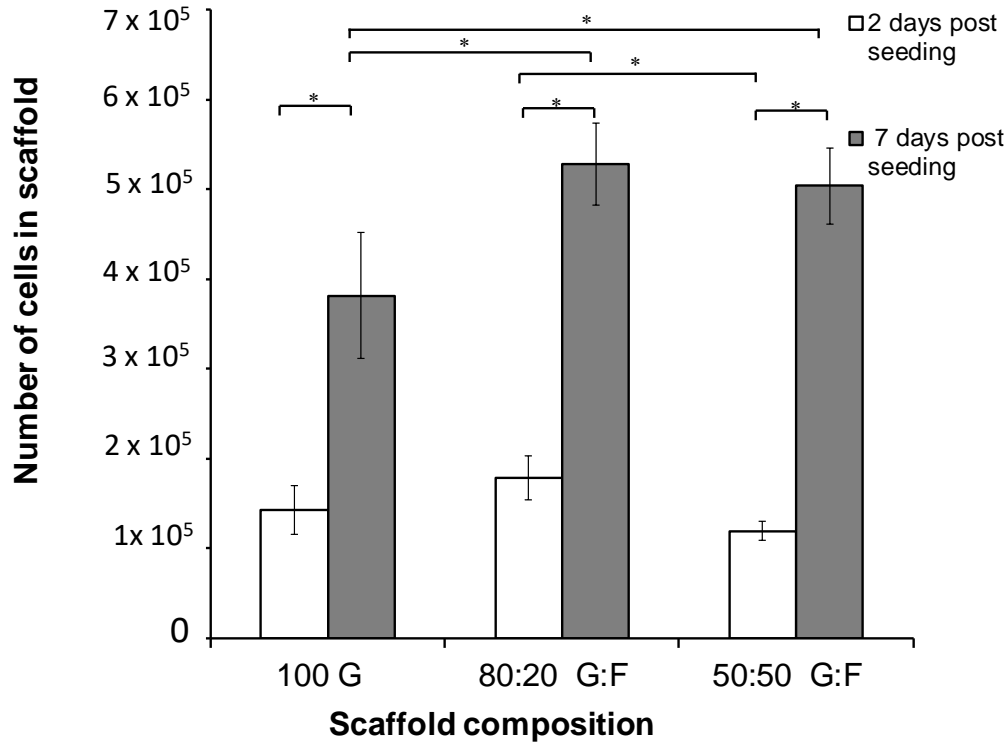
Figure 9 Cell Proliferation results after 2 and 7 days post seeding in 100 G, 80:20 G:F, and 50:50 G:F electrospun scaffolds. Average cell number per scaffold is reported for the two time points. Error bars shown are standard deviation. (* p<0.05; n=6)

For the 100 G scaffolds, the average percentage of cell migration through the scaffold depth after 2 and 7 days was 36.16% ± 2.07% and 91.66% ± 1.7% respectively. For the 80:20 G:F scaffolds, the average percentage of cell migration after 2 and 7 days was 45.36% ± 2.85% and 90.96% ± 1.41% respectively. For 50:50 G:F the average percentage of cell migration after 2 and 7 days was 35.53% ± 1.04% and 97.66% ± 2.05% respectively. In Figure 10B, a composite from

multiphoton imaging of the 80:20 flat sheets 7 days post SMCs seeding is shown. It is possible to observe that cells (DAPI 2PEF, nuclei shown in blue) have migrated down through the material fibers (gelatin and fibrinogen autofluorescence 2PEF, fibers shown in green).
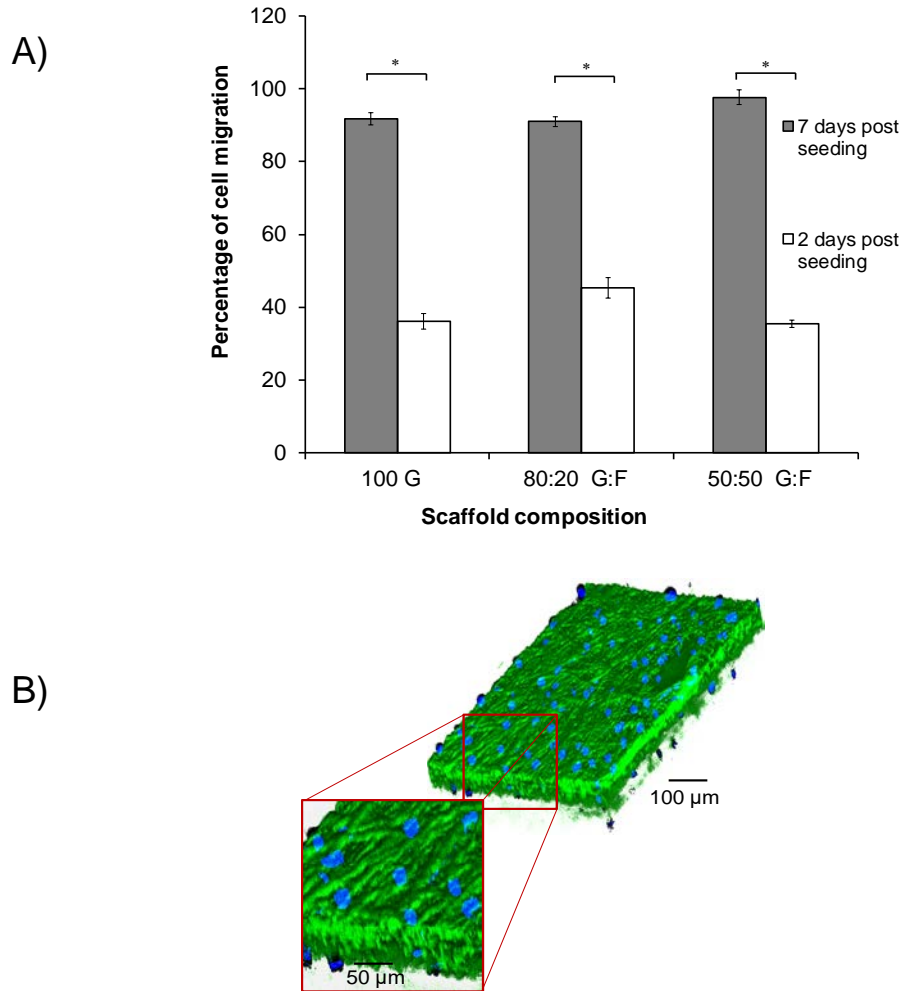
Figure 10 A) Cell infiltration results after 2 and 7 days post seeding in 100 G, 80:20 G:F, and 50:50 G:F electrospun scaffolds. Error bars shown are standard deviation (*p<0.05; n=2). B) Representative multiphoton image of an 80:20 G:F flat sheet with cells after 7 days in culture. The material fibers are shown in green, and cell nuclei in blue. Image was acquired at a magnification of 20x.

2.3.3 Effect of exogenous TGFβ2 in cell proliferation, migration, and collagen production

SMCs were seeded on 80:20 G:F flat sheets, TGFβ2 was added to the culture medium at different concentrations, and cell proliferation, migration and collagen production was assessed after 7 days in culture. Exogenous TGFβ2 at concentrations ≤ 1ng/ml had a positive effect over cell count (proliferation) compared to the control (Figure 11). At concentrations >1ng/ml, TGFβ2 suppressed cell growth. The largest number of cells in scaffolds was found in cultures where TGFβ2 was added to the medium at a concentration of 0.1ng/ml with a significant main effect
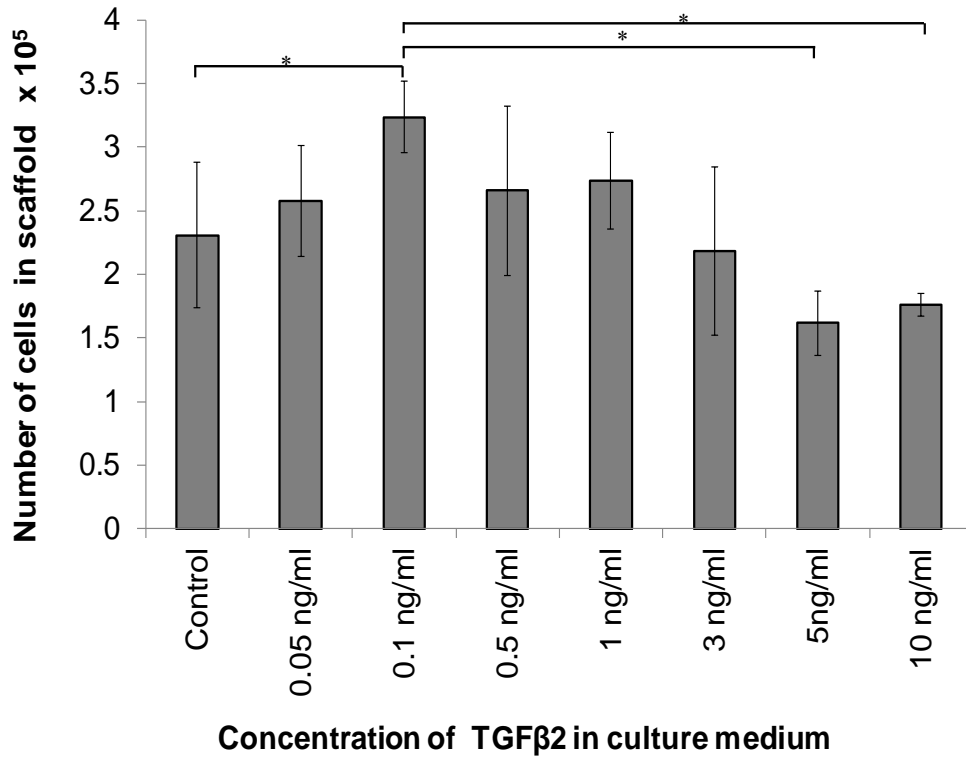
Figure 11 Cell Proliferation results after 7 days post seeding in 80:20 G:F electrospun scaffolds, when different concentrations of exogenous TGFβ2 were added to the culture medium. Average cell number per scaffold is reported for the 8 different culture conditions. Error bars shown are standard deviation (∗p<0.05; n=6).

(p<0.05) compared to the control ($3.24 \times 10^5 \pm 2.81 \times 10^4$ vs. $2.31 \times 10^5 \pm 5.75 \times 10^4$). The lowest number of cells growing in the scaffolds was obtained with TGFβ2 at 5ng/ml and 10ng/ml with a significant reduction compared to the control ($3.24 \times 10^5 \pm 2.81 \times 10^4$ vs $1.62 \times 10^5 \pm 2.56 \times 10^4$, p<0.05 for the control vs 5ng/ml TGFβ2, and $3.24 \times 10^5 \pm 2.81 \times 10^4$ vs. $1.76 \times 10^5 \pm 8.78 \times 10^3$, p<0.05 for the control vs 10ng/ml TGFβ2).

A significant increase (p<0.05) in SMCs migration was found when TGFβ2 was at 0.1ng/ml compared to the control (99% ± 0.5% vs. 83.88% ± 0.8%) and a significant reduction (p<0.05) in cell migration in 10 ng/ml TGFβ2 samples compared to the control (14.28% ± 1.14% vs. 83.88% ± 0.83 (Figure 12).
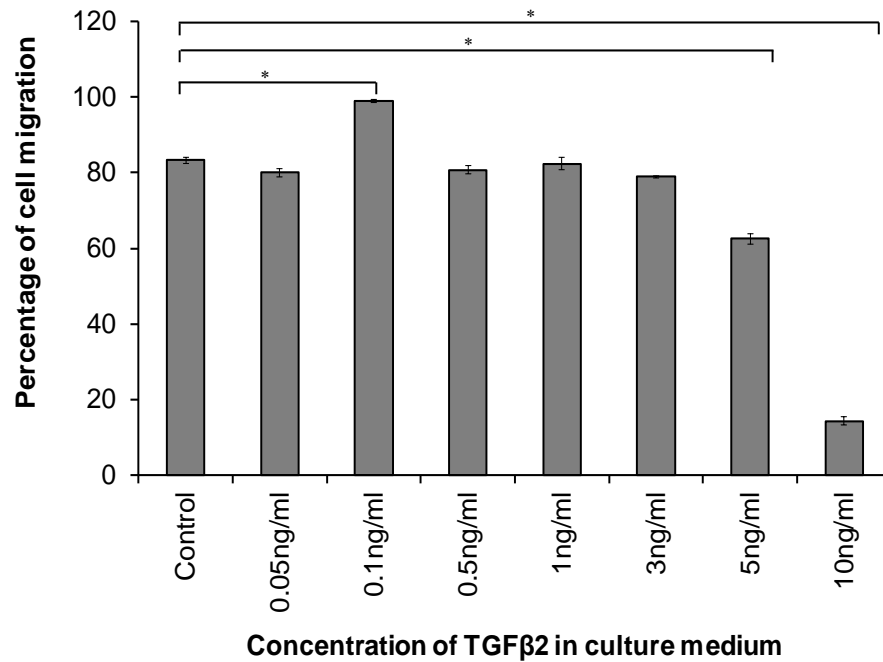
Figure 12 Cell infiltration results after 7 days post seeding in in 80:20 G:F electrospun scaffolds, when different concentrations of exogenous TGFβ2 were added to the culture medium. Error bars shown are standard deviation (∗ p<0.05; n=2).

Representative images from the multiphoton microscopy of the scaffolds when TGFβ2 was at 0.1ng/ml (Figure 13A) and 10ng/ml (Figure 13B) are shown as composites. The 80:20 G:F sheets are displayed in green (autofluorescence 2PEF) and cell nuclei in blue (DAPI 2PEF).
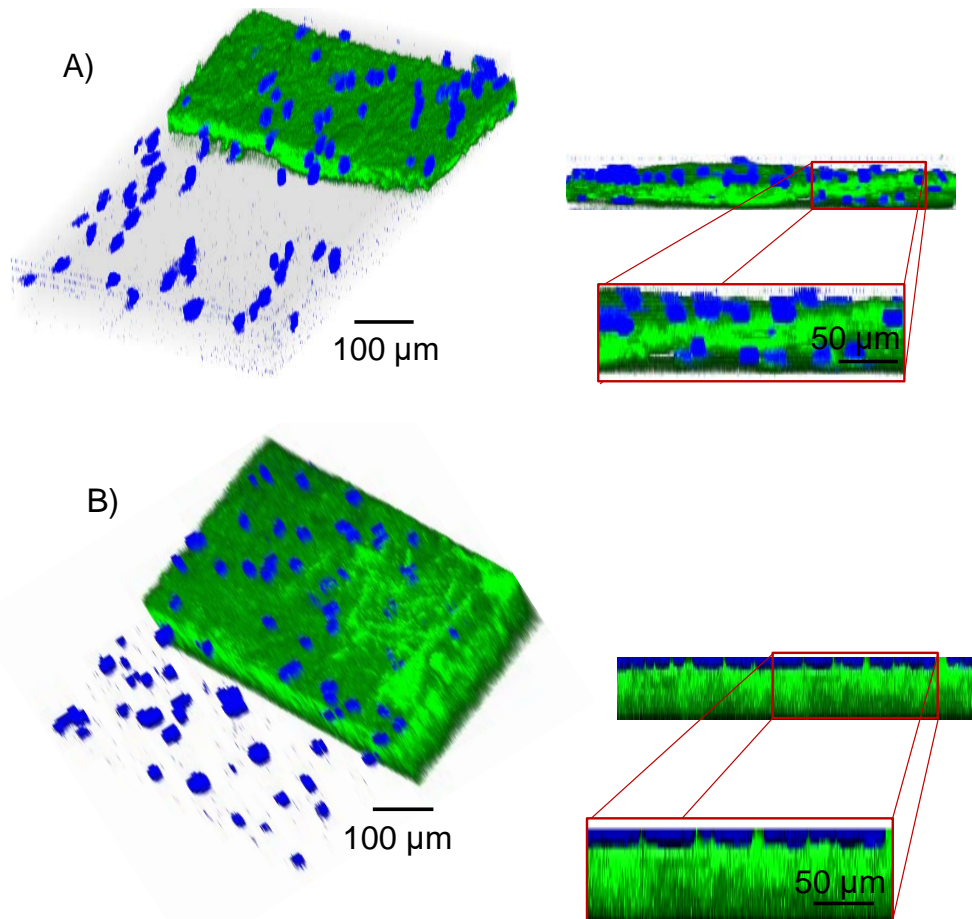
Figure 13 Representative multiphoton images of an 80:20 G:F flat sheet with cells after 7 days in culture when the concentration of TGFβ2 in culture media was A) 0.1ng/ml, and B) 10ng/ml. The material fibers are shown in green, and cell nuclei in blue. In the left image a 3D render of the scaffold is shown with the *y* plane clipped for the green channel. The right image is the *xz* view of the 3D render. Image was acquired at a magnification of 20x.

The left side is a 3D rendering of the scaffold where the *y* plane of the green channel was clipped to facilitate cell location visualization. The Right side is the *xz* view of the 3D render where the cell position along the *z* plane is shown. In Figure 13A it is possible to observe how the cells migrated through the entire scaffold depth and they are located in different positions along the *z* plane. In Figure 13B it is possible to see that the cells remained in the scaffold surface since the migration was limited.

Collagen production was assessed in growth medium and in the actual scaffold. Figure 14A shows the results for the collagen dissolved in growth media that was produced from day 6 to day 7. The amount of collagen was normalized by the number of cells in the flat sheet. The largest amount of collagen was produced when the concentration of TGFβ2 was 10ng/ml (8.89×10^{-5} μg/cell $\pm 5.63 \times 10^{-5}$ μg/cell), and the least amount of collagen was obtained when the TGFβ2 was 0.1ng/ml (3.17×10^{-5} μg/cell $\pm 1.35 \times 10^{-5}$ μg/cell), which is lower than the control (4.37×10^{-5} μg/cell $\pm 2.38 \times 10^{-5}$ μg/cell). A similar tendency was obtained when the collagen was measured in the scaffolds (Figure 14B). The largest amount of collagen in the flat sheets was obtained with a concentration of TGFβ2 of 10ng/ml (2.19×10^{-3} μg/cell$\pm 2.95 \times 10^{-4}$ μg/cell) and the lowest amount when the TGFβ2 concentration was 0.1ng/ml (2.45×10^{-4} μg/cell $\pm 1.58 \times 10^{-5}$ μg/cell). Moreover, a significant main effect was identified ($p<0.05$) for 5ng/ml and 10ng/ml compared with the control (1.11×10^{-3} μg/cell $\pm 5.42 \times 10^{-5}$ μg/cell, 2.19×10^{-3} μg/cell $\pm 2.95 \times 10^{-4}$ μg/cell vs. 3.63×10^{-4} μg/cell $\pm 6.62 \times 10^{-5}$ μg/cell).
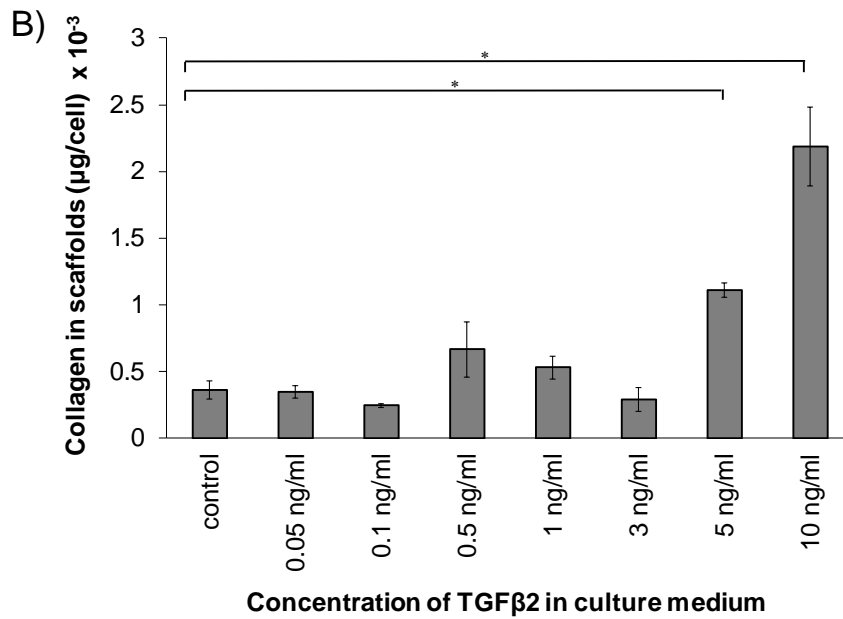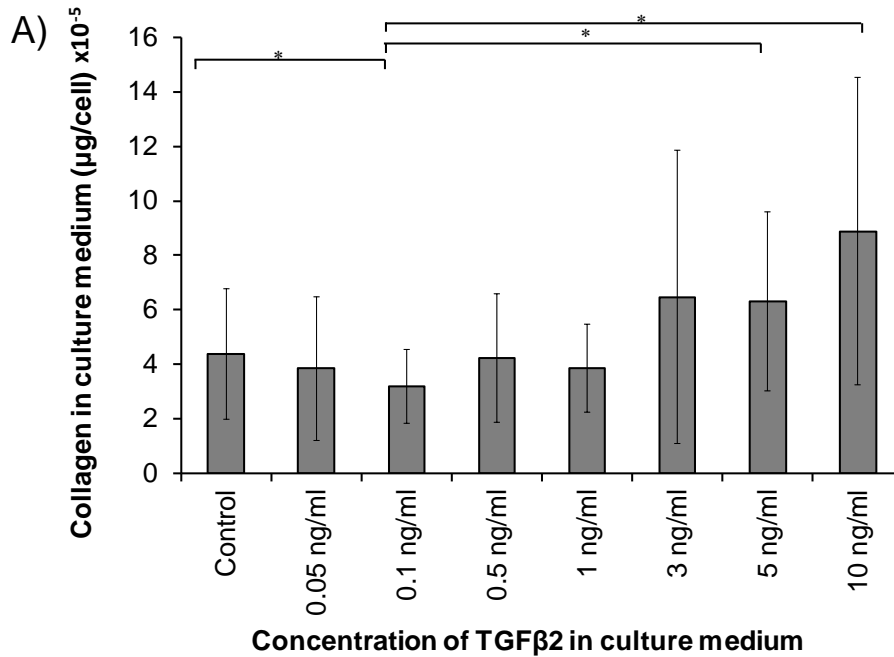
Figure 14 Collagen produced by SMCs growing on 80:20 G:F electrospun scaffolds, when different concentrations of exogenous TGFβ2 were added to the culture medium. A) Average amount of collagen/cell dissolved in culture medium is reported. Collagen dissolved was assessed over 24h from day 6 to day 7 after cell seeding. B) Average amount of collagen/cell deposited in the scaffolds after 7 days in culture is reported. Error bars shown are standard deviation (∗p< 0.05; n=6).

2.4   DISCUSSION

The data suggest that scaffolds composed of 80:20 G:F are more suitable for SMCs growth in both early (2days) and later (7 days) stages in culture, since cells have shown to adhere and proliferate more compared with 100 G and 50:50 G:F (Figure 9, Figure 10). We found a differential effect of TGFβ2 concentration on the SMCs growing in 80:20 G:F sheets. When these constructs were treated with TGFβ2 at concentrations ≤1 ng/ml the cell proliferation and migration increased, and the collagen production was not significantly affected. In contrast, when the constructs were treated with high TGFβ2 concentrations (>1 ng/ml), cell proliferation and migration decreased and the collagen production increased (Figure 11, Figure 12, Figure 13, and Figure 14).

In the study of Balasubramanian et al, 2013 [86], the authors were studying cell growth in scaffolds with a composition of 80% gelatin-20% fibrinogen and 60% gelatin-30% fibrinogen compared with constructs made of 100% fibrinogen. Their findings stated that the addition of gelatin to the fibrinogen scaffolds is beneficial for cell growth since their constructs with 80:20 G:F composition were more likely to cause better cell attachment and growth [86]. When looking closer at our results for differences in proliferation between the scaffolds after 2 and 7 days, it is possible to observe that at 2 days post seeding 100 G flat sheets had a higher number of cells attached than 50:50 G:F. In contrast, at 7 days 100 G scaffolds showed the lowest number of cells growing in the scaffold (Figure 9). This could indicate that gelatin may be more suitable for cell attachment while fibrinogen may help to promote cell proliferation. It is possible to attribute these results to the fact that gelatin is partially hydrolyzed collagen which preserves the arginine-glycine-aspartic acid (RGD) sequence along its structure [97, 98]. This particular amino acid sequence is a specific integrin location for focal adhesion which encourages cell attachment [97-99]. Furthermore, it has been strongly suggested that fibrinogen and its degradation products can

stimulate the SMCs DNA synthesis as in mitosis and consequently their proliferation. Thus fibrinogen can be considered as a mitogenic stimulus [86, 100-103].

Cell infiltration results show that SMCs can migrate through the fibrous scaffold, and that migration is progressive along the time in culture, with more than 90% of the scaffold thickness infiltrated after 7 days post seeding (Figure 10A). A representative image of the cell seeded scaffolds is shown in Figure 10b, where it is possible to observe that the cells were homogenously placed on the flat sheets and they were located in different points along the z plane. It is well known that the porus size and fiber diameter affect the migration of cells in electrospun scaffolds. Generally, cell seeded in electrospun scaffolds with a percentage of porosity higher than 35%, present good migration [104-106]. In Rnjak-Kovacina et al (2011), authors demonstrated that fibroblasts seeded in electrospun synthetic human elastin was improved when the porosity of the constructs was increased from $14.5 \pm 0.8\%$ to $34.4 \pm 1.3\%$. Authors observed that in the upper limit of porosity, at 3 post-seeding cells had migrated half way through the scaffold and by day 8 post-seeding they spanned the entire scaffold [104]. From the characterization of our electrospun gelatin-fibrinogen sheets, we found that the fiber diameter was comparable among the different scaffold composition, and the porosities range from 45% - 79%, fact that did not affect cell migration as it is possible to observe in Figure 10a. Our results are consistent with Rnjak-Kovacina et al (2011) observations since 2 days post seeding SMCs migrated between 35% and 45% and 7 days post seeding cells migrates between 90% and 97%.

Our findings on the effect of exogenous TGFβ2 over the SMCs after 7 days in culture suggest that different concentrations can produce different effect on cell proliferation, migration and collagen production. A positive effect over cell proliferation was observed when TGFβ2 was added at the more physiological concentrations of ≤1 ng/ml, with the highest SMCs growth detected at

0.1ng/ml (Figure 11). Nevertheless, when the culture medium was supplemented with higher, more non-physiological TGFβ2 concentrations (>1ng/ml), cell proliferation seemed to be inhibited with the lowest cell count obtained at 5 ng/ml and 10ng/ml (Figure 11). A similar trend was found in our cell infiltration results, where the highest and lowest scaffold infiltration was achieved when TGFβ2 was at 0.1ng/ml and 10ng/ml respectively (Figure 12). At 0.1ng/ml TGFβ cells migrated through 99% of the scaffold and were spread out along the *z* axis (Figure 13A). Conversely, at a concentration of 10 ng/ml TGFβ the cells only migrated through approximately 14% of the flat sheet (in the z axis direction), mainly remaining superficial (Figure 12, Figure 13B). Interestingly, when observing the influence of TGFβ2 over collagen production, a direct opposite outcome was found, with a negligible or negative effect obtained with TGFβ2 at concentrations ≤1ng/ml, and a positive effect when TGFβ2 was at concentrations >1ng/ml (Figure 14). Contrary to what was found for proliferation and migration, the highest collagen amount (for both dissolved in growth medium and deposited in the scaffolds), was obtained with 10ng/ml TGFβ2, and the lowest for 0.1ng/ml TGFβ2.

It is well know that SMCs can modulate from a mature or contractile phenotype, which is exhibited in mature tissue, to a proliferative or synthetic phenotype, found in new born arteries or under conditions such as injury or atherogenesis [34, 52] . In the contractile phenotype these cells have a low rate of proliferation, produce small amounts of ECM, and due to their contractile function, are less able to migrate [34, 52, 53]. In contrast, when SMCs are in a synthetic phenotype they are highly proliferative, are able to migrate and synthesize ECM [34, 52]. It has been demonstrated that SMCs can change between phenotypes depending on different environmental stimuli such as the concentration of TGFβ, which in fact is a key signaling factor for inducing, maintaining, or switching between SMCs phenotypes [53, 107-109]. Depending on its

concentration TGFβ is capable of either promoting or inhibiting SMCs proliferation [110, 111]. At low concentrations, TGFβ can stimulate SMC proliferation by promoting the platelet-derived growth factor (PDGF), which increases DNA synthesis [110-112]. However, at high TGFβ concentrations the expression of PDGF is downregulated, causing a reduction in SMCs proliferation [110]. Additionally, when SMCs are exposed to higher concentrations of TGFβ2, this growth factor can also induce proteins such as alpha-smooth muscle actin and desmin, typical of the contractile phenotype [34, 53]. In physiological conditions, SMCs in the contractile phenotype proliferate at an extremely low rate, and the production of ECM components such as collagen is low [34, 53, 108]. Nevertheless in the study of Kubota et al (2003), the authors validated that the treatment of vascular SMCs with a high concentration of TGFβ1 (10ng/ml) stimulated collagen synthesis and increased the level of collagen type I mRNA around 2 fold [113]. In a different study (Mann et al, 2001) authors showed that the use of TGFβ1 can increase the synthesis of ECM components on RGD-containing systems such as gelatin scaffolds [114]. In the context of these TGFβ1 studies, our results would suggest that the non-physiologically high TGFβ2 concentrations may be inducing signaling for ECM production through a TGFβ1 pathway [115]. Current literature indicates that when SMCs are exposed to low TGFβ2 concentrations, proliferation is promoted; and when SMCs are exposed to high concentrations of TGFβ2, proliferation is decreased, the contractile phenotype may be induced, and the production of ECM is stimulated [53, 110, 111, 113].

Our study was based on PAOSMCs, however our results can be translated to humans since human and porcine vascular smooth muscle cells (VSMC) have a comparable rate of proliferation, and have shown similar responses to different stimuli *in vitro* [116-121].

Additionally, it has been demonstrated that the biological analogies that establish the pig as physiologically the nearest animal to man, make swine potentially a good model for biomedical research [122, 123]. One of the fields in which the pig will make its greatest contribution to human health and longevity is that of research on the heart and circulatory system [122]. The distribution of blood supply by the coronary artery system is almost identical to that of humans, as well as the size of the heart and the different blood vessels [123].

One limitation of our study was the variability of the thickness of the sheets due to the inherent randomness of the electrospinning process. Our infiltration results had to be normalized by the flat sheet depth and then averaged with the aim of reducing the error introduced by the variability of the scaffold dimensions. Another limitation of the study included the sheets imaging under the multiphoton microscope being unable to capture the second harmonic generation (SHG) signal expected from the collagen produced by the cells. This led us the uncertainty of whether or not the collagen deposited was effectively assembled into a fibrillar form, or if the SHG signal was too low to be detectable by the photomultiplier tube (PMT) in the multiphoton microscope. We demonstrated by using a chemical reaction that SMCs growing in the scaffolds were synthetizing collagen, and also that this synthesis was affected when the cells were treated with different concentrations of TGFβ2. However, our results do not allow us to ensure that this collagen may be fibrillar as it is normally in soft tissue. Future studies will be focused on find for a strategy that allows us to assess if the collagen deposited by the SMCs in the electrospun flat sheets is in fact fibrillar collagen. Additionally, since the autofluorescence signal from the constructs is much higher than the fluorescence signal from the antibodies, our attempts to image SMCs growing in the flat sheets using ICC were not successful. This prevents us from obtaining important information about morphology and the expression levels of proteins related to SMC phenotype. In

order to be able to image SMCs growing in gelatin-fibrinogen constructs using ICC, it would be necessary to strategically increase the signal from the secondary antibodies. Some of the strategies consist in culture the cells for longer periods of time before performing ICC. Also increase the concentration and incubation times of both primary and secondary antibodies. In this way, it could be possible to obtain a more intense signal from the secondary antibodies, so the autofluorescence from the flat sheet cannot mask the fluorophores. Our observations suggest that high concentrations of TGFβ2 induce the contractile phenotype; nevertheless, morphology and protein marker expression would confirm these results. Since it is important to gain knowledge on how SMC phenotype is affected by a TGFβ stimulus, our future research will focus on the assessment of morphology and the expression levels of proteins such as alpha-smooth muscle actin, calponin, smooth muscle myosin heavy chain, and caldesmon [53]. Furthermore, as part of the study of the tissue engineered scaffolds, our future work also consists in the biomechanical characterization of the electrospun sheets seeded with SMCs and treated with exogenous TGFβ2 at different concentrations, including the "TGFβ2 switch". The biomechanical properties will be measured using a microbiaxial optomechanical device (MOD) designed in our laboratory to measure macroscopic and microstructural properties of planar and tubular samples [90, 124, 125]. The MOD is a single consolidated device for which simultaneous mechanical stimulation of the same fully hydrated sample can be done while performing multiphoton microscopy. The MOD has been specifically designed for integration with the AIM.

2.5   CONCLUSIONS

Electrospun scaffolds composed by 80% gelatin and 20% fibrinogen are attractive for SMC growth and migration, since gelatin facilitates cell attachment and fibrinogen seems to promote cell proliferation. When our tissue-engineered scaffolds were treated TGFβ2, a differential modulation was observed depending on the concentration, noticing that at low concentrations of TGFβ2 (≤1ng/ml) cell proliferation was enhanced with no significant effect over cell infiltration and collagen production. Increasing the concentration of TGFβ2 above 1ng/ml has an opposite effect on the cell behavior, where the mitotic function was lower, the migration was minimal, and the collagen production was increased. According to these results it is possible to propose a strategy that we call "The TGFβ2 switch" to biochemically control SMC function growing in tissue engineered scaffolds: In early stages, the SMC proliferation and migration will be promoted by treating the cells with low concentrations of TGFβ2, ideally 0.1ng/ml, as it has been demonstrated in this work. Subsequently, once the cells are distributed throughout the scaffold, the concentration of TGFβ2 will be significantly increased to 10ng/ml with the aim of promoting collagen production and possibly induce the contractile phenotype. Future research in our laboratory will further explore the implementation of "The TGFβ2 switch" strategy, evaluating cell proliferation, infiltration, collagen production and phenotype shifting of SMCs growing in 8:20 G:F electrospun scaffolds.

3.0   CHAPTER 3: SPECIFIC AIM 2

TGFβ2 RELEASE FROM TUBULAR ELECTROSPUN SCAFFOLDS TO MODULATE SMC FUNCTIONS

In view of vascular tissue engineering applications, in this aim I studied the possibility of integrating TGβ2 in electrospun tubular scaffolds with the goal of modulating the proliferation, infiltration and collagen production of SMC growing in the scaffolds. TGβ2 was loaded into tubular constructs fabricated from different ratios of gelatin and polycaprolactone. Scaffold morphology, degradation rate, TGβ2 release kinetics, and bioactivity were assessed.

This aim evaluated the possibility of having a TGβ2 releasing system using intelligently the biodegradation of natural and synthetic biomaterials to modulate different functions of SMC directly from the implanted TEVG.

This aim is based on the article "**Ardila D. C.,** Tamimi E., Wagner W., Doetschman T., Vande Geest J.P. Modulating smooth muscle cell response by the release of TGFβ2 in tissue engineered vascular grafts" Submitted to the Journal of Controlled Release on August 24, 2018

3.1 INTRODUCTION

The development of a functional tissue engineering vascular graft (TEVG) is one of the urgent necessities in the effort to improve the treatment of coronary heart disease [1-7]. An acellular and biodegradable TEVG must encourage healthy host cell infiltration while also providing a suitable environment for matrix production and proper long term function [8, 44, 68, 69, 126, 127]. TEVG scaffolds can also provide additional biofunctionality by locally delivering biomolecules to regulate SMCs response [128, 129]. Growth factors such as TGFβ2 can have a differential effect on SMCs proliferation, migration, and matrix deposition as was demonstrated in Aim 1. The data showed that the proliferation and migration of SMCs seeded in gelatin/fibrinogen scaffolds was increased in low concentrations of exogenous TGFβ2 ($\leq$ 2ng/ml in culture media) whereas the proliferation and migration of SMCs deceased in high concentrations of exogenous TGFβ2 ($\geq$ 5ng/ml) [78]. These results suggested that it is possible to modulate SMCs growth in a TEVG by using TGFβ2.

Biomolecules such as TGFβ2 can be incorporated into the polymeric scaffold using various different strategies such as physical encapsulation [49, 56], absorption of growth factors into the processed matrix surface [49, 56], covalent immobilization has also been used by researchers [58, 130-134], and ECM-inspired immobilization using heparin [49, 56, 135-137]. The release of TGFβ2 from the scaffolds will depend mainly from the degradation rate of the materials used in the encapsulation [138]. The use of synthetic biodegradable polymers such as PCL in a blend with natural polymers such as gelatin have been used to improve the mechanical properties and patency of scaffolds, and delay their degradation allowing for new tissue ingrowth and the control release of biomolecules such as growth factors [138-143].

The goal of this work was to create hybrid gelatin:polycaprolactone (G:PCL) tubular scaffold capable of releasing bioactive TGFβ2 to encourage SMC proliferation and migration. Electrospinning was used to prepare tubular scaffolds with increasing ratios of a G:PCL blend. TGFβ2 was loaded into the polymeric blends during the electrospinning process and genipin was used to crosslink the gelatin contained in the polymeric blends. The resulting scaffolds were evaluated for their porosity, fiber thickness, degradation rates, TGFβ2 release kinetics, bioactivity of the released growth factor, and their suitability for *in vitro* SMC culture.

3.2   MATERIALS AND METHODS

3.2.1   Preparation of TGFβ2 loaded polymeric scaffolds

Gelatin extracted from porcine skin and PCL (80,000 MW) (Sigma-Aldrich, USA) were mixed at three different percentages: 80% gelatin 20% PCL (80G:20PCL), 50% gelatin 50% PCL (50G:50PCL), and 20% gelatin 80% PCL (20G:80PCL). The polymeric blends were dissolved in 1,1,1,3,3,3-Hexafluoro-2-propanol (HFP) (Sigma-Aldrich, USA) to create a 10% (w/v) solution under continuous stirring. The polymeric solutions were loaded into a 5 ml BD syringe and lyophilized recombinant human TGFβ2 (R&D systems) was reconstituted with 4mM HCL containing 1mg/ml bovine serum albumin (BSA) (Sigma-Aldrich, USA). The TGFβ2 solution was mixed with the polymeric blends directly in the syringe immediately prior to electrospinning to create a final concentration of 1.3 µg/ml. A 23-gauge stainless steel dispensing blunt tip needle (CML supply, USA) was attached to the syringe which was then loaded onto a NE-1000 single syringe pump (New era pump systems inc., USA) set to a pumping rate of 30 µL/min and a total

dispensing volume of 300 µL. The distance from the needle tip to the target was 10 cm. The polymeric solutions containing TGFβ2 were electrospun at a high voltage of 15 kV, onto a grounded 1.4-mm metallic rod mounted onto a rotating and translating mandrel set to a rotation rate of 300 rpm and a translation rate of 300 mm/sec. The resulting tubular scaffolds were crosslinked in a 0.5% (m/v) genipin solution (Wako Chemicals, USA) in 200 proof ethanol for 24 hours at 37°C under constant stirring. The tubes were rinsed with ethanol to remove any genipin residues. Each scaffold had an approximate length of 8 cm, a dry weight of 10 mg, and a determined TGFβ2 density of 13 ng TGFβ2/ mg scaffold.

3.2.2   Scaffold characterization

Scaffold characterization was performed using scanning electron microscopy (SEM) on scaffolds with and without TGFβ2. Briefly, samples were mounted onto aluminum stubs, grounded with silver paint, and sputter coated with 6 nm gold/palladium (Cressington Sputter Coater Auto 108, Cressington, Watford, UK). Cross-sectional and en face views of the samples were imaged in a JEOL JSM-6335F scanning electron microscope (Peabody, MA) at 3 kV at a magnification of 2000x. The en face SEM images (n=3 for each group) were binarized and the porosity was calculated by dividing the total number of fiber pixels by the total number of pixels in the image. The fiber diameter was calculated by manually measuring the diameter of 40 randomly selected fibers per scaffold (n=3 for each group) via freehand lines superimposed over the SEM images in ImageJ.

3.2.3   Scaffold degradation rate

The degradation rate of the electrospun scaffolds was assessed in terms of dry weight change. For each group, 8-cm long dry crosslinked scaffolds were weighted and placed into 15 ml conical tubes containing 10 ml of 1X phosphate buffered saline (PBS) (Gibco, Life technologies) and incubated at 37°C. At predetermined time points, the samples were taken from the PBS, rinsed 2 times with deionized water, dried in a convection oven for 1 day at 42 °C and weighed. The samples were then put back in fresh 1X PBS and incubated at 37°C to continue the degradation study. The degradation of each scaffold was calculated as a percentage of dry weight remaining compared to their initial dry weight.

3.2.4   *In vitro* TGFβ2 release kinetics

TGFβ2 loaded scaffolds (8-cm long, 10 mg TGFβ2 total approximately) were put in 15 mL conical tubes and incubated in 10 mL of Dulbecco's Modified Eagle Medium (DMEM) supplemented with 10% Fetal Bovine Serum (FBS), 100U/mL of penicillin, 100 μg/mL of streptomycin, 5 μg/mL of amphotericin B and 25 mM HEPES (Gibco, Life technologies, USA) at 37°C and 5% CO_2. The release media was collected at predetermined time points and frozen at -80°C until assaying. The release medium was replenished with fresh medium to continue the release study. TGFβ2 concentrations were quantified using the Quantiquine human TGFβ2 immunoassay ELISA kit (R&D systems).

3.2.5 TGFβ2 bioactivity assay

The bioactivity of the released TGFβ2 was measured by its ability to modulate SMC proliferation. Scaffold groups of 80G:20PCL, 50G:50PCL, and 20G:80PCL containing 13 ng TGFβ2/mg scaffold and 100 ng TGFβ2/mg scaffold, were fabricated by electrospinning as previously described. Porcine aortic SMCs from passage 4 were seeded in wells of 96-well plates at a density of 7 x 10^3 cells/well. Cells were cultured in the above described culture media for 24 h at 37°C and 5% CO2 in a humidified atmosphere. Culture media was then changed in each cell seeded well and the scaffolds containing either 0ng, 13 ng, or 100 ng TGFβ2/mg of scaffold were cut into 7 mm pieces and submerged into the culture media without touching the cells. For this purpose, a HTS Transwell®-96 well permeable support (Corning, USA) was used, which allowed cells to interact with the released TGFβ2 without direct contact with the scaffold. The system was incubated for 5 days at 37°C and 5% CO2 in a humidified atmosphere. After the incubation period, the scaffolds and the permeable support were removed and the cells were detached from the wells using 0.25% trypsin (Gibco, Life technologies, USA). Cell number was determined using the Countess II-automated cell counter (Invitrogen). To calibrate the effect of TGFβ2 on porcine vascular SMC growth, cells were grown in culture media containing different concentrations of TGFβ2 ranging from 1 pg/ml to 10 ng/ml. Porcine aortic SMCs (PAOSMCs) were seeded in the wells of 96-well plates at a density of 7 x 10^3 cells/well in culture media for 24 hours. The media was then replaced with culture media with different concentrations of TGFβ2. The SMCs were incubated for additional 5 days and cell proliferation was evaluated by cell count

3.2.6   *In vitro* SMC growth within the TGFβ2 loaded scaffolds

To evaluate the ability of the TGFβ2 releasing scaffolds to support SMC growth, porcine vascular SMCs were seeded onto the scaffolds with or without TGFβ2. Cylindrical 80G:20PCL scaffolds containing 13 ng TGFβ2/mg of scaffold, were cut into 3 mm pieces. Each piece was placed upright in a well of a 96-well plate, and porcine vascular SMCs from passage 4 were pipette-seeded in the lumen at a density of 1 x 10^4 cells/scaffold, followed by a 15 min incubation period. A second seeding was performed by submerging the samples in 100 µl of a cell solution containing 1 x 10^4 cells, follow by a 15 min incubation period to let the cells attach to the outer surface. The samples were then rinsed with 1X PBS and transferred to new wells of a 96-well plate containing fresh culture media prepared as described above. The seeded scaffolds were cultured for 5 days in a humidified atmosphere at 37°C and 5% CO2. After the incubation, the samples were immediately fixed in 10% formalin for 24 hours at 4°C. Cell nuclei were stained with VECTSHIELD® mounting media containing 4',6-diamidino-2-phenylindole (DAPI) (Vector Laboratories, USA). The Advanced Intravital Microscope (AIM) for multiphoton imaging at the University of Pittsburgh's Soft Tissue Biomechanics Laboratory was used to observe the total cell distribution along the scaffold thickness. The Pitt AIM is an Olympus BX51 upright laser-scanning microscope coupled to a Coherent 120-fs tunable pulsed Titanium-Sapphire laser (Santa Clara, CA). For this study a 4X air objective was used. Incident light was focused on the sample and the backscattered signal was collected over a 1500 x1500 µm field of view at 5 µm steps, imaging through the scaffold depth. Cross-sections and en face images of each scaffold were captured. The laser was centered at λ=750 nm to excite DAPI, and 2-photon excited fluorescence (2PEF) was split with a 505 nm dichroic mirror and collected through a 460/80 bandpass filter. The fibers were imaged colocalized using the autofluorescence signal from genipin collecting the light with a 620/50

bandpass filter. The optics were chosen to maximize discrimination between the polymeric fibers and DAPI fluorescence. The colocalized image stacks from nuclei and fibers were merged to visualize the 3D cell location in the scaffolds. Maximum intensity projections from the cross sectional images were binarized and used to calculate the area covered by the cells in 3 different regions: inner (luminal), middle (medial), and outer (abluminal) third through the thickness.

3.2.7   Statistical methods

All values are presented as the mean ± standard deviation unless otherwise specified. For the porosity values and fiber thickness individual Students t-tests were performed. For all statistical tests, a critical p-value of 0.05 was used to define significance. The statistical analysis for the effect of different concentrations of TGFβ2 on SMCs proliferation was performed using a one-way ANOVA with the Dunnet's comparison procedure. For the bioactivity assay and nuclei area coverage in the cell seeded scaffolds the analysis was completed using a two-way ANOVA with a *post hoc* analysis using a Bonferroni correction to account for family-wise error.

3.3   RESULTS

3.3.1   Scaffold porosity and fiber thickness

The tubular electrospun scaffolds with and without TGFβ2 were found to have porosities above 35% and fiber thickness below 1μm (Table 1).

Table 1 Scaffold porosity and fiber thickness. Average value ± standard deviation is presented. (n=3 in each)

	Without TGFβ2		
Scaffold	*80G:20PCL*	*50G:20 PCL*	*20G:80PCL*
Porosity (%)	43.6 ± 3.1	37.5 ± 4.6	41.1 ±1.7
Fiber thickness (μm)	0.7 ± 0.58	0.63 ± 0.51	0.44 ± 0.35
	With TGFβ2		
Porosity (%)	45.6 ± 1.6	38.9 ± 3.7	41.24 ± 3.7
Fiber thickness (μm)	0.65 ± 0.46	0.57 ± 0.48	0.44 ± 0.28

The addition of TGFβ2 did not significantly change the porosity or fiber thickness in scaffolds with the same gelatin:PCL (referred to as G:PCL) composition. Fiber thickness was significantly lower ($p < 0.05$) in the 20G:80PCL compared to the 80G:20PCL in scaffolds with and without TGFβ2.
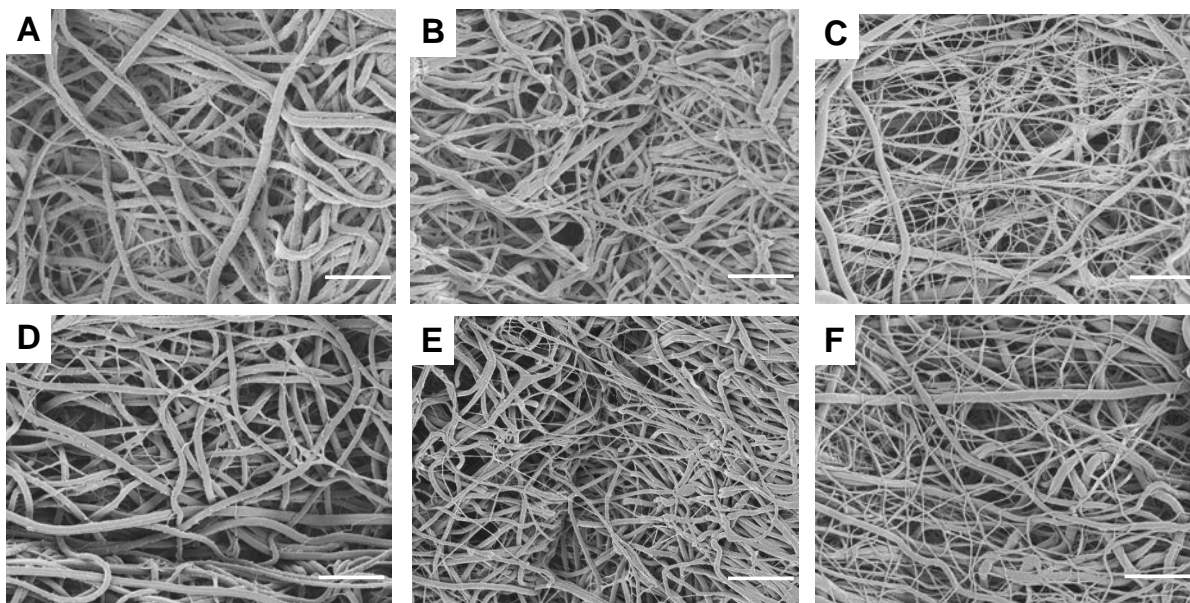
Figure 15 Representative SEM en face images of tubular scaffolds excluding (A-C) and including (D-F) TGFβ2. A and D are composed of 80G:20PCL; B and E are composed of 50G:50PCL; C and F are composed of 20G:80PCL. Scale bar is 10µm.

The *en face* SEM images of the electrospun scaffolds are shown in Figure 15, where interconnected pores are observed in all the samples. It is also noticeable that thick and thin fibers were formed regardless of the scaffold composition.

However, as the content of gelatin decreases and PCL increases the difference in thickness between the thick and thin fibers is lower which contributed to the reduction in the fiber size variance. This behavior was observed in scaffolds with and without TGFβ2.

3.3.2   Degradation rate

Figure 16 shows the scaffolds' weight percentage remaining as a function of time after incubation in PBS. These results demonstrate that the degradation rate of the blended G:PCL scaffolds increased as gelatin content increased, with the lowest weight percentage remaining of

80% ± 1.2% in the 80G:20PCL scaffolds after 42 days of incubation in a aqueous solution. For the 50G:50PCL and 20G:80PCL, the weight remaining after 42 days was 91%±0.81%, and 94.1 ± 0.88%, respectively
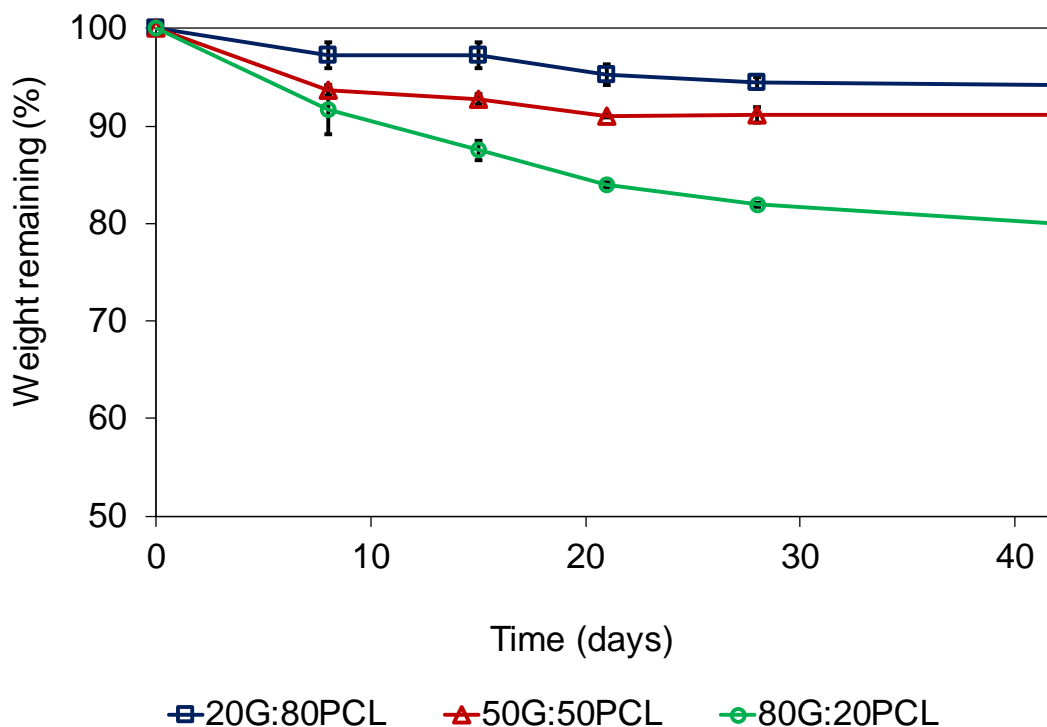
Figure 16 Degradation rate of TGFβ2 releasing scaffolds over the course of 42 days. Error bars shown are standard deviation (n=4)

3.3.3   Release of TGFβ2 from crosslinked gelatin:PCL electrospun scaffolds

TGFβ2 released from the crosslinked G:PCL electrospun scaffolds was evaluated by ELISA. Figure 17 presents the release profile of TGFβ2 of the 80G:20PCL, 50G:50PCL, and 20G:80PCL constructs.

All the samples showed a slow sustained release over the course of approximately 15 days before reaching a plateau. The scaffolds with higher percentage of gelatin exhibited higher

amounts of TGFβ2 eluted. The 80G:20PCL constructs had the maximum TGFβ2 percentage release of 3.1% over the course of 42 days. The maximum percentage release over 42 days for the 50G:50PCL, and 20G:80PCL constructs was 0.22% and 0.07% respectively.
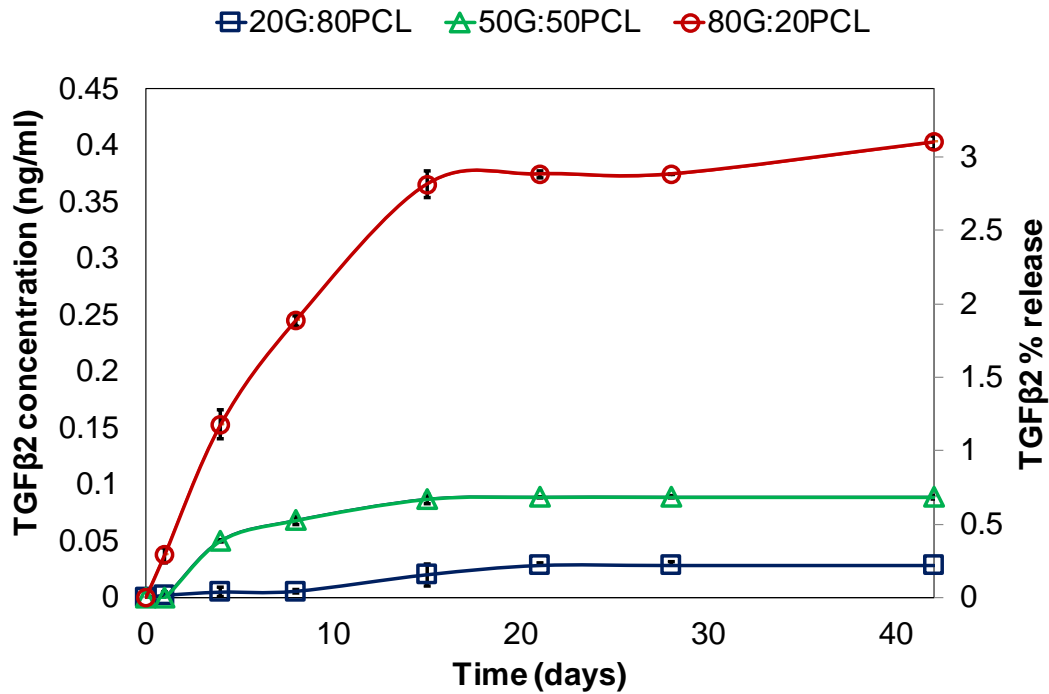
Figure 17 Cumulative release of TGFβ2 from electrospun scaffolds with different G:PCL compositions. Error bars shown are standard deviation (n=4)

3.3.4   Bioactivity of released TGFβ2

A calibration curve of the cell number after 5 days of culture with a range of TGFβ2 concentrations shows an increase in cell number when growing in media with added TGFβ2 at 0.1ng/ml to 1 ng/ml as it is possible to observe in Figure 18. It is also noticeable that when the concentration of TGFβ2 in the media increases to 5 ng/ml and 10 ng/ml, the cell count decreased.

Scaffolds loaded with 13 ng TGFβ2/mg scaffold had a positive effect over cell proliferation as shown in Figure 19. The 80G:20PCL constructs with 13 ng TGFβ2/mg scaffold significantly increased cell number relative to scaffolds without TGFβ2 (p=0.016), as well as scaffolds containing 100 ng TGFβ2/mg of scaffold (p=0.011).
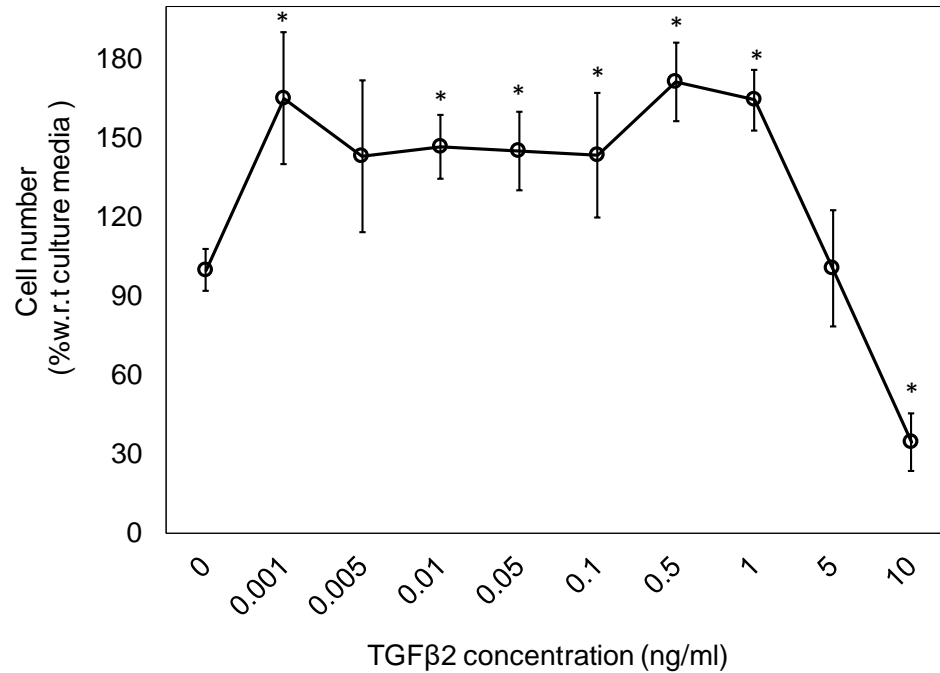
Figure 18 Effect of exogenous TGFβ2 dose on proliferation of SMCs growing in monolayer for 5 days. Error bars shown are standard deviation (n=6)

Scaffolds composed by 20G:80PCL with 13 ng TGFβ2/mg of scaffold and 100 ng TGFβ2/mg of scaffold had a significant positive effect on cell proliferation compared to scaffolds without TGFβ2 (p=0.012, and p=0.032 respectively). The 80G:20PCL and 50G:50PCL constructs loaded with 100 ng TGFβ2/mg of scaffold had an inhibitory effect over cell proliferation, while the 20G:80PCL scaffolds with this high TGFβ2 content show an increase in cell number.
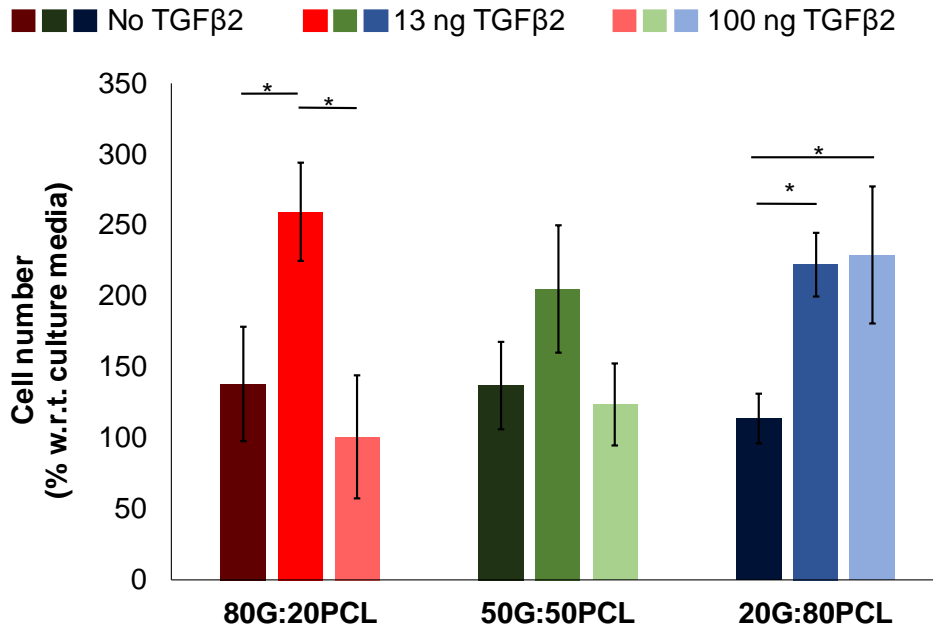
Figure 19 Bioactivity of released TGFβ2 from electrospun scaffolds on cells growing in monolayers. Scaffolds loaded with 13 ng and 100 ng of TGFβ2/mg of scaffold were submerge in the culture media without having direct contact with the cells. A permeable support was used to elevated the scaffolds above the cell level. Cell count was assessed after 5 days in culture. Error bars shown are standard deviation (*p < 0.05; n = 6).

3.3.5   In vitro cell growth of SMCs in the TGFβ2-releasing scaffolds

Cells seeded and cultured for 5 days in the eluting scaffolds were quantified by calculating the area covered by the nuclei in the maximum intensity projection of the multiphoton images of the scaffold cross-sections.

A representative image from the 2-photon 3D reconstructions of the seeded 80G:20PCL scaffolds loaded with 13 ng TGFβ2/mg of scaffold is shown in Figure 20.
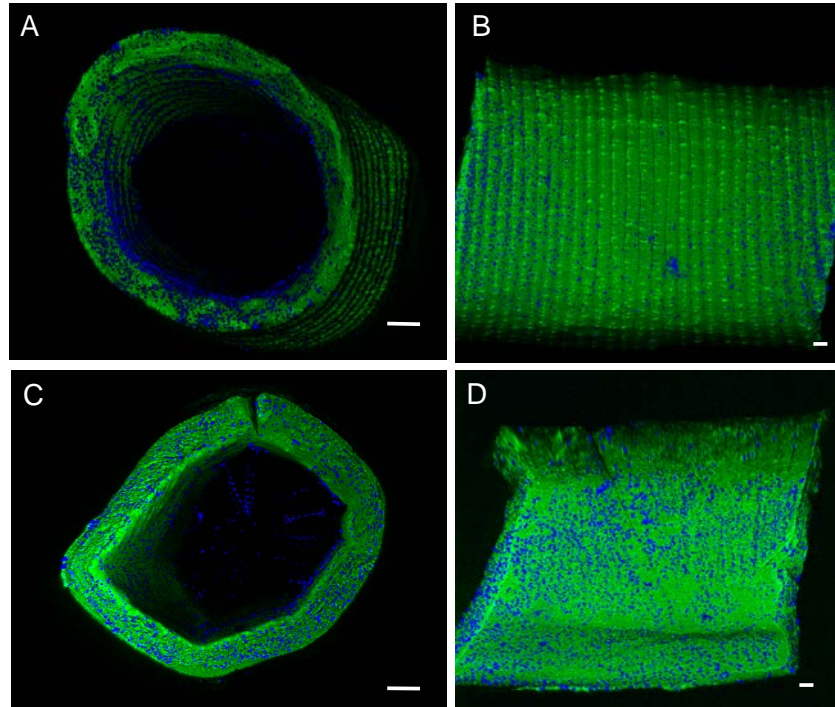
Figure 20 Representative multiphoton images of the 80G:20PCL electrospun scaffolds without (A and B) and with (C and D) TGFβ2 cultured with SMCs for 5 days. A and B are cross-sectional and *en face* images of the scaffold without TGFβ2, respectively. C and D are cross-sectional and *en face* images of the TGFβ2 releasing scaffolds. Green - electrospun fibers; Blue – nuclei. Scale bar sown is 100μm

The TGFβ2-eluting scaffolds had a more even cell distribution in both the radial direction and along the circumference. These scaffolds also exhibited higher number of nuclei along the scaffold length. A representative image from the 2-photon 3D reconstructions of the seeded 80G:20PCL scaffolds with and without 13 ng TGFβ2/mg is shown in Figure 6. The TGFβ2 eluting scaffolds had a more even cell distribution in both the radial direction and along the circumference. These scaffolds also exhibited higher number of nuclei along the scaffold length.

Binary images (Figure Figure 21A) were used to calculate the percentage of the cross-sectional area occupied by cell nuclei. These results showed that scaffolds releasing TGFβ2 have significantly higher cell numbers in the middle section of the construct relative to scaffolds without TGFβ2 (p=0.037, Figure Figure 21B).

A **Without TGFβ2**

With TGFβ2

B
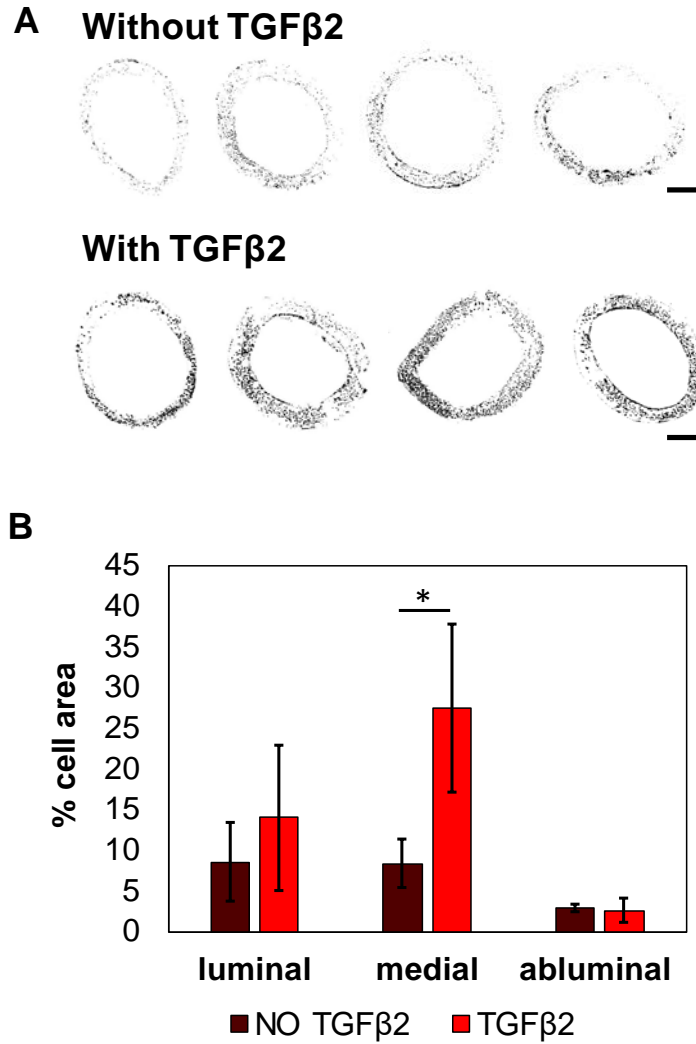
Figure 21 A) Binary multiphoton images of the 80G:20PCL electrospun scaffolds without (top row) and with (bottom row) TGFβ2 cultured with SMCs for 5 days. The four cross-sections in each group correspond to four different replicates. Scale bar is 200 µm. B) Quantification of the cross-sectional area occupied by cell nuclei. The thickness of the scaffold was divided in 3 different regions, each one corresponding to one third of the thickness: inner (luminal), middle (medial), and outer (abluminal). Error bars shown are standard deviation (*p < 0.05; n = 4)

3.4   DISCUSSION

Results from aim 2 show that electrospun scaffolds from a blend of natural and synthetic polymers have the ability to elute bioactive and functional TGFβ2. The data also demonstrate that electrospinning our biomaterials results in fibrous scaffolds with interconnected pores (Figure 15). The obtained porosities range from 37% to 45%, with fiber thickness ranging from 440 nm to 700 nm, decreasing and becoming more uniform as gelatin content in the scaffold decreases (Table 1). We found that scaffolds with higher gelatin content degrade faster as constructs composed of 80G:20PCL had less weight remaining at all the time points compared to the 50G:50PCL, followed by 20G:80PCL (Figure 16). The TGFβ2 release profile showed a slow sustained release over the course of 15 days before getting into a plateau that is extended until 42 days. No burst release was observed for any of the scaffolds. It was also noticeable that the elution of TGFβ2 is higher as gelatin content in the scaffold increases as the 80G:20PCL scaffolds had the greater TGFβ2 elution followed by the 50G:50PCL and the 20G:80PCL (Figure 17). This eluted TGFβ2 is bioactive and has a differential effect on SMC growth (in monolayers) depending on its concentration (Figure 18 and Figure 19). The released TGFβ2 also increased cell infiltration and proliferation of cells growing in 3D 80G:20PCL TGFβ2 loaded scaffolds (Figure 20 and Figure 21)

Rnjak-Kovacina et al. in 2014 [104] used image analysis to calculate the porosity of their electrospun scaffolds. The authors demonstrated that tubular scaffolds fabricated from synthetic human elastin with porosities higher than 35% promoted early attachment, spreading and proliferation of primary dermal fibroblasts, as well as migration and infiltration into the construct. In this work we also used image analysis to determine the porosity of our scaffolds obtaining values ranging from 35% to 47%. This combined with the fact that the cells seeded in our scaffolds were able to migrate through the construct indicates that our porous scaffolds are suitable for cell

infiltration. Heydarkhan-Hagvall et al. [144] have created three-dimensional gelatin:PCL and collagen:elastin:PCL electrospun scaffolds with fiber sizes ranging from 590-880 nm, which favored the attachment of adipose derived stem cells. Similarly, Fu et al., [145] fabricated tubular electrospun gelatin/PCL and collagen/PCL constructs. These researchers obtained scaffolds with fiber diameters ranging from 300 nm to 400 nm, favoring the adhesion and proliferation of human umbilical cord SMCs *in vitro* and *in vivo*. Our electrospun scaffolds are composed of fibers with thicknesses ranging from 440 nm - 700 nm on average which are similar to that obtained by Heydarkhan-Hagvall et al. and Fu et al. Looking closer into the scaffold fiber structure, the blends of gelatin and PCL resulted in electrospun matrixes with thick and thin fibers with thickness distribution that becomes more uniform as the gelatin content decreased. These results are comparable to the ones obtained by Gautam, et al., 2013 [146] who also showed a relationship between increasing PCL content and fiber size distribution. We have successfully seeded and cultured SMCs in our electrospun scaffolds with and without TGFβ2, demonstrating that the microstructure of our scaffolds is suitable for cellular growth and infiltration.

The results state that the hydrolysis of the hybrid material and the elution of the growth factor from the scaffolds strongly depend on the gelatin content. Our findings are consistent with the study of Munj et al. 2017 [138], who studied the release of rodamine B from gelatin:PCL scaffolds with different compositions of the two polymers. Their study concluded that the degradation of the polymeric matrix is faster as gelatin content increases in the scaffold. The authors also found that increasing the PCL content decreased the elution of the dye which also prevented its burst release. Our results show that the degradation of the 80G:20PCL in PBS is faster compared to the degradation of 50G:50PCL, and 20G:80PCL; obtaining the slowest degradation rate for the 20G:80PCL. Our release profiles also suggested that the TGFβ2 elution

rate from the scaffolds depends directly on the gelatin amount in the polymeric blend. The highest percentage released was obtained for the 80G:20PCL constructs and the lowest for the 20G:80PCL. Only sustained release was achieved from the three gelatin:PCL blends with no observed burst release. This type of profile may be due to the addition of PCL to the scaffolds, and also to the crosslinking of gelatin, which prevents the fast hydrolysis of gelatin.

Our release profiles are also similar to the ones obtained in the work of Nada et al. 2016 [147], where the elution of chloramphenicol from electrospun gelatin crosslinked with poly aldehyde β- cyclodextrin (PA-β-CD) was studied. They show that crosslinked gelatin fibers have a sustained release of the drug with a lack of rapid release, as opposed to the profile obtained using uncrosslinked fibers where more than 90% of the chloramphenicol was eluted in the first 30 min of the study. Nada et al. concluded that the addition of a crosslinker is necessary to maintain the integrity of the gelatin containing electrospun fibers avoiding rapid elution of the drug.

Different authors have studied the release of growth factors from polymeric matrixes for a number of tissue engineering applications. The obtained percentage release values depend on the materials used for the scaffold fabrication. For instance, Sohier et al. 2006 [148] studied the release of TGFβ1 from Poly(ethylene glycol)-terephthalate/poly(butylene terephthalate)(PEGT/PBT) and poly(ethylene glycol)-succinate)/ poly(butylene succinate) (PEGS/PBS) in view of cartilage regeneration. TGFβ1 was loaded into the PEG/PBS using an emulsion-coating method which used chloroform and high vacuum to force the emulsion solution through a premade porous scaffold. The release of the TGFβ1 depended on the PEG hydrolysis in media which was incomplete after 50 days obtaining a maximum percentage release of 13% of the total amount loaded. Another example is the work of Wang et al. 2016 [149] who created electrospun PCL:hyluronan (HA) constructs loaded with epidermal growth factor (EGF) for wound healing. EGF was directly mixed

with the polymers prior to electrospinning. The authors found that the addition of HA increased the hydrophilicity of the scaffold and increased the release speed of the EGF to a maximum of 30% elution after 33 days. In that study the researchers did not use a crosslinker to stabilize the HA, however they obtained an incomplete release of EGF that can be attributed to the presence of PCL which may have prevented the short term degradation of the scaffold. These studies have release systems that either only contained synthetic polymers that don't need to be crosslinked or are aimed at applications that don't require the natural polymer to display mechanical strength. In our study the maximum TGFβ2 release from our 80G:20PCL scaffolds was 3.1% of the total amount loaded. These results are comparable to those obtained by Wang et al. 2015 [150] who fabricated electrospun and EDC crosslinked gelatin:PCL scaffolds functionalized with heparin and loaded with VEGF. The growth factor was bound to the scaffold through its affinity to heparin. The authors observed a sustained release of the VEGF that increases by increasing the amount of gelatin in the blend. The percentage release never exceeded 2.7%. However, the released VGEF was able to promote the *in vitro* proliferation of endothelial cells and the *in vivo* vascularization of a subcutaneous implant. We believe that the addition of PCL, which slows the degradation of the construct, as well as crosslinking method may have been responsible for our low growth factor recovery. In this study, we added a relatively high amount of TGFβ2 to our scaffolds due to our a priori knowledge of the inhibiting effect of crosslinking on gelatin hydrolysis. This high degree of crosslinking may have significantly decreased the degradation of gelatin which would have influenced the release of TGFβ2. Additionally, since our crosslinking method consisted in submerging the scaffolds in a liquid solution of genipin in ethanol, it is possible that surface adsorbed TGFβ2 was released in this crosslinking fluid resulting in a low content of TGFβ2 in the scaffold. Moreover, since genipin is a protein crosslinking agent [151, 152], it is possible that it

may have reacted with some of the available amine groups from TGFβ2, rending the growth factor unrecognizable by the antibodies in our ELISA kit. However, gelatin is a very linear molecule that has all its amine groups exposed and available for crosslinking, increasing the likelihood that the genipin reacts with the gelatin over the amine groups of TGFβ2, which exhibit a non-linear three dimensional structure and post-translational glycosylation [153]. This hypothesis is also supported by the bioactivity results in Figure 5, where it is observed that the released TGFβ2 either promoted or prevented SMCs proliferation depending on its concentration in the media. This demonstrates that the eluted TGFβ2 maintained its structure as evident by its ability to influence SMC growth.

Overall, the behavior of SMCs exposed to eluted TGFβ2 are consistent with the behavior of SMCs exposed to exogenous TGFβ2 in media (Figure 4). Additionally, our previous work demonstrates similar SMC behavior, in which different concentrations of exogenous TGFβ2 were added to PAOSMCs growing on electrospun gelatin:fibrinogen flat sheets, where cell migration, proliferation and collagen production on the flat scaffolds were differentially modulated by TGFβ2 [78]. Furthermore, our *in vitro* experiments of SMCs growing on 80G:20PCL scaffolds with and without TGFβ2 showed that it is possible to obtain higher cell numbers and improved migration from TGFβ2-eluting constructs loaded with 13 ng TGFβ2/mg of scaffold. After 5 days of culture, the cells growing on the TGFβ2-eluting scaffolds were more evenly distributed throughout the construct. These results confirmed both qualitatively and quantitatively the bioactivity of the TGFβ2 released from our TEVG.

The exposure of TGFβ2 to a liquid genipin solution is a potential limitation of our approach. To overcome the low recovery of TGFβ2, further experiments with different drug-loading methods will be necessary to further explore this issue. One possibility could be to incorporate TGFβ2 by adsorption after the crosslinking of the scaffolds, which would limit TGFβ2

exposure to the fluid and to the crosslinker. However, this may result in an initial burst release from the fiber surface [138]. Another alternative would be to covalently immobilize TGFβ2 to already crosslinked fibers which could reduce the initial burst release. However, this may cause the loss of bioactivity, since the immobilization can change the conformation of the growth factor. Another alternative is to encapsulate TGFβ2 into biodegradable microspheres that would be further incorporated into the polymeric blend before electrospinning. With this method the TGFβ2 would be protected from the crosslinker, and the release would mainly depend on the degradation of the microspheres and not the degradation of the scaffolds. Therefore, it may be important to choose encapsulating materials with similar degradation rates to the currently studied electrospun fibers. It is important to note that any inclusion of particles to electrospun fibers could have implications over the electrospinning process and consequently, affect the mechanical properties of the scaffold. In our laboratory, we have studied and modulated the mechanical properties of electrospun gelatin to create tubular scaffold compliance matched with a porcine coronary artery [154]. To obtain similar biomechanical properties to the biological sample it is necessary to include a synthetic biopolymer in our scaffold and also to use gelatin crosslinking agents to both preserve the three-dimensional structure of the electrospun fibers and give them enough strength to be used as a deliverable TEVG [154]

Another limitation of this work is that we have only evaluated TGFβ2 release *in vitro*. We expect a faster degradation of our constructs *in vivo* due to the presence and effect of macrophages and other immune cells. This may contribute to an accelerated TGFβ2 release from the implanted construct. However, we are also expecting a decrease in the local concentration of the growth factor due to hemodynamic and interstitial flow increasing washout from the scaffold.

Further *in vivo* experiments will be required using TGFβ2 eluting-scaffolds to evaluate the effect of the released TGFβ2 on scaffold cell infiltration, growth, and remodeling.

Our future work will focus on continuing to design a TGFβ2-eluting electrospun scaffold that can release low amounts of TGFβ2 initially to increase SMC proliferation and migration through the scaffold. The scaffolds will be designed to subsequently provide a late release of higher amounts of TGFβ2, thus reducing SMC proliferation and migration while also promoting collagen production as the TEVG degrades. In this study we have evaluated the effect of TGFβ2 on SMC migration and proliferation from TGFβ2-loaded constructs. However, we recognize that it is important to gain knowledge on how SMC phenotype is affected by a TGFβ stimulus. Further *in vitro* studies will investigate the expression levels of proliferative and contractile markers of SMC stimulated with different concentrations of TGFβ2.

3.5   CONCLUSIONS

To the best of my knowledge this is the first study investigating a release system to modulate SMC growth and infiltration in TEVGs using TGFβ2. SMCs are essential for the formation of a vascular media that can modulate vascular tone and ECM remodeling, making the control of SMC recruitment, infiltration, and proliferation an important aspect of a TEVG development. Here, we demonstrated the fabrication of gelatin/PCL hybrid biodegradable scaffolds with the ability of releasing bioactive TGFβ2. This releasecan be tuned using the degradation properties of natural and synthetic polymers in a blend allowing control of SMC growth and infiltration of our TGFβ2-releasing conduits, thus making these scaffolds attractive for vascular tissue engineering applications.

4.0 <u>CHAPTER 4</u>: SPECIFIC AIM 3

ENDOTHELIALIZATION STUDIES

In this aim, human umbilical cord blood derived endothelial cells (hCB-ECs) were used to seed surface modified planar electrospun scaffolds. The important characteristics of a healthy endothelium were evaluated under static conditions using human umbilical vein endothelial cells (HUVECs) as a positive control. We found that scaffolds composed of polycaprolactone/gelatin/fibrinogen, that were surface modified by a thermoforming process and coated with ECM proteins, are the most suitable for endothelial cell growth. hCB-ECs growing on these scaffolds can proliferate and form a stable monolayer on the surface of the planar scaffold, produce endothelial nitric oxide synthase (eNOS), respond to the addition of interleukin 1 beta (IL-1β), and reduce platelet deposition and activation rate. This research evaluates the suitability of a surface modified biomaterial for the endothelialization of a vascular graft as well as the use of hCB-ECs as a cell source for cardiovascular tissue engineering applications

This aim is based on the manuscript "**Ardila D. C.,** Maestas D., Liou J, Slepian M., Badowski M., Harris D., Vande Geest J.P. In-Vitro Characterization of Human Cord Blood-derived Endothelial Cells for Vascular Tissue Engineering Applications", submitted to the Journal of Clinical Medicine, Special Issue: Biobanking and Regenerative Medicine on September 5, 2018.

4.1   INTRODUCTION

Surface modification of biomaterials is a popular method for increasing the biocompatibility of a polymeric scaffold. In tissue engineering it is known that the chemical and physical architecture of the scaffold surface is the principal characteristic responsible for the attachment, viability, and biological response of cells in the biomaterial. Some of the most common surface modification techniques include heparinization, plasma treatment, alkaline or acid hydrolysis, and coating with ECM proteins among others [155].

For a TEVG to be successful it needs to have the ability to promote the formation of a healthy endothelial cell monolayer in the inner lumen of the graft [156]. Endothelial cells play a wide variety of critical roles in the control of vascular function. They participate in all aspects of the vascular homeostasis, but additionally are critical in physiological or pathological processes like regulation of vascular tone, inflammation, and prevention of both thrombosis and intimal hyperplasia [32, 33, 54]. Therefore, a correct establishment of a healthy endothelium is crucial for the long term success of a TEVG [156]. Some studies have reported the application of polycaprolactone (PCL) scaffolds for the fabrication of TEVGs [143, 157, 158]. Previously we found that the incorporation of both gelatin and fibrinogen enhances the compliance which is very critical for vascular grafts [159].

In recent years human umbilical cord blood derived endothelial cells (hCB-ECs) have been garnering more attention for tissue engineering applications, due to their highly proliferative capacity *in vitro* [160]. Different studies have shown that endothelial cells derived from human umbilical cord blood develop a homogeneous population and can be passaged 50–60 times before senescence, or the loss of their differentiated endothelial cell phenotype [160, 161]. These studies compared the protein profile of hCB-ECs with human umbilical vein endothelial cells (HUVECs),

concluding that hCB-ECs display a higher proliferative capacity, higher sensitivity to angiogenic factors, and a differentiated production of the anti-oxidant enzyme manganese superoxide dismutase, which makes hCB-ECs more tolerant to oxidative stress than HUVECs [160, 162-167].

However, whether the combination of gelatin, fibrinogen, and polycaprolactone can provide a better environment for hCB-EC cell growth is unclear. In this study, gelatin/fibrinogen and gelatin/fibrinogen/polycaprolactone scaffolds were electrospun and surface modified through a thermoforming process and coating with a blend of collagen IV and fibronectin. hCB-ECs were tested for their ability to proliferate and remain on the surface of the scaffold in the formation of a monolayer. We also assessed whether the attached cells could function as a mature endothelium. In order to quantify this, we focused on important characteristics of mature and healthy endothelium, including the response to pro-inflammatory cytokine interleukin 1 beta (IL-1β), the production of endothelial nitric oxide synthase (eNOS), and antithrombotic capacities compared to HUVEC as a positive control.

4.2 MATERIALS AND METHODS

4.2.1 Cell isolation and characterization

HUVECs were purchased from ATCC as a positive control (ATCC, Manassas, VA). Cell culture was per manufacturer's instructions. hCB-ECs were isolated and identified by our group as follows: de-identified umbilical cord blood (UCB) was obtained from the University of Arizona Biorepository per protocols approved by the University of Arizona's Institutional Review Board (IRB). After collection, the isolation and differentiation procedures followed those described by

Javed et al., 2008 [168], with minor modifications. Briefly, UCB (20-100ml) was diluted 1:1 with Hank's balanced salt solution, and then overlaid onto an equivalent volume of Histopaque 1077 (Sigma Aldrich, USA). To isolate mononuclear cells (MNCs), the diluted UCB was centrifuged for 30 minutes at room temperature at 740 xg. The isolated MNCs were washed and re-suspended in 12 mL complete EGM-2 plus medium (Lonza, USA), supplemented with 15% FBS. The cells were seeded onto 6-well plates pre-coated with rat tail collagen I (Life Technologies, USA) and maintained in a humidified environment at 37°C and 5% CO_2. Medium was changed daily for the first 7 days and then every other day until the first passage. Colonies of endothelial cells appeared between 5 and 22 days of culture. Cell identity was confirmed by flow cytometry and immunocytochemistry (ICC) as previously described [169] using mouse anti-human primary conjugated monoclonal antibodies purchased from BD Biociences, USA. For flow cytometry, fluorescein isothiocyanate (FITC) conjugated antibodies, allophycocyanin (APC) conjugated antibodies, and phycoerythrin (PE) conjugated antibodies were used to target CD31, CD105, and CD45 respectively. Fluorescence intensity per cell produced by the bound antibodies was measured, and cells were counted using the LSRII flow cytometer (BD Biosciences, USA). For each ICC and flow cytometry experiments, 10,000-30,000 cells were used, which were gated from a population of 500,000 cells. For the ICC, cells were cultured on glass coverslips coated with rat tail collagen I and the immunostaining was performed using the aforementioned FITC conjugated CD31 antibodies. Cell nuclei were counterstained using VECTSHIELD® mounting media containing 4',6-diamidino-2-phenylindole (DAPI) from Vector Laboratories, USA. Additionally, the cells were qualitative characterized by their ability of aligning with flow. For this purpose, cells glass slides were coated with rat tail collagen I and HUVEC and hBC-ECs were seeded at a concentration of 1 million cells per slide. Once a monolayer was acquired, the slides were imaged

in a phase contrast inverted microscope to get time point 0 h (no flow). Then the slides were punt in a flow chamber (Appendix 0) at a shear stress of 25 dyne/cm^2 and imaged once more at 24h and 48h. For all experiments performed, cells from passages 2-6 were used.

4.2.2 Scaffold fabrication and scaffold characterization

Flat sheet scaffolds were fabricated by electrospinning. Gelatin extracted from porcine skin and fraction I bovine fibrinogen (Sigma-Aldrich, St. Louis, MO) were mixed at a ratio of 80% gelatin-20% fibrinogen w/w (thereafter **GF**) [78, 86, 159]. A second polymeric blend consisting of 50% polycaprolactone, (PCL, 80,000 MW; Sigma-Aldrich, St. Louis, MO), 40% gelatin, and 10% fibrinogen in mass was created (thereafter **PCL-GF**). The polymeric blends were dissolved in 1,1,1,3,3,3-Hexafluoro-2-propanol (Sigma-Aldrich, St. Louis, MO) to create a 10% w/v solution under constant stirring. The solutions were loaded into a 5 ml BD syringe with a 23-gauge stainless steel dispensing blunt tip needle attached (CML Supply, Lexington, KY). The syringe was then loaded into a NE-1000 single syringe pump (New Era Pump Systems Inc, Farmingdale, NY) set to a pumping rate of 30 μl/min. The distance from the needle tip to the target was 8 cm. The polymeric solutions were electrospun with an applied voltage of 15 kV, onto glass coverslips attached to a metallic target to create fine fibers. The resulting flat sheets were crosslinked in 25% glutaraldehyde (Sigma-Aldrich, St. Louis, MO) in vapor phase for 24 hours. The glutaraldehyde was then removed in a convection oven overnight at 42°C which is a temperature below the denaturation point of gelatin and fibrinogen. Additionally, the scaffolds were rinsed with deionized water to remove any crosslinker residues and uncrosslinked gelatin [78]. This method of removing glutaraldehyde was previously used by our group demonstrated no cytotoxicity of the crosslinked scaffolds for the proliferation of smooth muscle cells [78]. After crosslinking, the scaffolds were

thermoformed by a technique previously used by our group, with the aim of reducing the surface roughness [170]. The scaffolds were immersed in a water bath at 45°C for 2 minutes, and quickly placed in between 2 glass slides. A pressure of approximately 45 mmHg [171] was constantly applied using a 25 mm wide binder clip while the scaffolds were immersed once more in the 45°C water bath for 5 minutes. The scaffolds were equilibrated at room temperature for 10 minutes before the pressure was released. The scaffolds were then designated as thermoformed.

GF and PCL-GF scaffolds, both non-treated and thermoformed were imaged using atomic force microscopy (AFM). All AFM data was collected with a Cypher (Asylum Research and Oxford Instruments company, Santa Barbara, CA) using AC Topography mode in air. The probes used were NSC15 tapping mode probes (Mikromasch, Watsonville, CA). For each scaffold treatment, 3 samples were imaged in 4 random areas of 25 μm^2, and roughness values (Ra) were calculated and averaged after applying a first order flatten on all surfaces using Asylum Research software version 14.13.134. Fiber diameter was calculated for each scaffold treatment measuring thirty random fibers among three different AFM images using ImageJ

4.2.3   Selection of surface modification

Thermoformed and non-thermoformed scaffolds were sterilized with 70% ethanol solution for 1 hour, rinsed 3 times with sterile 1X PBS and then placed under UV light (254 nm) for 1 hour. The sterile scaffolds were then pipette coated with a solution 1:1 of collagen IV and fibronectin in HBSS with a final concentration of 5 µg/ml for 24 hours at 4°C. This coating was selected as explained in (Appendix A.3) The coating solution was carefully rinsed with sterile 1X PBS. hCB-ECs and HUVECs were seeded at $1x10^4$ cells/scaffold and cultured for 7 days.

The culture medium was changed every other day and cultures were maintained in a humidified environment at 37°C and 5% CO_2. For cell imaging, the sheets were fixed with a solution of 2% formaldehyde and Alexa Fluor® 568 phalloidin (Life Technologies, Carlsbad, CA) to visualize f-actin following the manufacturer's instructions. To stain the nuclei, the scaffolds were treated for 24 hours with VECTASHIELD® mounting medium with DAPI (Vector Laboratories, Burlingame, CA). The Advanced Intravital Microscope (AIM) for multiphoton imaging at the University of Arizona's BIO5 Institute was used to observe scaffold coverage, cell morphology, and total cell migration through the scaffold depth [89, 90]. An Olympus XLUMPLFL 20x water immersion objective with a numerical aperture of 0.9 was used. Signal was collected over a 400 x 400 μm field of view at 5 μm step along the scaffold thickness, imaging through the flat sheet to a depth of approximately 100 μm. The nuclei, fibers, and f-actin were imaged simultaneously and colocalized using three different photomultiplier tubes (PMTs). The laser was centered at λ=780 nm to excite simultaneously DAPI, the autofluorescence signal from the scaffolds (NADH), and Alexa Fluor® 568. In the first PMT, DAPI signal was split with a 505 nm dichroic mirror and collected through a 460/80 bandpass filter. In the second PMT, signal from the scaffolds was split with a 568 nm dichroic mirror and collected through a 525/50 bandpass filter. Alexa Fluor® 568 signal was acquired in the third PMT by splitting the signal with a 568 nm dichroic mirror and collecting using a 607/70 bandpass filter. The colocalized image stacks from the cell nuclei, the fibers, and f-actin were merged to visualize the cell location in the flat sheet. Maximum intensity projections (MIPs) were produced to calculate the cell coverage by color-based thresholding using ImageJ. Infiltration was calculated as the percentage of cell migration through the flat sheet (from the surface to the bottom) relative to the flat sheet thickness

4.2.4 Cell growth and cell proliferation

All experiments performed to evaluate cell functionality were carried out using PCL-GF scaffolds that were thermoformed and coated with the Collagen IV/Fibronectin mixture (hereafter labeled as **TC**). Non-treated scaffolds (not thermoformed or coated, hereafter labeled as **NT**) were used as the control. The samples were seeded with hCB-ECs and HUVECs at a cell density of $1x10^4$ cell/scaffold. The culture medium was changed every other day and cultures were maintained in a humidified environment at 37°C and 5% CO_2. For each experiment, separate cultures were used. All experiments had 4 replicates. Cell growth was evaluated after 2 and 7 days in culture. A sample of approximately 25 mm^2 was cut from each construct, and cell number was measured by the MTS assay as explained above.

4.2.5 Platelet activation and platelet adherence

De-identified adult human blood-derived platelet samples were obtained at the University of Arizona Sarver Heart Center in accordance with IRB approved protocols. Briefly, 30 mL of whole blood was drawn through venipuncture into 3 mL of acid citrate dextrose A. Subsequently, the blood was centrifuged at 500 xg for 15 minutes to obtain platelet-rich plasma, which was gel-filtered through a column of Sepharose 2B beads (GE Healthcare Life Sciences, Marlborough, MA) with HEPES-modified Tyrode's buffer to collect gel-filtered platelets. The platelet concentration was then diluted to a count of 20,000 platelets/μL in HEPES-modified Tyrode's buffer, with 3mM $CaCl_2$ added 10 minutes prior to any experiment.

Platelet activity state (PAS) was measured using a modified-prothrombinase assay reported in [172, 173]. Briefly, after 7 days in culture, a sample of 20,000 platelets/μL was perfused onto

the surface of the cell-seeded scaffolds and incubated at 37°C for 0, 1, and 2 hours. After incubation, 100 pM factor Xa, 5 mM calcium, and 200 nM acetylated prothrombin, were added and incubated for 10 minutes. Thrombin generation was quantified through spectrophotometric analysis over 7 minutes at an absorbance wavelength of 405 nm to obtain the PAS values, using Chromozym-TH (Roche, Penzberg, Germany) as the thrombin-specific chromogenic peptide substrate. Relative platelet number was calculated based on the absorbance for thrombin activity. The more platelets present, the higher absorbance detected. The platelets in a control tube were fully activated by sonication. Each PAS value was the platelet number normalized to the platelet number obtained after sonication [173]. The platelet activation rate (PAR) for each experiment was obtained taking the slope of the PAS values over two hours. The experiments had 4 replicates.

After the final time point of the PAS assay, platelet deposition upon each surface was quantified. Samples were prepared for scanning electron microscopy (SEM) following Merkle et al., with minor modifications [173]. Non-adherent platelets were gently washed away with DPBS 1X, and the samples were immediately fixed with a solution composed of 2% formaldehyde and 2% glutaraldehyde in 1X DPBS for a minimum of 4 hours. The samples were then washed 3 times in 25% ethanol for 5 minutes and then dehydrated by serial washes in 50%, 75% and 100% Ethanol performed in 15 min intervals. The samples were then treated with critical point drying in CO_2 using an E3100 Critical Point Dryer (Quorum Technologies LTDA, England). Each sample was then mounted with carbon tape and coated with platinum for 30 seconds in a Hummer 6.2 argon gas sputter system (Anatech LTD, Battle Creek, MI). All samples were imaged using a field emission SEM (Hitachi S-4800) with the working distance and accelerating voltage set to enhance the contrast of adhered platelets against the cell surfaces. Platelet deposition on scaffolds was determined using ImageJ. For each manual count, 10 random 40,000 μm^2 sections of area in 4

samples were selected and averaged to estimate the relative adherence of platelets on each scaffold treatment [173, 174]. Platelets were characterized based on their characteristic size (2.3-4.3μm) and shape [175]. When platelet counts required higher resolution, images of the same sections at higher magnifications were used.

4.2.6 Evaluation of inflammatory response

After 4 days of culture, recombinant human interleukin 1 beta (IL-1β; Life Technologies Carlsbad, CA) was added to each scaffold at a final concentration of 0.5 ng/ml. After 3-day additional culture time [176], the scaffolds were fixed with 2% formaldehyde and a sample of 25 mm^2 was cut and transferred to a 96 well plate. In-cell ELISA was performed using mouse anti intracellular adhesion molecule 1 (ICAM-I; Abcam, Cambridge, United Kingdom) and mouse anti vascular cell adhesion protein (VCAM-I; Abcam) primary monoclonal antibodies. Primary antibodies were conjugated with HRP rabbit anti-mouse polyclonal secondary antibodies (Abcam). 1-step ultra TMB ELISA (Thermo Fisher Scientific, Waltham, MA) was used to detect HRP activity following the manufacturer's instructions. Absorbance was read at 450 nm in a Synergy H1 plate reader (BioTek, Winooski, VT).

4.2.7 Endothelial nitric oxide synthase production

After 7 days in culture, the scaffolds were fixed with 2% formaldehyde and a sample of 25 mm^2 was cut and transferred to a 96 well plate. In-cell enzyme-linked immunosorbent assay (ELISA) was performed using mouse anti-eNOS primary monoclonal antibodies (Abcam). Primary antibodies were conjugated with HRP rabbit anti-mouse polyclonal secondary antibodies

(Abcam). 1-step ultra TMB ELISA (Thermo Fisher Scientific, Waltham, MA) was used to detect HRP activity as described above. The results were normalized by the average cell number found with the MTS assay after 7 days in culture and were compared with the ones obtained using glass micro-coverslips as the cell growing surface.

4.2.8   Statistical analysis

All values are presented as the mean ± standard deviation unless otherwise specified. The statistical analysis was performed using the software package SPSS (IBM, Armonk, NY). For surface roughness, fiber diameter, cell proliferation, and ELISA analyses, the statistical analysis was completed using two-way ANOVA with Tukey's range tests to compare between two cell types and two scaffolds. For nitric oxide synthase production, platelet activity assay, and platelet adherence analyses, one-way ANOVA was performed with a post-hoc analysis using individual two sample two-tailed t tests. Significant difference was determined when the p value <0.05.

4.3   RESULTS

4.3.1   Cell characterization

Figure 22 shows the results of the flow cytometry represented in histograms. The blue histogram characterizes the signal obtained from the cells treated with the antibodies and the gray histogram represents the cells that were not.
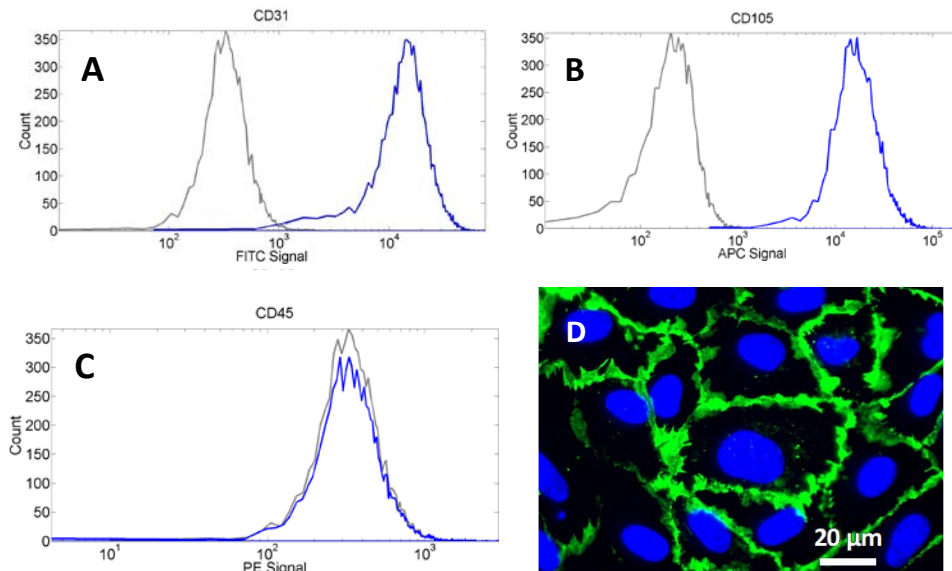
Figure 22 Characterization of hCB-EC monolayers using flow cytometry and immunochemistry. (A-C) hCB-ECs were characterized by flow cytometry of (A) CD31, (B) CD105, and (C) CD45. Results show that hCB-ECs are positive for CD31 and CD105 and negative for CD45. (D) Immunocytochemistry of CD31 shows the expression of CD31 labeled in green in the cell membrane while the cell nuclei are labeled in blue.

A shift in the histogram indicates a relative increase in the average cell fluorescence. Antibodies against CD31 (Figure 22A) and CD105 (Figure 22B) were attached to the cell, confirming the expression of these two endothelial cell-specific markers in our hCB-ECs. In contrast, the blue histogram for the cells treated with the antibodies against CD45 did not shift

(Figure 22C), which can be interpreted as a lack of CD45 expression in the studied cells. These results confirm that hCB-ECs were successfully produced and there is no contamination from the hematopoietic lineage. Additionally, the ICC orroborated the expression of CD31 exclusively in the cell membrane at the cell-cell junctions (Figure 22D).

Figure 23 shows that after 48 h of dynamic culture with a shear stress of 25 dyne/cm^2, hCB-ECs were able to align with the flow direction. This result is comparable with the one obtained for HUVEC.
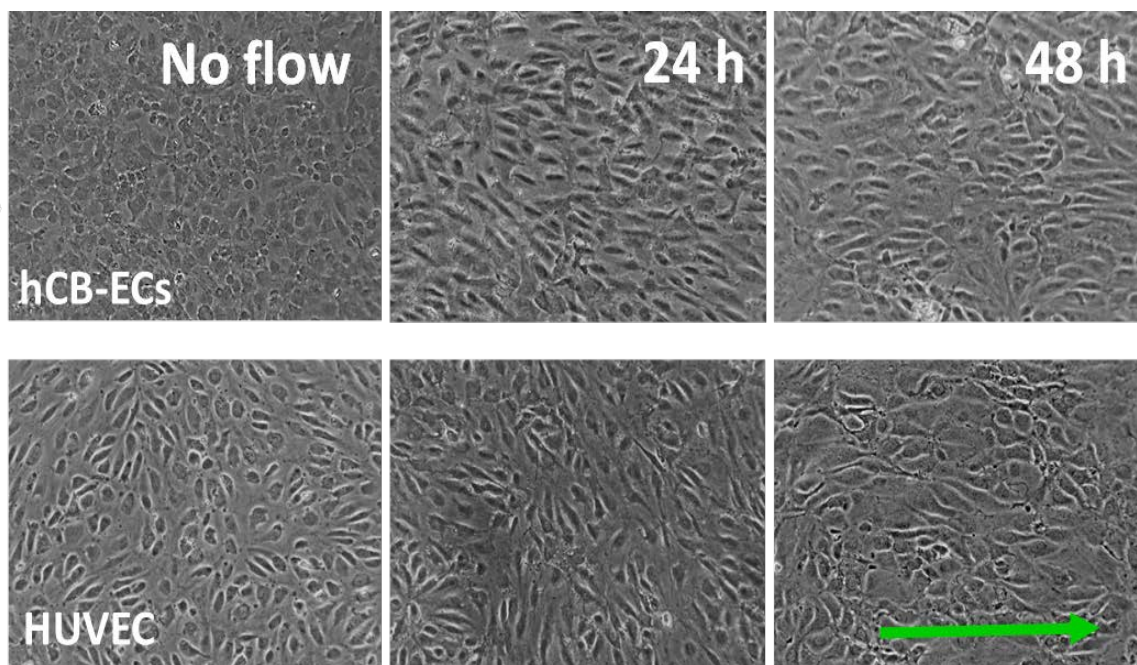
Figure 23 A confluent monolayer of hCB-ECs and HUVEC in glass slides were culture for 48h in a flow chamber with a shear stress of 25 dyne/cm^2 . The green arrow is showing the flow direction. After 48h hCB-ECs and HUVEC to aligned with the flow.

84

4.3.2 Scaffold characterization

AFM was performed in order to study the effect that adding PCL and thermoforming our GF scaffolds had on surface roughness and fiber diameter. Surface roughness is reported as Ra (Figure 24A) which represents the average change in height on the surface with respect to a reference point. In this case the reference points are the glass coverslips which the individual samples were laid on prior to imaging. Out of the 4 different scaffold groups, the thermoformed PCL-GF scaffolds displayed the lowest roughness value (299.30 nm ± 27.53 nm). However, no significant differences were identified among the 4 sample groups.
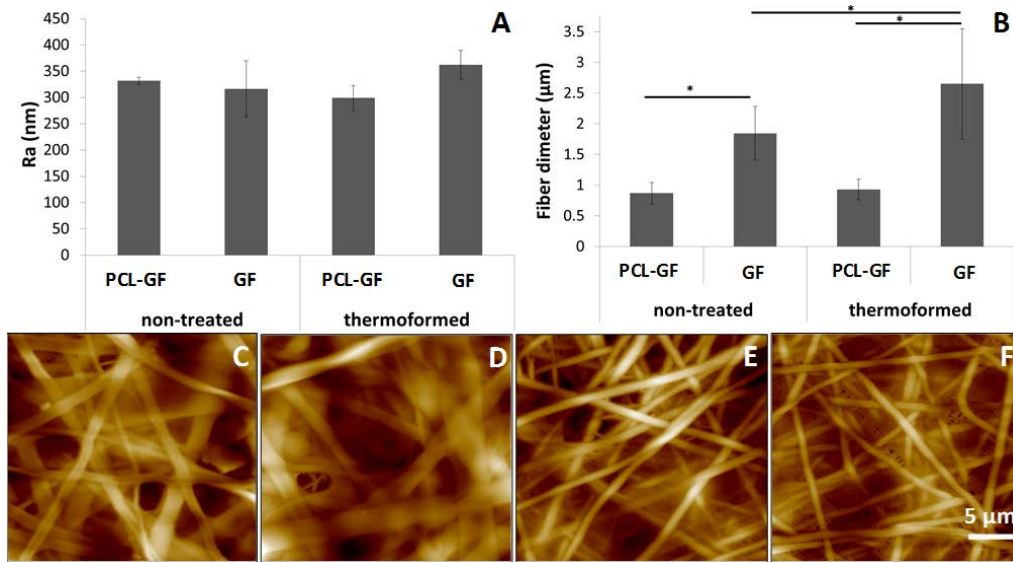
Figure 24 Effect of thermoforming on surface roughness and fiber diameter of polycaprolactone/gelatin/fibrinogen (PCL-GF) and gelatin/fibrinogen (GF) scaffolds. (A) Surface roughness and fiber diameter results obtained by AFM for non-treated or thermoformed scaffolds. Average roughness values (Ra) in nm. No significant difference was detected. (B) Fiber diameter in μm are reported for the four groups. Error bars shown are standard deviations (*p<0.05; n=3). (C-F) Representative AFM images of (C) non-treated GF scaffolds, (D) thermoformed GF scaffolds, (E) non-treated PCL-GF scaffolds, and (F) thermoformed PCL-GF scaffolds.

Fiber diameter was measured from the AFM images, using thirty random fibers among the three images for each scaffold treatment (Figure 24B). In general, GF scaffolds presented significantly larger fibers compared to PCL-GF (1.84 ± 0.43 vs 0.86 ± 0.17, p= 2.31 x 10^{-16} for the non-treated scaffolds and 2.65 ± 0.89 vs 0.92 ± 0.16, p=0.17 for the thermoformed scaffolds). Thermoforming significantly increased the GF fiber diameter (2.65 µm± 0.89 µm vs $1.841.84\pm0.43$, p=0.000045). Figure 24C-E are representative AFM images of the studied scaffolds demonstrating that the addition of PCL (Figure 24E-F) reduces construct fiber size.

4.3.3   Surface modification selection

An arrangement of MIPs from each image stack taken is shown in Figure 25. Cell coverage and scaffold infiltration were calculated from the MIPs and the image stacks, respectively. According to our results, lower percentages of migration were found for the PCL-GF constructs while the highest percentages of coverage were found in the GF samples. Nevertheless, the combined surface modification of thermoforming and coating favor the spread of hCB-ECs on the surface while limiting their migration though the PCL-GF, leading to the lowest ratio of infiltration/coverage. In order to be able to get an infiltration/coverage ratio < 1 it is necessary to strategically orchestrate a combination of PCL-GF scaffolds, thermoforming and coating, and hCB-EC as a cell source.
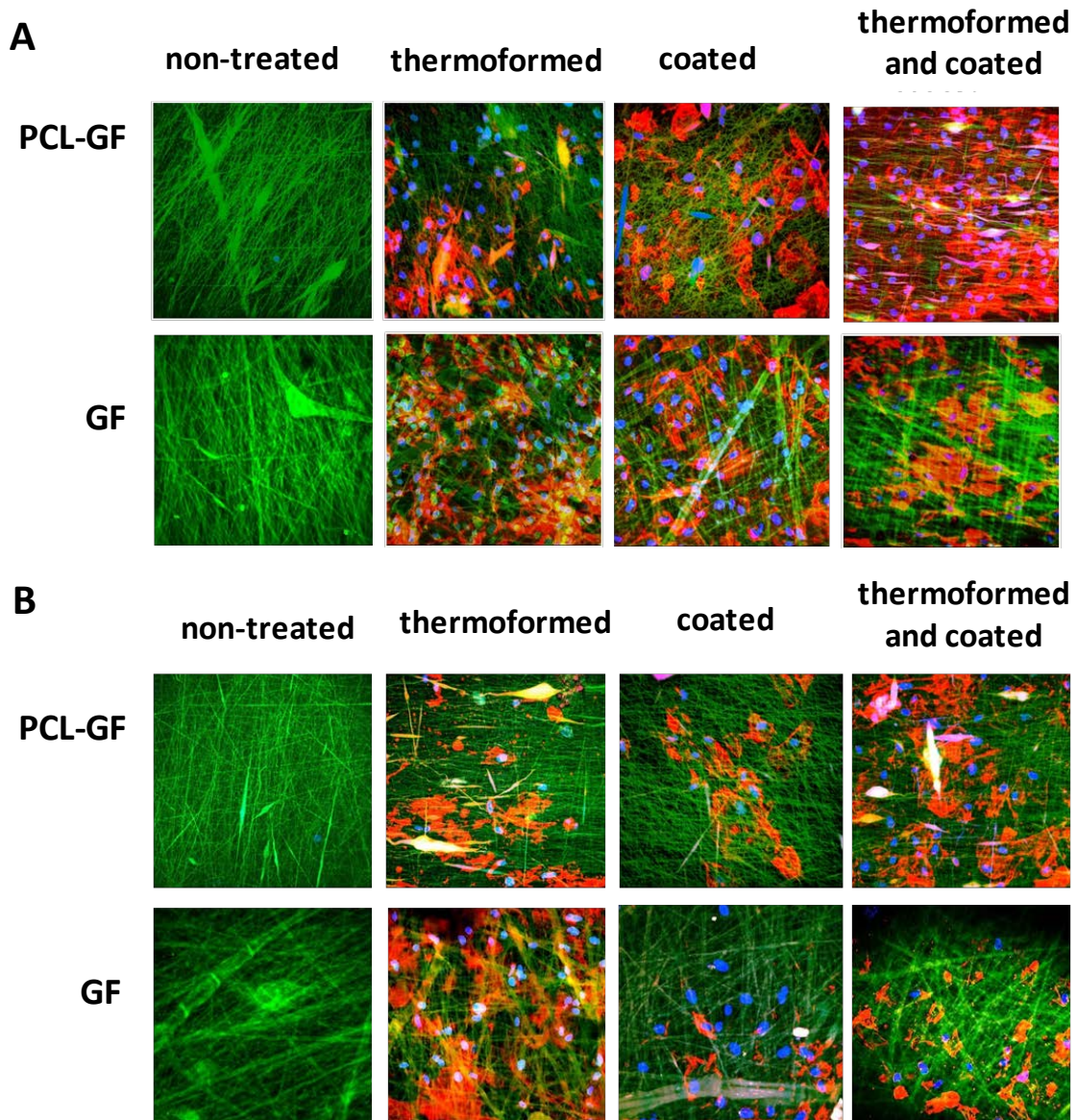
Figure 25 Effect of thermoforming and coating with gelatin and fibronectin on PCL-GF or GF scaffolds. (A) Representative maximum intensity projections of hCB-ECs seeded on PCL-GF or GF scaffolds with four surface modifications (non-treated, thermoformed, coated with collagen IV/fibronectin, or thermoformed and coated). For hCB-ECs, thermoformed and coated PCL-GF scaffolds promote the highest cell attachment. (B) Representative maximum intensity projections of HUVECs seeded on PCL-GF or GF with four surface modifications. The material fibers are shown in green, f-actin in red, and cell nuclei in blue.

4.3.4 Cell growth and proliferation

Cell proliferation results showed that the hCB-ECs and HUVECs have a similar number of cells after 2 days in culture ($7.50 \times 10^3 \pm 7.9 \times 10^2$ vs. $8.03 \times 10^3 \pm 4.89 \times 10^2$). Nevertheless, the cell count at 7 days indicated an increase in cell number for the hCB-ECs ($7.50 \times 10^3 \pm 7.9 \times 10^2$ at 2 days and $1.09 \times 10^4 \pm 4.79 \times 10^3$ at 7 days) and a decrease for HUVECs ($8.03 \times 10^3 \pm 4.89 \times 10^2$ at 2 days compared to $5.40 \times 10^3 \pm 1.18 \times 10^3$ at 7 days). No significant difference was identified between the two cell types at 2 days or 7 days (Figure 26)
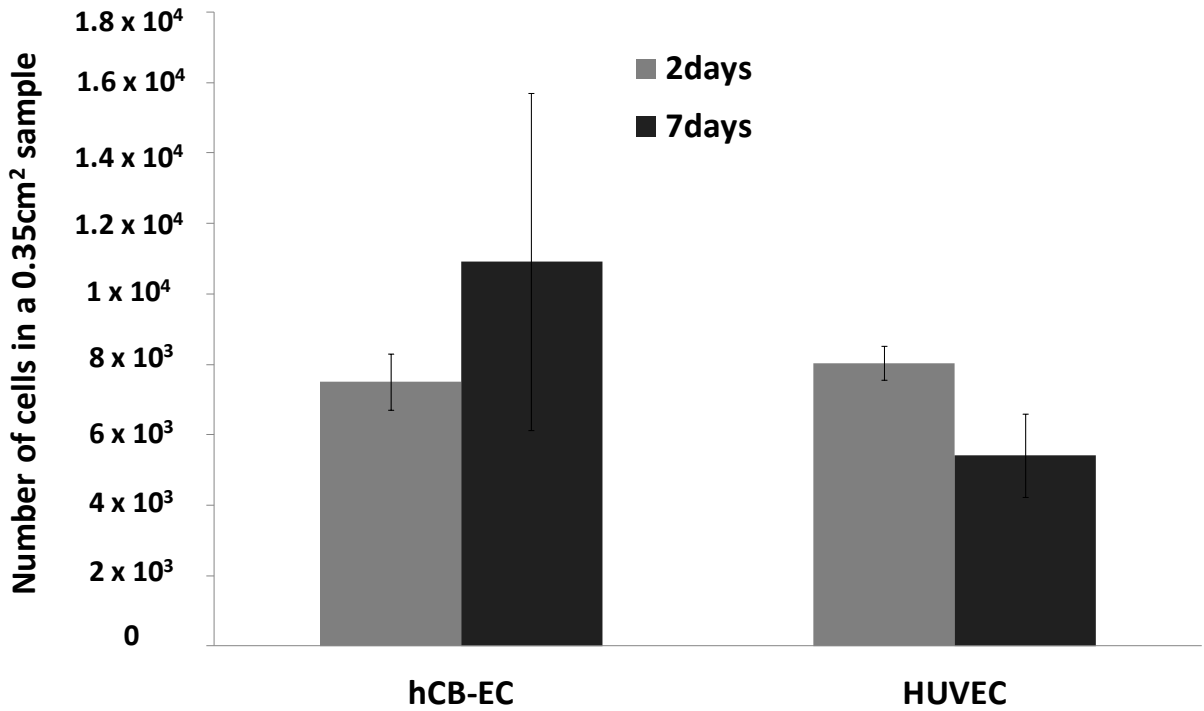
Figure 26 Proliferation results of hCB-ECs and HUVECs after 2 and 7 days post seeding on thermoformed and coated PCL-GF scaffolds. Average cell number in a 25 mm2 sample is reported. Error bars shown are standard deviations (n=4).

4.3.5 Platelet activation and adherence

PAS was calculated for platelets on non-treated and TC PCL-GF scaffolds both seeded with hCB-ECs and HUVECs (Figure 27A). We observed that in the TC samples, regardless of the cell type, PAS values decrease after 1h indicating a possible deactivation of platelets.
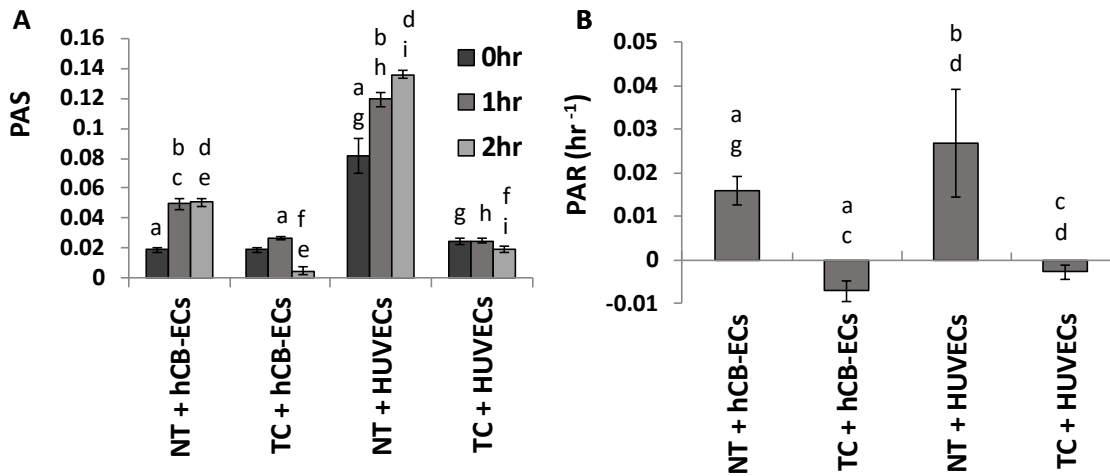
Figure 27 Platelet activation of hCB-EC-seeded or HUVEC-seeded PCL-GF scaffolds. (A) Platelet activation state (PAS) of platelets deposited on hCB-EC-seeded or HUVEC-seeded PCL-GF scaffods thermoformed/coated with Collagen IV/Fibronectin (TC) compared to non-treated (NT) controls at 0, 1, and 2 hours. For bars with the same letter, the difference between the means is statistically different (*p<0.05, n=4). (B) Platelet activation rate (PAR) of platelets was calculated over the 2 hours. For bars with the same letter, the difference between the means is statistically different (*p<0.05, n=4).

On the contrary, in the non-treated scaffolds the PAS values increase over time suggesting a constant activation of platelets. Comparisons were made between treatments within the same cell type, and also between cell types growing in scaffolds with the same treatment. A significant difference in absorbance for thrombin generation was found for the NT and TC scaffolds seeded

with hCB-ECs at 1h (0.049 ± 0.003 nm vs 0.026 ± 0.001 nm, p=0.0002) and 2h (0.05 ± 0.003 nm vs 0.0049 ± 0.002 nm, p=2.03 x 10^{-10}) of platelets-prothrombinase incubation. Also, when comparing the thrombin absorbance results for the NT and TC scaffolds seeded with HUVECs, a significant difference in absorbance was found at 0h (0.081 ± 0.01 nm vs 0.024 ± 0.002 nm, p=0.001), after 1h (0.12 ± 0.04 nm vs 0.024 ± 0.001 nm, p=9.83 x 10^{-7}), and after 2h (0.135 ± 0.03 nm vs 0.019 ± 0.001 nm, p=4.3 x 10^{-10}) of incubation. A significant decrease in thrombin generation was found in the NT scaffolds seeded with hCB-ECs compared to the ones with HUVECs at 0 h (0.018 ± 0.001 nm vs 0.081 ± 0.01 nm, p=0.001), after 1h (0.049 ± 0.003 nm vs 0.024 ± 0.001 nm, p=5.46 x 10^{-7}), and 2h (0.05 ± 0.003 vs 0.135 ± 0.002, p=2.44 x 10^{-9}) of prothrombinase reaction. For the TC scaffolds seeded with hCB-ECs, the thrombin generation by the perfused platelets was significantly lower when comparing to the TC scaffolds seeded with HUVECs after 2h of incubation (0.0049 ± 0.002 nm vs 0.019 ± 0.001 nm, p=4.3 x 10^{-10}). In Figure 27B the PAR is quantified, showing negative values for the platelets seeded on the TC scaffolds indicating again a potential platelet deactivation. Significantly lower PAR was found when hCB-ECs were seeded on the TC as compared to the non-treated samples (-0.006 ± 0.0027 h^{-1} vs 0.0159 ± 0.003 h^{-1}, p=0.0019). The same trend was found for HUVECs (-0.002 ± 0.0016 h^{-1} vs. 0.026 ± 0.012 h^{-1}; p=0.00031).

Platelet count results are presented in Figure 28, where a significant reduction was found in the number of platelets adhered to both non-treated (186.9 ± 56.39 vs 242.5 ± 39.22 p=0.025) and TC (65.77 ± 5.51 vs 65.77 ± 5.51 p=0.0033) scaffold surfaces when hCB-ECs were pre-seeded. When assessing the differences between scaffold types, the TC had a significantly lower

number of platelets deposited as compared to the non-treated with either hCB-ECs (55.4 ± 7.31 vs. 186.9 ± 56.39; p=0.000017) or HUVECs (65.77 ± 5.51 vs. 242.5 ± 39.22; p=8.4x10^{-11}). In Figure 28B and Figure 28C, representative SEM images of hCB-EC seeded scaffolds are shown for non-treated and TC samples, respectively. The black arrows indicate single platelets while the white arrows designate aggregated platelets. It is important to note that in the non-treated scaffolds there are some open areas where the cells failed to make tight junctions and several platelets aggregated. In the TC samples, hCB-ECs were able to cover the entire scaffold surface with very tight cell-to-cell junctions and consequently less platelets adhered and aggregated. Figure 28D and
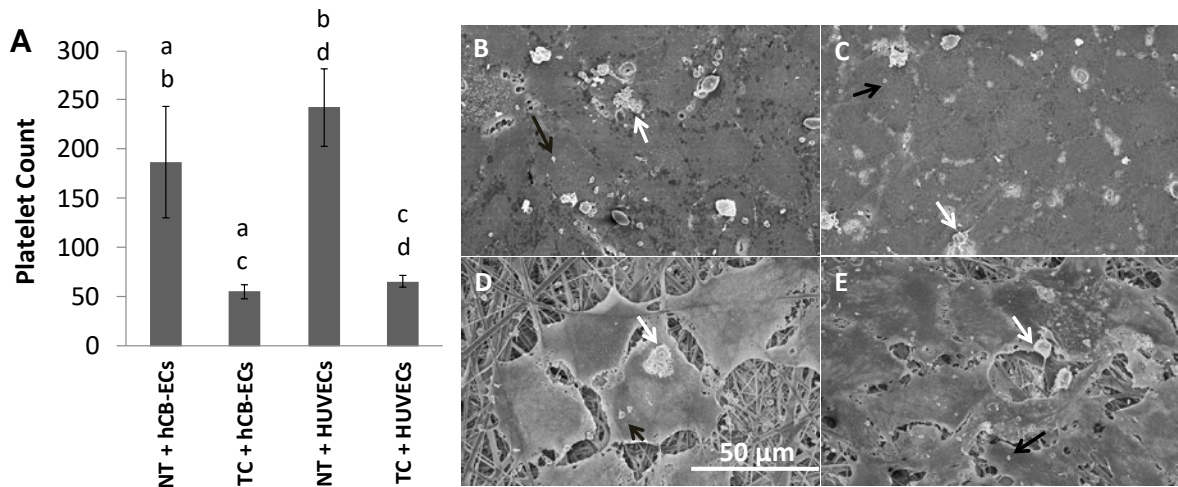
Figure 28 Assessment of platelet adherence of hCB-ECs and HUVECs cultured on thermoformed and coated (TC) compared to non-treated (NT) PCL-GF scaffolds. (A) Platelet adherence results for PCL-GF thermoformed/coated (TC) and non-treated (NT) scaffolds, pre-seeded with either hCB-ECs or HUVECs. Average platelet count is reported. For bars with the same letter, the difference between the means is statistically different (*p<0.05, n=4). (B-E) Representative SEM images of the platelets adhered to (B) hCB-ECs cultured on non-treated scaffolds, (C) hCB-ECs cultured on thermoformed/coated scaffolds, (D) HUVECs cultured on non-treated scaffolds, and (E) HUVECs cultured on thermoformed/coated scaffolds. Black arrows are pointing to single platelets, and white arrows to aggregated platelets.

Figure 28E show the NT and TC scaffolds, respectively, seeded with HUVECs. It can be clearly observed from these images that these cells were not able to cover the entire surface of the scaffold, which is made evident by the presence of material fibers where many platelets are deposited. However, in the TC scaffolds, more HUVECs were attached which reduced the platelet count.

4.3.6 Inflammatory response and eNOS production

For the hCB-ECs and HUVECs seeded onto TC PCL-GF scaffolds the addition of IL-1β to the cultures increased the absorbance at 450 nm. An increase in absorbance is directly related to the expression of inflammation associated proteins VCAM-1 and ICAM-1 (Figure 29). All absorbance values were normalized by the average number of cells calculated after 7 days growing in the aforementioned scaffolds. A significant decrease in the VCAM-1 production was found comparing hCB-ECs to HUVECs after the injection of IL-1β (1.47 ± 0.17 vs. 2.34 ± 0.17; p=0.00058). The expression of ICAM-1 is also significantly lower in hCB-EC as compared to HUVEC seeded scaffolds before (0.65 ± 0.11 vs. 1.01 ± 0.089; p=0.0015) and after (0.86 ± 0.07 vs. 1.56 ± 0.19; p=0.00067) IL-1β stimulation. The absorbance at 450 nm as a result of eNOS production per number of cells in static conditions was also found to be significantly lower in hCB-ECs as compared to HUVECs (0.64 ± 0.18 vs 1.18 ± 0.24; p=0.00016) when the cells are grown on TC PCL-GF scaffolds. The production of eNOS by hCB-ECs growing in the scaffolds

is significantly lower as compared to their eNOS production when these cells are seeded in glass coverslips (1.66 ± 0.47 vs. 1.28 ± 0.26; p=0.00027).
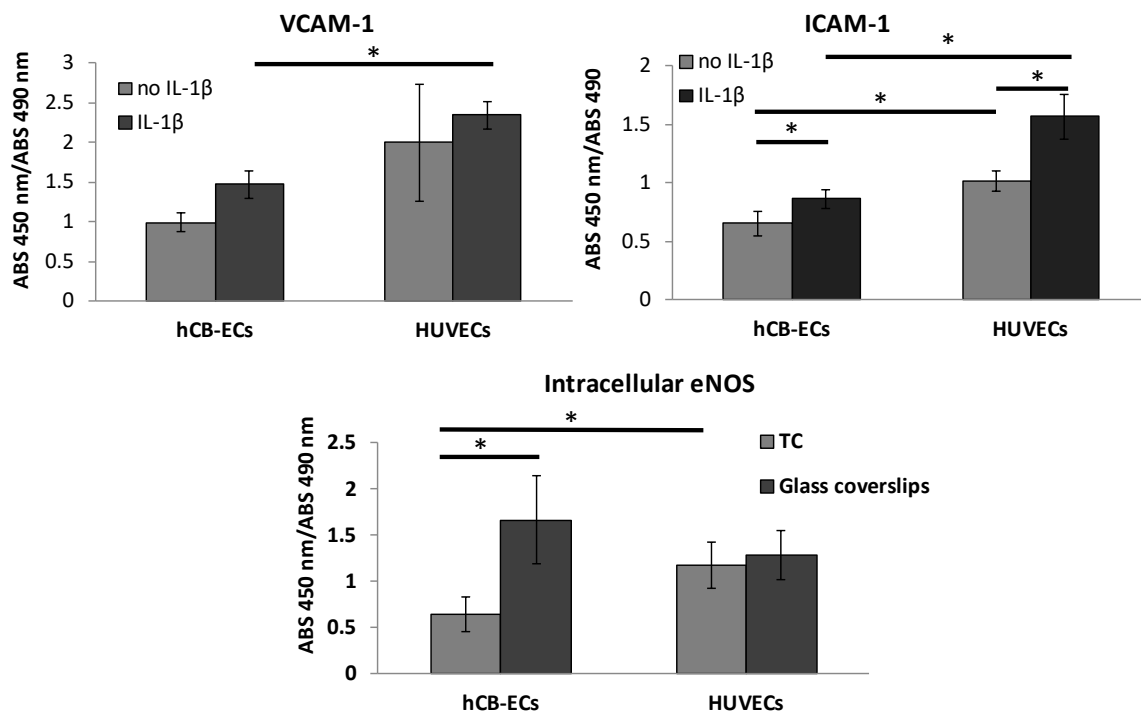
Figure 29 Evaluation of inflammatory response of hCB-ECs and HUVECs cultured on thermoformed and coated PCL-GF scaffolds. In-cell ELISA results for the intracellular expression of VCAM-1, ICAM-I, and eNOS in hCB-ECs and HUVECs growing in thermoformed/coated (TC) PCL-GF. VCAM-1 and ICAM-I levels were evaluated before and after the addition of 0.5ng/ml of IL-1β. As a baseline, eNOS production was evaluated when the cells were cultured on glass coverslips. Average absorbance of eNOS ELISA was normalized to the absorbance of MTS assay (*p<0.05; n=4).

4.4   DISCUSSION

With this Aim I have demonstrated the possibility of isolating mononuclear cells from human umbilical cord blood, and successfully differentiate them into endothelial cells. In this work, I have also demonstrated the ability of culturing derived hCB-ECs on electrospun scaffolds

while maintaining endothelial cell phenotype. The data suggest that scaffolds composed of polycaprolactone/gelatin/fibrinogen that have been surface treated by thermoforming and coated with a mixture 1:1 collagen IV to fibronectin will promote the formation of a functional endothelium. In these scaffolds, cell growth is encouraged but through thickness cell infiltration is limited, resulting in a monolayer of endothelial cells mimicking the tunica intima. According to these results, hCB-ECs seem to proliferate more robustly on our surface modified scaffolds than HUVEC, and the maintenance of the endothelial cell function of both hCB-ECs and HUVEC is comparable. hCB-ECs seeded on the constructs upregulated the adhesion molecules ICAM-1 and VCAM-1 when stimulated with the pro-inflammatory cytokine IL-1β. Our hCB-ECs also displayed the ability to produce the vaso-regulatory and hemocompatibility related enzyme eNOS and also reduce platelet adhesion and activation.

Different efforts have been made for the endothelialization of small diameter vascular grafts, and many of them have used surface modified scaffolds fabricated with synthetic polymers which have excellent biomechanical properties but have shown low biocompatibility [4, 177-185]. The surface modifications of these synthetic polymer scaffolds have been necessary to reduce the hydrophobicity of the material and therefore increase biocompatibility. Immobilization of peptide ligands onto these grafts is one of the most popular techniques for improving biocompatibility and the endothelial cell adhesion to biomaterials. Peptide sequences such as RGD, GRGDSP, and DGEA have been widely used since they have the ability to interact directly with endothelial cell receptors, increasing their attachment [186].

In this work, it is demonstrated that a construct made of a blend of synthetic and natural polymers such as PCL, gelatin, and fibrinogen improves hCB-ECs growth following thermoforming and coating with a mixture of collagen IV and fibronectin. This unique, hybrid

biomaterial possesses the RGD peptide from gelatin [187, 188], fibrinogen [189] and fibronectin [190], GRGDSP from fibronectin [191], DGEA from gelatin [192], and FYFDLR from collagen IV [193]; all of them important peptides recognized by integrins in the endothelial cell membrane [193-196]. Furthermore, the inclusion of PCL to the polymeric blend reduced the fiber diameter which seems to promote cell attachment [197] and endothelial cell proliferation [198]. The thermoforming process was initially used with the aim of smoothing the surface of the electrospun scaffolds. Surprisingly, in this study, thermoforming did not significantly alter the surface roughness but did improve hCB-EC confluency and decrease cell migration in the radial direction, both of which favor the development of an endothelial cell monolayer. We hypothesize that the pressure applied to the scaffolds by thermoforming may lead to the production of a more compact fiber arrangement that aids with the retention of coating proteins facilitating better hCB-ECs attachment and growth. Future work will be needed to extract the mechanisms by which this process is governed.

The principal goal of this aim is not only to promote the attachment and growth of hCB-ECs to our electrospun scaffolds but also to assess whether the attached cells can function as a mature endothelium. For this purpose, three important functions of a healthy endothelium under static conditions were evaluated: the inflammatory response to a pro-inflammatory stimulus, the production of eNOS (enzyme directly related with nitric oxide generation), and the antithrombotic function. The inflammatory response was also investigated by exposing the hCB-ECs and HUVECs seeded in the studied scaffolds to the pro-inflammatory cytokine IL-1β and by assessing the production of VCAM-1 and ICAM-1. The results show that in both cell types VCAM-1 and ICAM-1 were upregulated, demonstrating a positive response to IL-1β as occurring in the healthy vasculature [199-202]. Interestingly, hCB-ECs intrinsically have a lower production of the

VCAM-1 and ICAM-1 which correlates to reduced recruitment of leucocytes and macrophages and the further probability of graft IH and atherosclerosis [203, 204]. In endothelial cells, eNOS is responsible for endothelium-derived NO production. *In vivo*, the predominant physiological stimulus for eNOS active phosphorylation and subsequent NO segregation is wall shear stress [205-207]. However, it has been demonstrated that eNOS is produced in less quantities in endothelial cells cultured in static flow conditions [205, 208, 209]. In this study, we measured intracellular eNOS production of hCB-ECs and HUVECs seeded in the studied constructs, as an indicator of correct EC functionality and it was compared with eNOS production when the cells are growing in glass coverslips as a basal control. According to these findings, both cell types expressed eNOS in static conditions in both the thermoformed/coated PCL-GF scaffolds and the glass coverslips, indicating that their endothelial cell phenotype is preserved. eNOS production in hCB-ECs is lower than the amount produced by HUVEC in both growing surfaces. These results are similar to that obtained by Brown et al. 2009, where the authors found that the hCB-ECs produced significantly fewer amounts of eNOS than aortic ECs in static and dynamic conditions [165]. Similar to other studies, the eNOS production may increase in hCB-EC-seeded constructs under flow conditions [165, 210].

Antithrombotic function was also assessed by evaluating platelet activation and deposition when in contact with either non-treated or thermoformed/coated PCL-GF scaffolds, pre-seeded with hCB-ECs or HUVECs. Figure 27A shows the results of the platelet activation state (PAS) assay where the PAS values represent the amount of acetylated thrombin formed by the platelets in contact with the studied samples [173]. Overall the PAS values over the course of 2 hours are lower for the TC constructs showing a deactivation after the first hour. It is known that platelets are deactivated by molecules secreted by the endothelium such as NO, PGI_2 and prostaglandin D

[211], and also that under normal conditions the coagulation cascade is self-regulated. Furthermore, molecules secreted by platelets and involved in further platelet activation, such as platelet activating factor, thrombin, and tumor necrosis factor-α (TNF-α), trigger the production of NO by the endothelial monolayer resulting in a negative feedback system which deactivates platelets [212-214]. This result becomes more evident in the calculation of the platelet activation rate (PAR). The PAR is calculated by taking the slope of the individual PAS values over the course of 2 hours and represents the overall rate of change of platelet activation [173]. In our work TC samples seeded with hCB-ECs produced the largest negative PAR values suggesting the highest amount of platelet deactivation. Positive PAR values represent an activation of platelets over time and the highest PAR values were found with the non-treated scaffolds seeded with HUVECs. The PAS and PAR results correlated with the number of platelets deposited in the scaffolds. It is possible to observe that there is a significantly lower number of platelets adhered to cell seeded TC scaffolds because of the development of a confluent monolayer. Even though the HUVECs formed a monolayer upon the TC samples, their cell-cell junctions were not as tight as the hCB-ECs which exposed material fibers and thus promoted platelet adhesion. In the non-treated constructs, the cells failed to cover the scaffold, leading to large areas where the material fibers were exposed and the rapid deposition of platelets. According to our findings, there is a clear inverse relationship between endothelial cell coverage and platelet activation and deposition on the surface. The PAR values and the platelet counts are higher in the scaffolds where the cells are not confluent and the material is uncovered. Previous studies have shown that endothelial progenitor cells (EPCs) such and hCB-ECs are able to inhibit the attachment and activation of platelets *in vitro* [215, 216].

Moreover, our results are also similar to the obtained by Brown et al, 2010 demonstrated that hCB-ECs have superior adhesion and proliferation to vessel derived cells such as human aortic endothelial cells (HAECs), and thus were able to reduce the platelet adhesion and prevented thrombosis in a vein graft [166].

One limitation of our study is that all the experiments were completed in static conditions. Although *in vitro* endothelialization studies of electrospun scaffolds are primarily made under zero flow [174, 217-219], we recognize the importance of testing endothelial cells under physiological shear stress, understanding that shear stress is the primary mechanical stimuli that lea to different cell function [220]. For example, one of the most important functions of endothelial cells in the vasculature is to produce NO, a potent vasodilator and anti-inflammatory mediator [221]. It is well reported that shear stress stimulates eNOS production, eNOS phosphorylation, and therefore NO synthesis [222-226]. Therefore, to be able to make further conclusions about the preservation of endothelial cell phenotype of hCB-ECs seeded in our thermoformed and coated PCL-GF scaffolds, future studies will focus on elucidating growth and functionality under physiological shear stress. Future pulsatile flow experiments will need to be performed both in a parallel plate flow chamber (for planar scaffolds) and in custom tubular bioreactors. Another limitation in our study is that all scaffolds reported were flat sheets rather than tubular constructs. One of our ongoing studies is to assess the hCB-EC cell growth in PCL-GF tubular constructs with and without fluid flow.

4.5   CONCLUSIONS

hCB-ECs grown on scaffolds composed of polycaprolactone, gelatin, and fibrinogen that are thermoformed and coated with collagen IV and fibronectin are attractive for endothelial cell growth and function. These cells have the capability to proliferate and form a stable monolayer on the surface of the planar scaffold. Upon monolayer formation, the hCB-ECs can produce eNOS, respond to the addition of IL-1β through the upregulation of VCAM-1 and ICAM-1, and reduce the platelet deposition and activation rate. Our hCB-ECs have similar or superior attachment and functionality compared to HUVECs grown on our electrospun scaffolds.

The goal of our research team is to create a TEVG for coronary artery replacement. This graft must support smooth muscle cell and endothelial cell growth and functionality, biomechanically match a native coronary artery and remain functional and durable post-implantation. We have developed an acellular TEVG from electrospun gelatin/fibrinogen that is suitable for porcine aortic smooth muscle cell proliferation and migration [78] that can also be fabricated to match the mechanical properties of a native porcine coronary artery [159]. With the present work, we demonstrate that adding PCL and thermoforming and coating our gelatin/fibrinogen constructs enhances hCB-ECs growth and improves maintenance of their EC phenotype *in vitro.* Future directions of our research will include the development and assessment of layered constructs as well as *in vivo* rat studies using an aortic implantation to functionally assess our TEVG.

5.0   CHAPTER 5: DISCUSSION

5.1   OVERVIEW

The term Tissue Engineering (TE) was first presented to the broad scientific community in 1993 by Langer and Vacanti [227]. Around that same time the pioneers on vascular tissue engineering research Weinberg, Bell and L'Heureux demonstrated that it was feasible to create a tubular scaffold made entirely using SMCs and fibroblasts [228, 229]. The field of vascular tissue engineering has had a significant progress in the past 25 years since the first tubular model of a vascular graft. However, many challenges in the development of a small diameter vascular graft have to be still overcome, and until then, the full clinical translation remains as an ambitious goal.

For the successful replacement of a small diameter blood vessel, a TEVG has to fulfill different characteristics, that as a whole make the design and fabrication of a tubular scaffold extremely challenging which is reflected in a limited clinical success. These characteristics include biocompatibility, biofunctionality, anti-thrombogenicity, be vasoactive, immune-compatible, have appropriate mechanical properties (compliance, suture strength, burst strength), and post-implantation function and durability. This thesis focused principally in the evaluation of biocompatibility, biofunctionality and antithrombogenicity. To evaluate biocompatibility, we assessed the ability of vascular SMCs (CHAPTER 2) and hCB-ECs (CHAPTER 4) to attach, grow and function in the electrospun scaffolds. We gave additional biofunctionality to the TEVG by using it as a release system of TGFβ2 to modulate SMC response (CHAPTER 3). Furthermore, we evaluate antithrombogenicity by quantifying the number of platelets attached to the hCB-ECs seeded scaffolds, and their platelet activation rate (CHAPTER 4).

In order to mimic the microstructure of the ECM in vasculature, we used electrospinning to create highly porous and fibrous scaffolds that resemble the ECM three-dimensional architecture. Also, we opted for developing a TEVG by electrospinning principally natural polymers such as gelatin (denatured collagen) and fibrinogen, which are proteins found in the ECM of vasculature. These natural polymers allowed for the improvement of cell attachment and proliferation and by consequence the biocompatibility of the scaffold. The inclusion of synthetic polymers such as PCL in a minor percentage have different purposes: PCL is a slow degrading polymer in aqueous media, and in the case of the TGFβ2 releasing scaffolds, it was electrospun in a blend with gelatin to inhibit the fast hydrolysis of gelatin, and such, it was possible to obtain a sustained elution profile over time, preventing the burst release of TGFβ2. For the purpose of the endothelialization studies, we performed an initial surface modification of the biomaterial by a thermoforming process to increase the attachment of hCB-ECs. This surface modification was possible by the inclusion of PCL, which can be thermoformed by applying pressure at a temperature close to its melting point of 40°C. Other natural polymers such as collagen IV and fibronectin, which are found in the basal lamina, were used to coat the thermoformed scaffolds, increasing the attachment of hCB-ECs.

An initial assessment of biocompatibility was performed in CHAPTER 2 by culturing SMCs in electrospun gelatin and fibrinogen scaffolds and using exogenous TGFβ2 at different concentrations to modulate cell migration, proliferation and collagen deposition. The results suggested that SMCs were able to grow, migrate and produce collagen in the scaffolds. Moreover, the SMCs were able to respond to the addition of different concentrations of TGFβ2.

CHAPTER 3 of this thesis outlined the development of a biofunctional tubular scaffold that can release TGFβ2. The combination of gelatin and PCL at different rations allowed for the

tunability of the elution, as scaffolds with higher gelatin content showed faster release of the growth factor. Moreover, the released TGFβ2 was bioactive and was able to modulate SMCs growth in vitro and in a 3D culture.

In CHAPTER 4 we evaluated antithrombogenicity and made an additional assessment of biocompatibility by culturing hCB-ECs in surface modified electrospun gelatin/fibrinogen/PCL scaffolds. The data showed that hCB-ECs were able to attach to thermoformed and coated scaffolds, decrease the platelet deposition and activation, produce eNOS in static conditions and respond to the addition of IL-1β by increasing the expression of ICAM-1 and VCAM-1.

5.2   SUMMARY OF RESULTS

5.2.1   CHAPTER 2: Differential effect of TGFβ2 on the growth, infiltration and collagen production of SMCs growing on electrospun scaffolds.

The development of a functional tissue engineering vascular graft (TEVG) is one of the urgent necessities in the effort to treat coronary heart disease [1-7]. A TEVG has to support the growth and induce matrix deposition of vascular smooth muscle cells (SMC), similar to the media layer of a coronary artery [8, 68, 69]. Consequently, the goal of this chapter was to evaluate the possibility of growing SMCs in electrospun scaffolds meant for vascular tissue engineering. Therefore, non-synthetic biopolymer-based planar scaffolds were created through the electrospinning of gelatin (G) and fibrinogen (F) at different mass ratios [86]. The scaffolds were seeded with porcine aortic smooth muscle cells (PAOSMCs), and cell proliferation and scaffold infiltration were assessed to determine the most suitable substrate for SMC attachment, growth,

and migration. Exogenous TGFβ2 was added to the culture medium at different concentrations to assess its effect on SMC proliferation, migration, and collagen production in the tissue engineered scaffolds. The overall goal of this chapter was to evaluate the suitability of electrospun natural polymers for the attachment and function of SMCs, and the cellular response to the addition of TGFβ2.

The data suggest that scaffolds composed of 80:20 G:F are suitable for SMCs growth in both early (2days) and later (7 days) stages in culture. We found a differential effect of TGFβ2 concentration on the SMCs growing in 80:20 G:F sheets. When these constructs were treated with TGFβ2 at concentrations ≤1 ng/ml the cell proliferation and migration increased, and the collagen production was not significantly affected. In contrast, when the constructs were treated with high TGFβ2 concentrations (>1 ng/ml), cell proliferation and migration decreased and the collagen production increased. With this knowledge it is possible to strategically use TGFβ2 to modulate SMCs response. In early stages in culture the SMC proliferation and migration will be promoted by treating the cells with low concentrations of TGFβ2, ideally 0.1ng/ml-1ng/ml, as it has been demonstrated in this work. Subsequently, once the cells are distributed throughout the scaffold, the concentration of TGFβ2 will be significantly increased to 10ng/ml with the aim of promoting collagen production and possibly induce the contractile phenotype. However, this is study is feasible only *in vitro* but not in *in vivo* applications when it is desirable to have a sustained release of the TGFβ2 factor from the scaffold. Then it is necessary to integrate the signaling factor into the scaffold during the fabrication process. This was the focus of CHAPTER 3

5.2.2 CHAPTER 3: TGFβ2 release from tubular electrospun scaffolds to modulate SMC functions

In Chapter 2 it was demonstrated that TGFβ2 can modulate SMCs response, but the integration of this growth factor within the TEVG is yet to be evaluated. Consequently, we sought to fabricate a tubular scaffold that is able to release bioactive TGFβ2. For this purpose, TGβ2 was loaded into tubular constructs fabricated from different ratios of gelatin (G) and PCL. Scaffold morphology, degradation rate, TGβ2 release kinetics, and bioactivity were assessed. The TGFβ2 release profile showed a slow sustained release over the course of 15 days before getting into a plateau that is extended until 42 days. No burst release was observed for any of the scaffolds. It was also noticeable that the elution of TGFβ2 is higher as gelatin content in the scaffold increases, since the 80G:20PCL scaffolds had the greater TGFβ2 elution followed by the 50G:50PCL and the 20G:80PCL. This eluted TGFβ2 is bioactive and has a differential effect on SMC growth depending on its concentration. The released TGFβ2 also increased cell infiltration and proliferation of cells growing in 3D 80G:20PCL TGFβ2 loaded scaffolds. These results show that TGFβ2 was successfully integrated into the biomaterial, that its bioactivity is consistent with our prior results suggesting an increased SMC infiltration into our constructs when loading low amounts TGFβ2. Overall, this releasing scaffolds were deemed to represent a promising system for the control of SMC response in TEVGs. This is possible by tunability of the release using the degradation properties of natural and synthetic polymers in a blend.

5.2.3 CHAPTER 4: Endothelialization studies

In the first two results chapters of this thesis we performed an initial assessment of biocompatibility and biofunctionality of the designed TEVGs. We demonstrated the ability of SMCs to grow, migrate and function in electrospun scaffolds fabricated using natural and synthetic polymers. We also show that SMCs growing in the scaffolds were able to respond to exogenous and released TGFβ2. The integration of bioactive TGFβ2 into the polymeric material gave the scaffold additional biofunctionality. To further investigate the biocompatibility and antithrombogenicity of the polymeric grafts, gelatin/fibrinogen and gelatin/fibrinogen/polycaprolactone scaffolds were electrospun and surface modified through a thermoforming process and coating with a blend of collagen IV and fibronectin. hCB-ECs were tested for their ability to proliferate and remain on the surface of the scaffold in the formation of a monolayer. We also assessed whether the attached cells could function as a mature endothelium. In order to quantify this, we focused on important characteristics of mature and healthy endothelium, including the response to pro-inflammatory cytokine interleukin 1 beta (IL-1β), the production of endothelial nitric oxide synthase (eNOS), and antithrombotic capacities compared to HUVEC as a positive control. The data suggest that scaffolds composed of polycaprolactone/gelatin/fibrinogen that have been surface treated by thermoforming and coated with a mixture 1:1 collagen IV to fibronectin will promote the formation of a functional endothelium. In these scaffolds, cell growth is encouraged but through thickness cell infiltration is limited, resulting in a monolayer of endothelial cells mimicking the tunica intima. According to these results, hCB-ECs seem to proliferate more robustly on our surface modified scaffolds than HUVEC, and the maintenance of the endothelial cell function of both hCB-ECs and HUVEC is comparable. hCB-ECs seeded on the constructs upregulated the adhesion molecules ICAM-1 and

VCAM-1 when stimulated with the pro-inflammatory cytokine IL-1β. Our hCB-ECs also displayed the ability to produce the vaso-regulatory and hemocompatibility related enzyme eNOS and also reduce platelet adhesion and activation. This chapter we evaluated the biocompatibility of the electrospun scaffoldas and suitability of surface modifications of a biomaterial for vascular tissue engineering applications. It also gave insight into the use of an autologous source of endothelial cells towards the formation of a functional and mature endothelium that will provide an anti-thrombogenic interphase.

5.3   LIMITATIONS AND FUTURE WORK

The work presented in this dissertation is an initial assessment of biocompatibility and antithrombogenicity of electrospun scaffolds made from natural and synthetic polymers in a blend. Given the exploratory nature of this work, there is room for more advanced future work. Based on the observations presented in this dissertation, this section proposes future work that can be performed.

Our principal assessment of biocompatibility was based on the proliferation, infiltration and collagen deposition of SMCs and their response to the presence of TGFβ2. It is well known that SMCs can modulate from a synthetic to a contractile phenotype depending to on the stimulus such as the concentration of TGFβ, which in fact is a key signaling factor for inducing, maintaining, or switching between SMCs phenotypes [53, 107-109]. The transition between these phenotypes is crucial for the proper function of the blood vesse TGFβ is capable of either promoting or inhibiting SMCs proliferation [110, 111]. At low concentrations, TGFβ can stimulate SMC proliferation by promoting the platelet-derived growth factor (PDGF), which increases DNA

synthesis [110-112]. However, at high TGFβ concentrations the expression of PDGF is downregulated, causing a reduction in SMCs proliferation [110]. Additionally, when SMCs are exposed to higher concentrations of TGFβ2, this growth factor can also induce proteins such as alpha-smooth muscle actin and desmin, typical of the contractile phenotype [34, 53]. In physiological conditions, SMCs in the contractile phenotype proliferate at an extremely low rate, and the production of ECM components such as collagen is low [34, 53, 108]. Nevertheless in the study of Kubota et al (2003), the authors validated that the treatment of vascular SMCs with a high concentration of TGFβ1 (10ng/ml) stimulated collagen synthesis and increased the level of collagen type I mRNA around 2 fold [113]. In a different study (Mann et al, 2001) authors showed that the use of TGFβ1 can increase the synthesis of ECM components on RGD-containing systems such as gelatin scaffolds [114]. In a different study Blanchette, et al., demonstrated that the treatment of fibroblastic cells with 10 ng/ml of TGFβ2 translates in the increase of bioactive TGFβ1 presence. In the context of these TGFβ1 studies, our results would suggest that the non-physiologically high TGFβ2 concentrations may be inducing signaling for ECM production through a TGFβ1 pathway [115]. Current literature indicates that when SMCs are exposed to low TGFβ2 concentrations, proliferation is promoted; and when SMCs are exposed to high concentrations of TGFβ2, proliferation is decreased, the contractile phenotype may be induced, and the production of ECM is stimulated [53, 110, 111, 113]. We demonstrated that using TGFβ2 it is possible to switch SMCs from a migratory and proliferative state to a more quiescent but ECM producing condition. Knowing the exact phenotype is important for the future development of the TEVG, since the final product is ideally a tubular construct with a layer of SMCs that resembles the tunica media in a native artery, exhibiting contractility and a low proliferative rate.

Future studies with SMCs growing in tubular scaffolds have to be done to study the effect of TGFβ2 on cell phenotype with the aim of tuning the cell response. In this way it will be possible to have a proliferative and migratory phenotype in early stages to populate the scaffold with SMCs, followed by a switch to a ECM remodeling phenotype to start building new tissue that maintain the mechanical properties and enhance the function of the reconstructed artery. And finally a contractile phenotype that is able to respond to vasoactive molecules to modulate vascular tone.

We demonstrated that is possible to incorporate TGFβ2 into our polymeric solution and to further fabricate an electrospun tubular scaffold that is able of releasing this growth factor in a sustained manner. This was possible by combination of a fast degrading natural polymer with a slow degrading synthetic polymer. We also demonstrated that this TGFβ2 was bioactive and have an effect on SMC growth. One limitation of this study is the low recovery of the growth factor. We hypothesize that the crosslinking of the TGFβ2 loaded scaffolds with a liquid solution of genipin in ethanol is the main cause of these results. To overcome the low recovery of TGFβ2, future experiments with different drug-loading methods will be necessary to further explore this issue. One possibility could be to incorporate TGFβ2 by adsorption after the crosslinking of the scaffolds, which would limit TGFβ2 exposure to the fluid and to the crosslinker. Another alternative would be to covalently immobilize TGFβ2 to already crosslinked fibers which could reduce the initial burst release. A different possibility is to encapsulate TGFβ2 into biodegradable microspheres that would be further incorporated into the polymeric blend before electrospinning. With this method the TGFβ2 would be protected from the crosslinker, and the release would mainly depend on the degradation of the microspheres and not the degradation of the scaffolds. These loading methods will decrease the exposure of the growth factor to the liquid genipin solution and to the crosslinking agent. However, all these techniques have some disadvantages that

have to be further evaluated. An important limitation of covalent immobilization is a possible change in the tree-dimensional conformation of the growth factor resulting in a loss in bioactivity. Moreover, the use of electrospun microspheres can affect the mechanical properties of the scaffold.

Another limitation of this work is that we have only evaluated TGFβ2 release *in vitro*. Future *in vivo* experiments are necessary to evaluate the effect of the blood flow, and the immune response in the degradation of the tubular scaffold, and consequently in the release of TGFβ2. We expect a faster degradation of the constructs *in vivo* due to the presence and effect of macrophages and other immune cells. This may contribute to an accelerated TGFβ2 release from the implanted construct. However, we are also expecting a decrease in the local concentration of the growth factor due to hemodynamic and interstitial flow increasing washout from the scaffold.

Making a further use of our observations, and with future studies of the TGFβ2 effect on SMCs phenotype, the future design of a TEVG will include the release of different amounts of TGFβ2 over time to modulate cell response at different stages of the TEVG cellularization and remodeling. This can be done using different fabrication approaches such as the production of a layered construct with low amounts of TGFβ2 in a fast degrading layer to promote cell proliferation and infiltration, and slower degrading layer loaded with high amounts of TGFβ2 to promote collagen production, and further contractile phenotype. Another possibility is to combine traditional electrospinning with co-axial electrospinning to combine fast and slow degrading fibers; each of them containing different amounts of TGFβ2 to modulate cell response over time.

In this dissertation we assessed antithrombogenicity by seeding hCB-ECs in a surface modified scaffold. One of the main limitations of this work is that the endothelial cell function was evaluated under static conditions. We recognize the importance of testing endothelial cells under physiological shear stress, understanding that shear stress is the primary mechanical stimuli that

lead to different cell function [220]. For example, one of the most important functions of endothelial cells in the vasculature is to produce NO, a potent vasodilator and anti-inflammatory mediator [221]. It is well reported that shear stress stimulates eNOS production, eNOS phosphorylation, and therefore NO synthesis [222-226].

Therefore, to be able to make further conclusions about the preservation of endothelial cell phenotype of hCB-ECs seeded in our thermoformed and coated PCL-GF scaffolds, future studies will focus on elucidating growth and functionality under physiological shear stress. In order to increase the clinical relevance of the electrospun scaffolds, future pulsatile flow experiments will need to be performed in custom bioreactors for tubular grafts.

One possible limitation of this dissertation is that we implemented a prothrombinase assay to assess the antithrombogenic capacity of the cells. For this purpose, we used a low platelet concentration (20,000 platelets per microliter) that is not physiologically relevant and can be related with thrombocytopenia in vivo. The low platelet concentration was intentionally used to avoid the probability of platelet-platelet activation. The prothrombinase assay used in this dissertation is meant to assess the platelet activation upon contact only with the cell seeded electrospun scaffolds. In order to better study the level of platelet activation it would be necessary to use more sensitive methods such as immunocytochemistry and flow cytometry using activated platelets specific markers such as CD62 or binding to annexin V. Moreover, a more physiologically relevant assay will include a platelet agonist such as flow.

The hCB-ECs inflammatory response was evaluated by quantifying the expression of ICAM-1 and VCAM-1 after the treatment of IL-1β for 72 h (3 days). This IL1-β exposure time was used before in the study by O'Carroll et al. [176], who used brain endothelial cells. The authors found the maximum expression of inflammation molecules such as ICAM-1 and VCAM-1 after 72h of

treatment with IL-1β. However, it is necessary to assess the optimal exposure time of hCB-ECs to pro-inflammatory cytokines to obtain the most accurate quantification of ICAM-1 and VCAM-1. Future experiments will evaluate the inflammatory response of hCB-ECs at different time points from 0-72 h.   Our studies of biocompatibility and anti-thrombogenicity using both SMCs and hCB-ECs were made in an independent manner using one cell type at a time. It is important to understand the interaction between SMCs and ECs when are co-cultured in a TEVG, as their crosstalk is essential for the homeostasis of blood vessels. Then, future studies need to be done by culturing SMCs and hCB-ECs simultaneously in tubular scaffolds. For the purpose of endothelialization, the inner layer of a electrospun tubular scaffold will be designed to be thin and have low porosity. This inner layer will be subsequently thermoformed and coated with collagen IV and fibronectin. In this way the formation of an endothelial cell monolayer will be promoted. In order to promote SMC response, the thicker outer layer of the scaffold will be highly porous and also will be loaded with TGFβ2. In this configuration the endothelial cells will be also exposed to TGFβ2. In this work we principally studied the effect of TGFβ2 on SMCs, then further studies have to be done to study the effect of the different concentrations of TGFβ2 on endothelial cell function. Different authors have shown that ECs can undergo endothelial to mesenchymal transition (EndMT) after a vascular graft implantation. This process causes ECs to lose their endothelial phenotype markers and acquire SMCs cell-like properties such as collagen production and ECM remodeling [230, 231]. One of the major inducers of EndMT is TGFβ2; and depending on its concentration, TGFβ2 can induce or inhibit the endothelial transdifferentiation to SMC-like cells. In ECs, low levels of TGFβ2 would prevent EndMT. Contrary, when TGFβ2 is at high levels, EndMT may occur [231]. This differential effect of TGFβ2 over ECs, allows for the control of the EndMT by timing the release of low or high doses of TGFβ2. In the study of Pinto et al [232],

authors showed that human coronary artery ECs and microvascular pulmonary artery ECs cultured in static conditions, started acquiring SMCs markers with the addition of 2, 5 and 10 ng/ml of TGFβ2. The cells didn't lose their ECs markers, and changes in expression of these ECs specific proteins did not occur all at once. This suggests ECs exposed to exogenous TGFβ2 concentrations between 2 and 10 ng/ml can be stimulated to become an intermediate phenotype of EndMT, without a loss of ECs functions [83]. Shear stress is also an important modulator of EndMT. It has been demonstrated that proper hemodynamic shear patterns can inhibit EndMT. We hypothesize that the concentrations of TGFβ2 here used to modulate SMCs growth and infiltration can start the EndMT in ECs used to endothelialize our TEVG. However, this partial EndMT can be reversed or prevented by applied dynamic and pulsatile flow to encourage the expression of ECs markers. Then it is necessary to study the co-culture of ECs and SMCs in a TGFβ2 eluting construct using bioreactors that allowed pulsatile flow that creates the necessary shear stress to encourage ECs phenotype.

This dissertation presents the possibility of creating a release system of a growth factor using a combination of electrospun natural and synthetic polymers. It was demonstrated here that TGFβ2 was successfully integrated into a tubular scaffold, and that the released growth factor was bioactive. This release system can be used also for the elution of other signaling factors that can promote cellularization and remodeling of the TEVG. One possibility is the integration of an endothelialization promoting cytokine such as VEGF or bFGF to further increase the possibility of having a stable endothelium in the lumen of the graft. In the TEVG model presented above for the co-culture of SMCs and ECs, the endothelialization promoting cytokine will be integrated only in the inner layer of the scaffold, while TGFβ2 will be integrated in the outer layer that will be populated with SMCs. The controlled release of these growth factors will allow for the regulation

of arterial wall homeostasis and the possible prevention of conditions such as of intimal hyperplasia.

Our concept of biocompatibility *in vitro* is based on the assessment of the cell ability to attach, grow and function as in native tissue. However, a further insightful and clinically relevant assessment of biocompatibility has to be done *in vivo* using tublar scaffolds. According to the FDA guidance for Biocompatibility of medical devices (International Standard ISO 10993-1, "Biological evaluation of medical devices - Part 1: Evaluation and testing within a risk management process") in order to guarantee biocompatibility it is necessary to conduct *in vivo* preclinical and/or clinical evaluations of devices to assess cytotoxicity, sensitization, hemocompatibility (hemolysis and thrombogenisity), pyrogenicity, implantation, genotoxicity, carcinogenicity, reproductive and developmental toxicity, and in vivo degradation assessment.

Our source of endothelial cells is cord blood, which is characterized by a unique richness in highly proliferative stem and progenitor cells [233]. Cord blood is readily available, can be collected non-invasively without risk to the mother or infant donor and can be tested and preserved for long periods of time for future use [166]. This source of endothelial cells has many advantages compared to bone marrow and peripheral blood. Some of the main advantages are the proliferative capacity of the cord blood progenitor cells, the low risk of thrombus formation while the mobilizations of the progenitor cells as compared with bone marrow progenitor cells, and it can be use in treatment of acute ischemic disease, in aging patients, and patients with risk of cardiovascular disease as opposed to peripheral blood derived endothelial cells [234]. The endothelial cells from cord blood will be treated as a non-autologous source of cells that has to be donor matched [169, 235]. Generally, it has been accepted that human leukocyte antigen mismatches are better tolerated with cells derived from cord blood as oppose to bone marrow,

resulting in less graft vs host disease [234]. This suggests that endothelial cells derived from cord blood are more adaptable as they are young and not fully differentiated in early passages.

5.4   DISSERTATION CONCLUSIONS

The development of a TEVG is an urgent need for the replacement of a small diameter vessel such as the coronary arteries. For a TEVG to be successful has to be biocompatible, biofunctional, anti-thrombogenic, vasoactive and immune-compatible, have appropriate mechanical properties and post-implantation function and durability. This dissertation focused on the evaluation of <u>biocompatibility</u> by the evaluation of SMCs and hCB-ECs growth and function, <u>biofunctionality</u> by the fabrication of a tubular scaffold capable of releasing bioactive TGFβ2 to modulate SMC response, and <u>anti-thrombogenicity</u> by the evaluation of platelet attachment and activation to a monolayer of hCB-ECs growing in surface modified electrospun scaffolds.

In this work it was demonstrated that electrospun scaffolds composed by 80% gelatin and 20% fibrinogen are attractive for SMC growth and migration, since gelatin facilitates cell attachment and fibrinogen seems to promote cell proliferation. When the scaffolds were treated with TGFβ2, a differential modulation was observed depending on the concentration, noticing that at low concentrations of TGFβ2 (≤1ng/ml) cell proliferation was enhanced with no significant effect over cell infiltration and collagen production. Increasing the concentration of TGFβ2 above 1ng/ml has an opposite effect on the cell behavior, where the mitotic function was lower, the migration was minimal, and the collagen production was increased.

According to these results it is possible to propose a strategy that we call "The TGFβ2 switch" to biochemically control SMC function growing in tissue engineered scaffolds: In early stages, the SMC proliferation and migration will be promoted by treating the cells with low concentrations of TGFβ2. Subsequently, once the cells are distributed throughout the scaffold, the concentration of TGFβ2 will be significantly increased to 10 ng/ml with the aim of promoting collagen production and possibly induce the contractile phenotype.

To the best of my knowledge this dissertation presents for the first time a release system to modulate SMC growth and infiltration in TEVGs using TGFβ2. Here, it was demonstrated the fabrication of gelatin/PCL hybrid biodegradable scaffolds with the ability of releasing bioactive TGFβ2. This release can be tuned using the degradation properties of natural and synthetic polymers in a blend allowing control of SMC growth and infiltration of our TGFβ2-releasing conduits, thus making these scaffolds attractive for vascular tissue engineering applications.

This dissertation confirms the importance of bio-banking as it demonstrates the possibility of deriving highly adhesive and proliferative endothelial cells (hCB-ECs) from banked cord blood. It also demonstrates that in our surface modified biomaterial hCB-ECs can grow and function. These cells have the ability to proliferate and form a stable monolayer on the surface of the planar scaffold. Upon monolayer formation, the hCB-ECs can produce eNOS, respond to the addition of IL-1β through the upregulation of VCAM-1 and ICAM-1, and reduce the platelet deposition and activation rate. The derived hCB-ECs have similar or superior attachment and functionality compared to HUVECs grown on the surface modified electrospun scaffolds.

These results suggest that a biofunctional biopolymer based TEVG can be fabricated that can control SMC response and promote the formation of a functional endothelium.

A.1 FLOW CHAMBER FOR THE CHARACTERIZATION OF ENDOTHELIAL CELLS
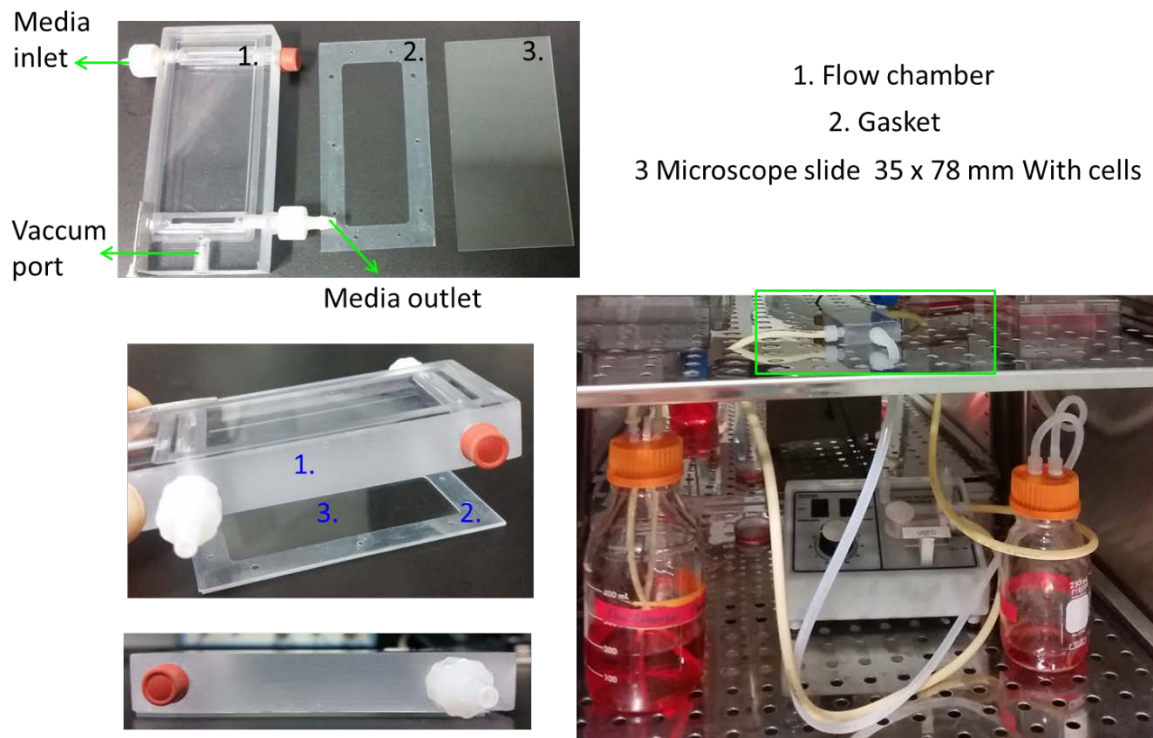
Figure A.1.1 Flow chamber used to characterize hCB-ECs

Here is shown a flow chamber for the characterization of endothelial cells. The polycarbonate plate, the gasket, and the glass slide with the attached cells are held together by a vacuum forming a channel of parallel plate geometry. The wall shear stress on the cell monolayer

in the flow chamber may be calculated using the momentum balance for a Newtonian fluid and assuming

parallel-plate geometry:

$t = 6Q\mu/bh2$

where Q is the flow rate (cm3/s); μ is the viscosity (.0.01 dyn s/cm2); h is the channel height (0.022 cm); b is the slit width, (2.5 cm); and t is the wall shear stress (dyn/cm2). The flow rate was controlled by a peristaltic pump

The Reynolds number of the flow through the chamber is given by:

$Re = Uhr/\mu = Q\rho/mb$

where U is the characteristic or mass average flow velocity; ρ is the density of the medium; and μ is the viscosity of the medium.

At 25 dyne/cm2 Re is approximately 20 indicating that fluid flow through the chamber was laminar.

This flow chamber was bought from Dr. John Frangos at La Joya Bioengineering institute. Here is the link of the paper where it is characterized. http://www.ncbi.nlm.nih.gov/pubmed/18587822

A.2   SELECTION OF A SURFACE MODIFICATION APPROACH FOR CULTURING ENDOTHELIAL CELLS

Porcine coronary artery endothelial cells (PCAECs) were cultured in 80:20 G:F electrospun constructs that were surface modified by air plasma treatment for 12 min, NaOH 0.5M for 30 min, and Fibronectin coating (5µg/ml) for 24h at 4°C. After 7 days in culture a proliferation assay was performed on every flat sheet using a sample with a surface area of approximately 35 mm2. Viable cell number was determined by the bioreduction of 3-(4,5-Dimethyl-thiazol-2yl)-5-(3-carboxymethoxyphenyl)-2-(4-sulfophenyl)-2H-tetrazolium and absorbance at 490 (Figure A.2.1). Additionally, the samples were fixed in paraformaldehyde and the cells were stained using alexafluor 568-phalloidin (red-f-actin) and dapi (blue-nuclei). The Advanced Intravital Microscope (AIM) for multiphoton imaging at the University of Arizona's BIO5 institute was used to observe the total cell migration along the scaffold (green) depth. PCAECs show a significant higher cell number ($p < 0.05$, n=4) in scaffolds coated with fibronectin compared to the control. Also from the 2-Photon images it is possible to observe that PCAECs presented a limited migration along the z direction of scaffolds treated with fibronectin. These results suggested that using a proteins present in the basal lamina such as fibronectin it is possible to encourage the cells form a monolayer on the scaffold surface (Figure A.2.1). Further experiments explored the used of other basal lamina proteins to encourage the attachment of ECs
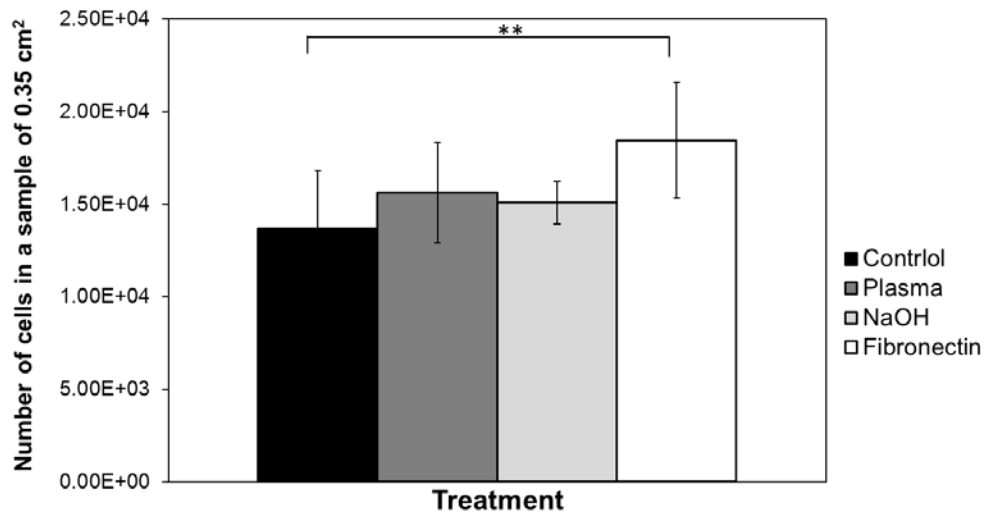
Figure A.2.1 Proliferation results of PCAECs cultured for 7 days in 80:20 surface modified gelatin: fibrinogen constructs. Error bars are standard deviation. (**p<0.05), n=4.
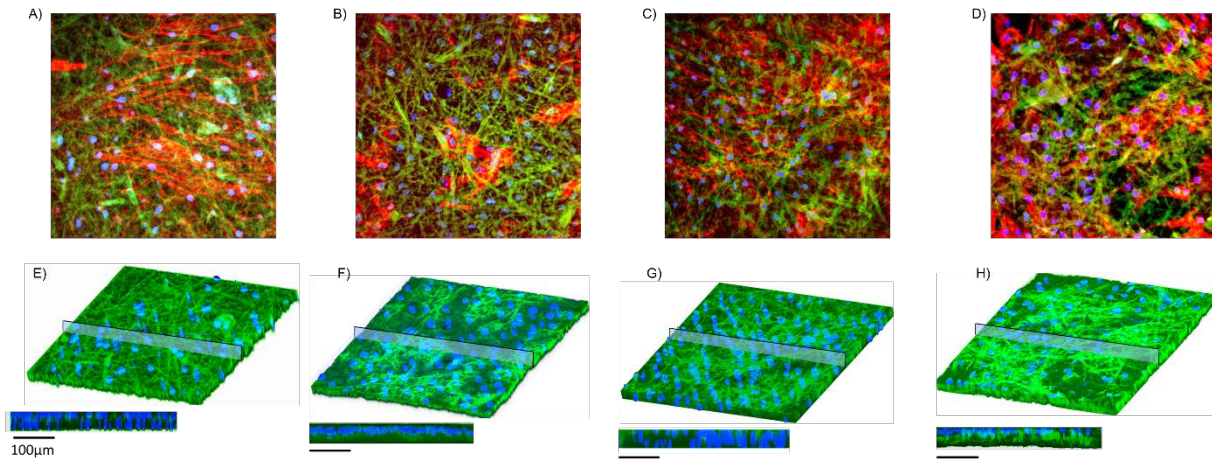
Fig. A.2.2 Top Row: Representative multiphoton image of an 80:20 G:F flat sheet with PCAECs after 7 days in culture. A) Control scaffold. Surface modified scaffold with B) air plasma C) NaOH D) Fibronectin coat. The material fibers are shown in green, the cell nuclei in blue, and F-actin in red. Image was acquired at a magnification of 20x. Bottom Row: Representative multiphoton images of an 80:20 G:F flat sheet with sheet with PCAECs cells after 7 days in culture. The material fibers are shown in green, and cell nuclei in blue. In each figure the top image is a 3D render of the scaffold. The bottom image is the xz view of the 3D render. Images were acquired at a magnification of 20x for E) Control scaffold. Scaffold surface modified with F) air plasma G) NaOH H) Fibronectin coat.

A.3   SELECTION OF A COATING FOR CULTURING ENDOTHELIAL CELLS

Glass micro coverslips were coated with either collagen I (ColI) from rat tail (Gibco, USA) in 20 mM acetic acid, collagen IV (ColIV) from human cell culture (Sigma-Aldrich, USA) in HBSS, fibronectin (Fib) from bovine plasma (Sigma-Aldrich, USA) in 1X PBS, or a mixture 1:1 of ColI and ColIV (ColI/ColIV) in 20 mM acetic acid, ColI and Fib (ColI/Fib) in 20 mM acetic acid, or ColIV and Fib (ColIV/Fib) in HBSS. All the solutions had a final concentration of 5 μg/ml. The coatings were incubated at 4°C for 24 hours. hCB-ECs and HUVECs were then seeded on the coated cover slips at a cell density of 1×10^3 cells/cover slip, and cultured in 96 well plates. After 2 hours of culturing, the coverslips were rinsed 3 times with sterile 1X PBS and then transferred to new 96 well plates. The culture medium was changed every other day and cultures were maintained in a humidified environment at 37°C and 5% CO2. Cell number after 3 days of culture was assessed using the MTS CellTiter 96® AQueous One Solution Cell Proliferation Assay (Promega, USA) following the manufacturer's instruction. Absorbance was read at 490 nm in a Synergy H1 plate reader from BioTek®. The experiments had 6 replicates.

The mixture of ColIV/Fib exhibited higher promotion of growth in both cell types compared with the other different coatings. HUVEC sow a better initial attachment, and a significant increase in cell number/well for the ColIV/Fib compared to ColIV and Fib (SPSS Bonferroni adjusted p values p=0.001and p= 0.002 respectively); and also for ColI/Fib compared to ColIV and Fib (SPSS Bonferroni adjusted p values p=0.019 and p=0.038 respectively).
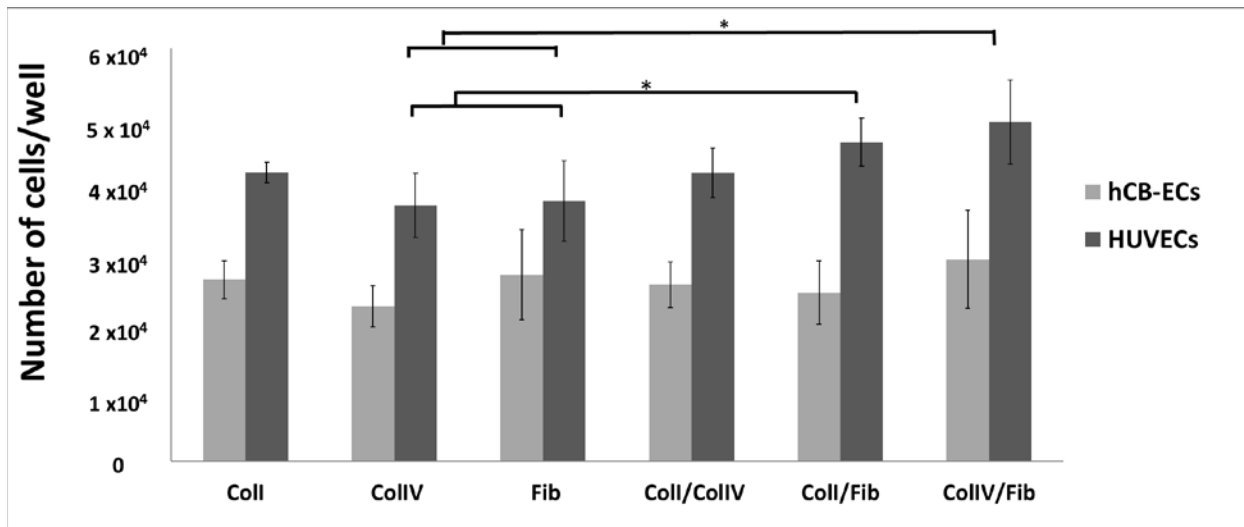
Figure A.3.1 Proliferation results of hCB-ECs and HUVECs 3 days post seeding in glass micro-coverslips coated with collagen I (ColI), collagen IV (ColIV), fibronectin, or a mixture 1:1 of ColI and ColIV (ColI/ColIV) ColI and Fib (ColI/Fib) or ColIV and Fib (ColIV/Fib). For culturing purposes, the micro-coverslips were placed in 96 well plates. Average cell number per well is reported for the two cell types. Error bars shown are standard deviations (*p<0.05; n=6).

A.4   RELEASE OF TGFβ2 FROM UNCROSSLINKED SCAFFOLDS

Gelatin extracted from porcine skin, human tropoelastin and PCL (80,000 MW) (Sigma-Aldrich, USA) were mixed as follows: 100% PCL, 50% gelatin-50% PCL (50G:50PCL), 50% tropoelastin 50% PCL (50T:50PCL), The polymeric blends were dissolved in 1,1,1,3,3,3-Hexafluoro-2-propanol (HFP) (Sigma-Aldrich, USA) to create a 10% (w/v) solution under continuous stirring. The polymeric solutions were loaded into a 5 ml BD syringe and lyophilized recombinant human TGFβ2 (R&D systems) was reconstituted with 4mM HCL containing 1mg/ml bovine serum albumin (BSA) (Sigma-Aldrich, USA). The TGFβ2 solution was mixed with the polymeric blends directly in the syringe immediately prior to electrospinning to create a final concentration of 1.3 µg/ml. A 23-gauge stainless steel dispensing blunt tip needle (CML supply, USA) was attached to the syringe which was then loaded onto a NE-1000 single syringe pump (New era pump systems inc., USA) set to a pumping rate of 30 µL/min and a total dispensing volume of 300 µL. The distance from the needle tip to the target was 10 cm. The polymeric solutions containing TGFβ2 were electrospun at a high voltage of 15 kV, onto a grounded 1.4-mm metallic rod mounted onto a rotating and translating mandrel set to a rotation rate of 300 rpm and a translation rate of 300 mm/sec. Each scaffold had an approximate length of 8 cm, a dry weight of 10 mg, and a determined TGFβ2 density of 13 ng TGFβ2/ mg scaffold.

The bioactivity of the released TGFβ2 was measured by its ability to modulate SMC proliferation. Porcine aortic SMCs from passage 4 were seeded in wells of 96-well plates at a density of 7 x 10^3 cells/well. Cells were cultured in the culture media for 24 h at 37°C and 5% CO2 in a humidified atmosphere. Then the culture media was removed and the release media from days 1, 21 and 42 from the 4 scaffold groups was added to the cells. Cells were culture with this media for 5 days. Then an MTS assay was used to assess cell number.

In Figure A.4.1 it was possible to observe that the release of the growth factor depends on the material used. The scaffolds containing tropoelastin presented a burst release in the first days. The scaffolds containing gelatin presented a sustained release for the course of the 42 days. The pure PCL scaffolds presented a limited release. In Figure A.4.2 it is possible to observe that the released TGFβ2 had a differential effect on cell proliferation depending on its concentration in culture media. In the first day the tropoelastin containing scaffolds released about 13% of the loaded growth factor corresponding to a concentration in culture media of 5ng/ml. This concentration of TGFβ2 decreased the proliferation of SMCs. Similarly, scaffolds containing gelatin had a sustained release of small amounts o TGFβ2 at every time point which increased cell proliferation
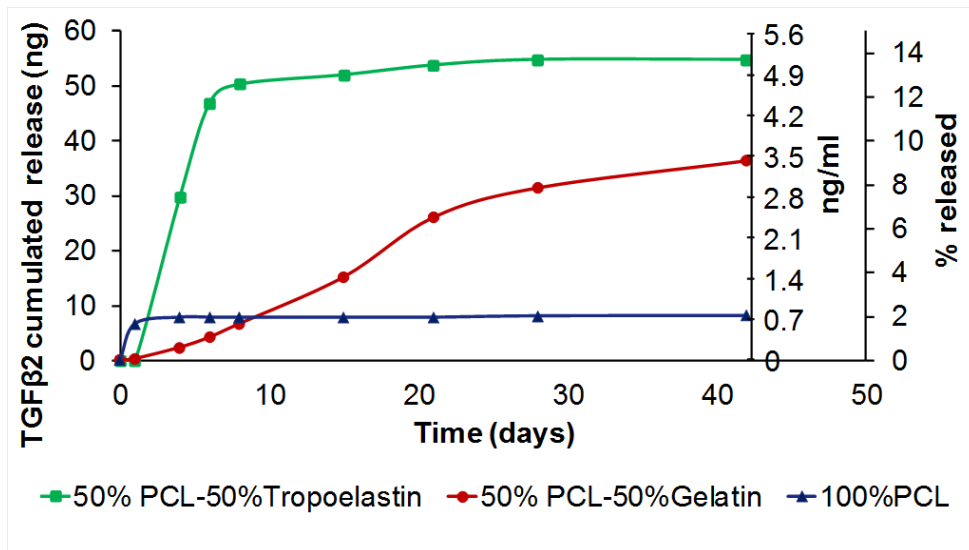
Figure A.4.1 Cumulative release of TGFβ2 from electrospun scaffolds with different containing gelatin, tropoelastin and PCL. (n=4)
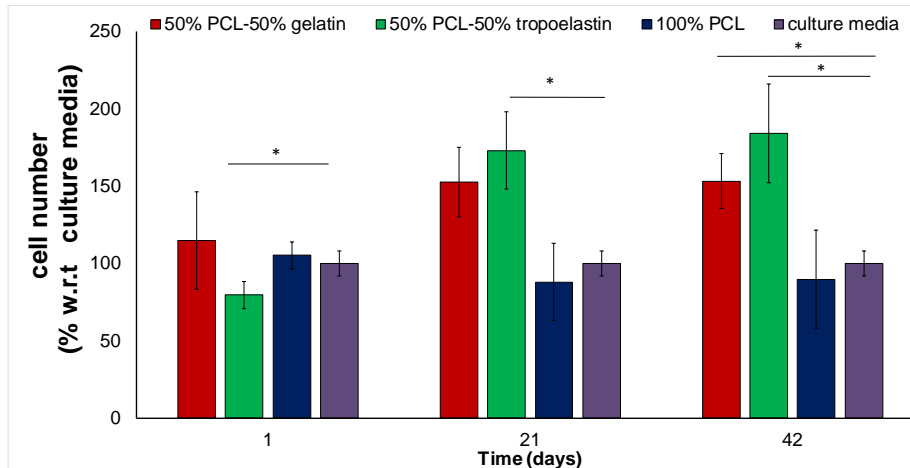
Figure A.4.2 Bioactivity of released TGFβ2 from electrospun scaffolds on cells growing in monolayers. Release media of scaffolds containing 13 of TGFβ2/mg of scaffold collected at time 1, 21 and 42 days was used to culture SMCs for 5 days .Cell count was assessed using an MTS assay. Error bars shown are standard deviation (*p < 0.05; n = 4).

A.5   FABRICATION OF A TUBULAR SCAFFOLD USING A GELATIN FLAT SHEET AND TROPOELASTIN HYDROGEL

To create a tubular scaffold with alternating layers of gelatin/fibrinogen and tropoelastin, first it is necessary to create an electrospun a 80:20 gelatin:fibrinogen flat sheet as explained in the methods presented in CHAPTER 2. Then a tropoelastin hydrogel was prepared as follows: 20 mg of tropoelastin were dissolved in 180 μl of cold PBS (tropoelastin will only dissolve in ice cold PBS) It is very important to maintain the tropoelastin solution at 4°C at all times to prevent its coadservation. After tropoelastin is completely dissolved in PBS, add 20 μl of BS3 (crosslinker) 12.5 mM, to a final concentration of final concentration of 1mM BS3 and 100mg/ml of tropoelastin.

The electrospun flat sheet was hydrated in cold PBS and placed completely flat on top of a cold surface. The excess of PBS was removed carefully using a Kim wipe. Then, 100 µl of the cold tropoelastin solution was pipetted on top of the sheet. Using a teflon or a stainless steel rod of 2 mm diameter, the sheet with the tropoelastin solution were rolled up carefully as shown in figure A.5.1. The rolled tube was immediately incubated at 37°C, for 24h. Histology of an acellular rolled tube is presented in figure A.5.2. stress strain curves of are shown in figure A.5.3. Histology and multiphoton images of a cellularized rolled construct are presented in figure A.5.4. For these cellularized construct the gelatin/fibrinogen flat sheet used for rolling was first seeded with SMCs and cultured in complete DMEM for 7 days. After rolling the constructs were incubated in bioreactors for 7 days.

Hydrogel

80:20 gelatin/fibrinogen
electrospun flat sheet
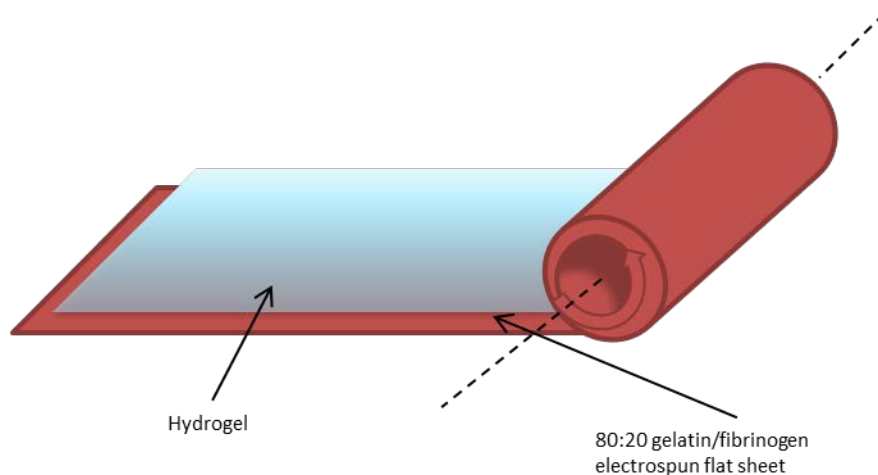
Figure A.5.1 Representation of the rolling procedure
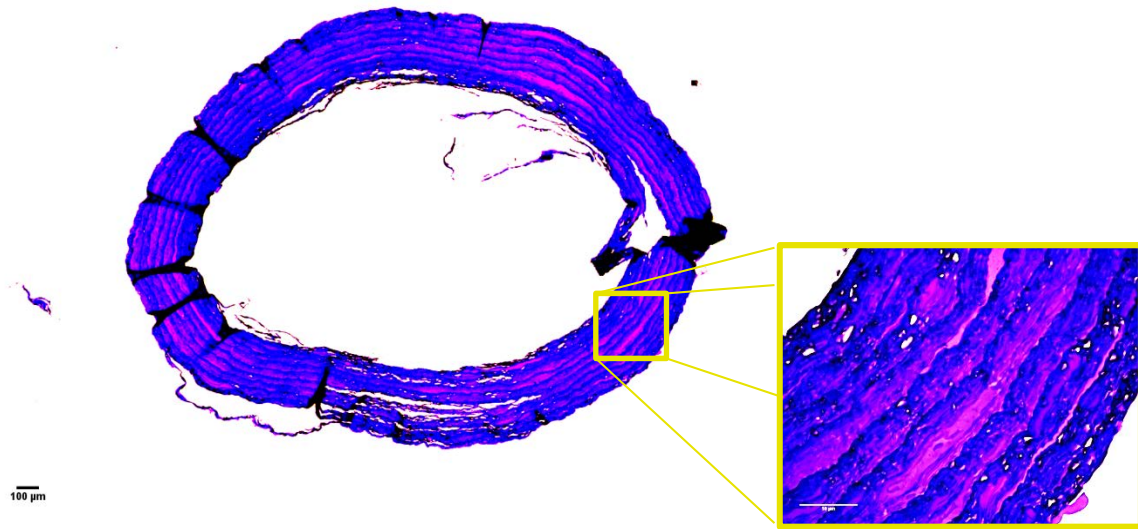
Figure A.5.2 Crossection of an 80:20 G:F flat sheets rolled with a 100mg/ml tropoelastin hydrogel on top, to create an acellular tubular construct. H&E stained. Colors were enhanced to show the differences between the G:F fibers (purple) and the tropoelastin hydrogel (pink).
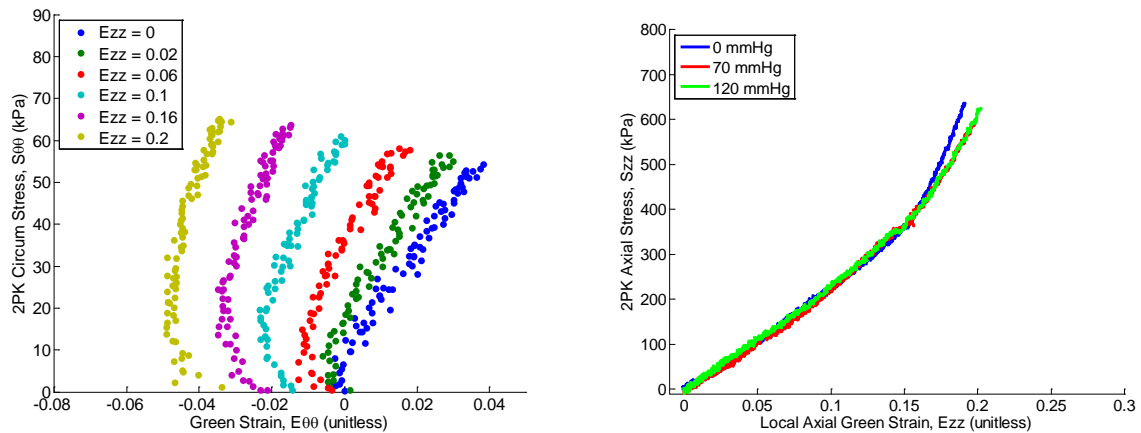
Figure A.5.3 Stress strain curves in the circumferential direction (left) and axial direction (right) of an 80:20 G:F flat sheets rolled with a 100mg/ml tropoelastin hydrogel on top, to create an acellular tubular construct. Thickness was245 microns and length was 9.9 mm

Dapi fluorescence 4x

126

H&E stain   4x   **Dapi+ autofluorescence 4x**

100 µm

Dapi fluorescence 4x   **Dapi+autofluorescence+ alpha actin (fitc)**

100 µm

H&E stain   4x   **Dapi+ autofluorescence 4x**

100 µm

100
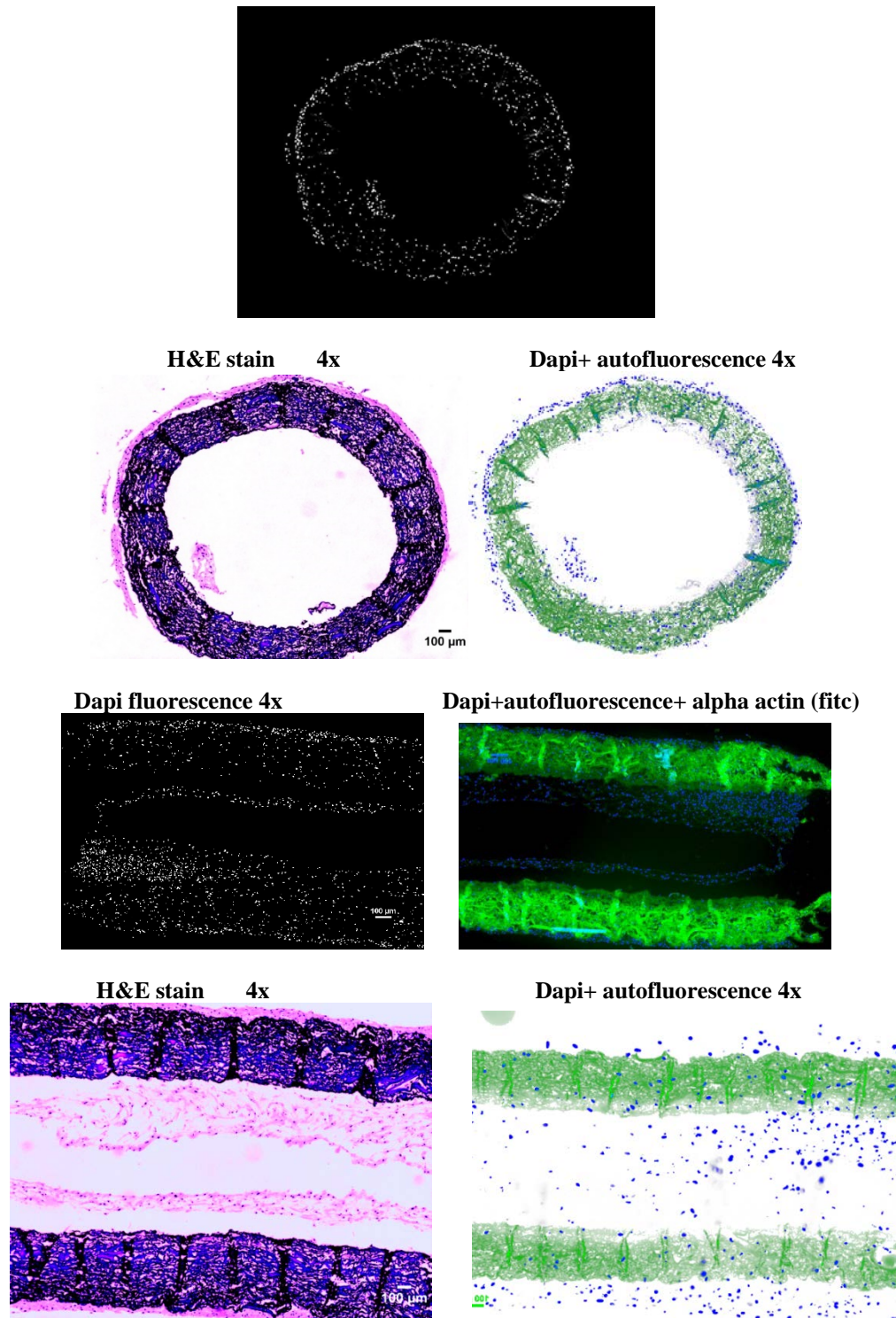
Figure A.5.4 Hystology and 2-photon images of the cellularized rolled constructs. 80:20 G:F flat sheets seeded with SMAs for 1 week were rolled with a 100mg/ml tropoelastin hydrogel on top. The rolled constructs were incubated for additional 7 days using bioreactors

BIBLIOGRAPHY

1. Centers for Disease Control and Prevention, N.C.f.H.S., *Multiple Cause of Death 1999-2015 on CDC WONDER Online Database, released December 2016. Data are from the Multiple Cause of Death Files, 1999-2015, as compiled from data provided by the 57 vital statistics jurisdictions through the Vital Statistics Cooperative Program. Accessed at http://wonder.cdc.gov/mcd-icd10.html.* 2016.

2. Serruys, P.W., et al., *Five-year outcomes after coronary stenting versus bypass surgery for the treatment of multivessel disease: the final analysis of the Arterial Revascularization Therapies Study (ARTS) randomized trial.* Journal of the American College of Cardiology, 2005. **46**(4): p. 575-581.

3. Benjamin, E.J., et al., *Heart disease and stroke statistics—2017 update: a report from the American Heart Association.* Circulation, 2017. **135**(10): p. e146-e603.

4. McClure, M.J., et al., *A three-layered electrospun matrix to mimic native arterial architecture using polycaprolactone, elastin, and collagen: a preliminary study.* Acta Biomaterialia, 2010. **6**(7): p. 2422-2433.

5. McClure, M., et al., *Bioengineered vascular grafts: improving vascular tissue engineering through scaffold design.* Journal of Drug Delivery Science and Technology, 2011. **21**(3): p. 211-227.

6. Sell, S.A., et al., *Electrospinning of collagen/biopolymers for regenerative medicine and cardiovascular tissue engineering.* Advanced drug delivery reviews, 2009. **61**(12): p. 1007-1019.

7. Byrom, M.J., M.K. Ng, and P.G. Bannon, *Biomechanics and biocompatibility of the perfect conduit—can we build one?* Annals of cardiothoracic surgery, 2013. **2**(4): p. 435.

8. Ong, C.S., et al., *Tissue engineered vascular grafts: current state of the field.* Expert review of medical devices, 2017. **14**(5): p. 383-392.

9. L'Heureux, N., et al., *Technology insight: the evolution of tissue-engineered vascular grafts—from research to clinical practice.* Nature Clinical Practice Cardiovascular Medicine, 2007. **4**(7): p. 389-395.

10. Tan, A., et al., *Tissue engineering vascular grafts a fortiori: looking back and going forward.* Expert opinion on biological therapy, 2015. **15**(2): p. 231-244.

11. Roger, V.L., et al., *Heart disease and stroke statistics—2012 update a report from the American heart association.* Circulation, 2012. **125**(1): p. e2-e220.

12.   Mozaffarian, D., et al., *Executive Summary: Heart Disease and Stroke Statistics—2016 Update A Report From the American Heart Association.* Circulation, 2016. **133**(4): p. 447-454.

13.   Go, A.S., et al., *Heart disease and stroke statistics-2014 update.* Circulation, 2014. **129**(3).

14.   Fuchs, J.R., B.A. Nasseri, and J.P. Vacanti, *Tissue engineering: a 21st century solution to surgical reconstruction.* The Annals of thoracic surgery, 2001. **72**(2): p. 577-591.

15.   Langer, R. and J.P. Vacanti, *Tissue engineering.* Science, 1993. **260**(5110): p. 920-6.

16.   Vacanti, J.P. and R. Langer, *Tissue engineering: the design and fabrication of living replacement devices for surgical reconstruction and transplantation.* The Lancet, 1999. **354**: p. S32-S34.

17.   Chen, Q.-Z., et al., *Biomaterials in cardiac tissue engineering: ten years of research survey.* Materials Science and Engineering: R: Reports, 2008. **59**(1): p. 1-37.

18.   O'Brien, F.J., *Biomaterials & scaffolds for tissue engineering.* Materials Today, 2011. **14**(3): p. 88-95.

19.   Gunatillake, P.A. and R. Adhikari, *Biodegradable synthetic polymers for tissue engineering.* Eur Cell Mater, 2003. **5**(1): p. 1-16.

20.   Dhandayuthapani, B., et al., *Polymeric scaffolds in tissue engineering application: a review.* International Journal of Polymer Science, 2011. **2011**.

21.   Nikolovski, J. and D.J. Mooney, *Smooth muscle cell adhesion to tissue engineering scaffolds.* Biomaterials, 2000. **21**(20): p. 2025-2032.

22.   Kohane, D.S. and R. Langer, *Polymeric biomaterials in tissue engineering.* Pediatric research, 2008. **63**(5): p. 487-491.

23.   Oh, S.H. and J.H. Lee, *Hydrophilization of synthetic biodegradable polymer scaffolds for improved cell/tissue compatibility.* Biomedical Materials, 2013. **8**(1): p. 014101.

24.   Sell, S.A., et al., *The use of natural polymers in tissue engineering: a focus on electrospun extracellular matrix analogues.* Polymers, 2010. **2**(4): p. 522-553.

25.   Mano, J., et al., *Natural origin biodegradable systems in tissue engineering and regenerative medicine: present status and some moving trends.* Journal of the Royal Society Interface, 2007. **4**(17): p. 999-1030.

26.   Marler, J.J., et al., *Transplantation of cells in matrices for tissue regeneration.* Advanced drug delivery reviews, 1998. **33**(1): p. 165-182.

27.   Catto, V., et al., *Vascular tissue engineering: recent advances in small diameter blood vessel regeneration.* ISRN Vascular Medicine, 2014. **2014**.

28.   Faletra, F.F., N.G. Pandian, and S.Y. Ho, *Coronary Artery Anatomy.* Anatomy of the Heart by Multislice Computed Tomography: p. 88-107.

29.   AHA. *Whatch, learn live, Interactive cardiovascular library*. 2018; Available from: http://watchlearnlive.heart.org/CVML_Player.php?moduleSelect=corart.

30.   James, T.N., *Anatomy of the coronary arteries*. 1961: PB Hoeber.

31.   Childs, G. *Microanatomy web atlas*. 1998; Available from: http://microanatomy.net/cardiovascular/cardiovascular_system.htm.

32.   Waller, B.F., et al., *Anatomy, histology, and pathology of coronary arteries: A review relevant to new interventional and imaging techniques—Part I.* Clinical cardiology, 1992. **15**(6): p. 451-457.

33.   Michiels, C., *Endothelial cell functions.* Journal of cellular physiology, 2003. **196**(3): p. 430-443.

34.   Rensen, S., P. Doevendans, and G. Van Eys, *Regulation and characteristics of vascular smooth muscle cell phenotypic diversity.* Netherlands Heart Journal, 2007. **15**(3): p. 100-108.

35.   Hanson, M.A., et al., *Coronary artery disease.* Primary Care: Clinics in Office Practice, 2013. **40**(1): p. 1-16.

36.   Centers for disease, c., and prevention. *Coronary Artery Disease: Causes, Diagonosis & Prevention*. 2015; Available from: https://www.cdc.gov/heartdisease/coronary_ad.htm.

37.   Wilson, P.W., et al., *Prediction of coronary heart disease using risk factor categories.* Circulation, 1998. **97**(18): p. 1837-1847.

38.   McCullough, P.A., *Coronary artery disease.* Clinical Journal of the American Society of Nephrology, 2007. **2**(3): p. 611-616.

39.   Kappetein, A.P., et al., *Treatment of complex coronary artery disease in patients with diabetes: 5-year results comparing outcomes of bypass surgery and percutaneous coronary intervention in the SYNTAX trial.* European Journal of Cardio-Thoracic Surgery, 2013. **43**(5): p. 1006-1013.

40.   Lytle, B.W. and D.M. Cosgrove, *Coronary artery bypass surgery.* Current problems in surgery, 1992. **29**(10): p. 743-807.

41.   System, M.N.H., *Understanding Off-Pump Coronary Artery Bypass (CABG) Surgery.* 2016.

42.   Norouzi, M., et al., *Protein encapsulated in electrospun nanofibrous scaffolds for tissue engineering applications.* Polymer International, 2013. **62**(8): p. 1250-1256.

43.   Stegemann, J.P., S.N. Kaszuba, and S.L. Rowe, *Review: advances in vascular tissue engineering using protein-based biomaterials.* Tissue engineering, 2007. **13**(11): p. 2601-2613.

44.   Pashneh-Tala, S., S. MacNeil, and F. Claeyssens, *The tissue-engineered vascular graft—past, present, and future.* Tissue Engineering Part B: Reviews, 2015. **22**(1): p. 68-100.

45.   Greiner, A. and J.H. Wendorff, *Electrospinning: a fascinating method for the preparation of ultrathin fibers.* Angewandte Chemie International Edition, 2007. **46**(30): p. 5670-5703.

46.   Huang, Z.-M., et al., *A review on polymer nanofibers by electrospinning and their applications in nanocomposites.* Composites science and technology, 2003. **63**(15): p. 2223-2253.

47.   Stitzel, J.D., et al. *Electrospraying and electrospinning of polymers for biomedical applications. Poly (lactic-co-glycolic acid) and poly (ethylene-co-vinylacetate).* in *International SAMPE technical conference.* 2000.

48.   Martínez-Pérez, C.A., et al., *Scaffolds for tissue engineering via thermally induced phase separation*, in *Advances in Regenerative Medicine*. 2011, InTech.

49.   Guan, J., J.J. Stankus, and W.R. Wagner, *Biodegradable elastomeric scaffolds with basic fibroblast growth factor release.* Journal of Controlled Release, 2007. **120**(1-2): p. 70-78.

50.   Carrabba, M. and P. Madeddu, *Current Strategies for the Manufacture of Small Size Tissue Engineering Vascular Grafts.* Frontiers in bioengineering and biotechnology, 2018. **6**: p. 41.

51.   Wang, L., et al., *Fabrication of tissue-engineered vascular grafts with stem cells and stem cell-derived vascular cells.* Expert opinion on biological therapy, 2016. **16**(3): p. 317-330.

52.   Worth, N.F., et al., *Vascular smooth muscle cell phenotypic modulation in culture is associated with reorganisation of contractile and cytoskeletal proteins.* Cell motility and the cytoskeleton, 2001. **49**(3): p. 130-145.

53.   Beamish, J.A., et al., *Molecular regulation of contractile smooth muscle cell phenotype: implications for vascular tissue engineering.* Tissue Engineering Part B: Reviews, 2010. **16**(5): p. 467-491.

54.   Deanfield, J.E., J.P. Halcox, and T.J. Rabelink, *Endothelial function and dysfunction testing and clinical relevance.* Circulation, 2007. **115**(10): p. 1285-1295.

55.   Marti, C.N., et al., *Endothelial dysfunction, arterial stiffness, and heart failure.* Journal of the American College of Cardiology, 2012. **60**(16): p. 1455-1469.

56.   Wang, Z., et al., *Novel biomaterial strategies for controlled growth factor delivery for biomedical applications.* NPG Asia Materials, 2017. **9**(10): p. e435.

57.   King, T.W. and C.W. Patrick Jr, *Development and in vitro characterization of vascular endothelial growth factor (VEGF)-loaded poly (DL-lactic-co-glycolic acid)/poly (ethylene glycol) microspheres using a solid encapsulation/single emulsion/solvent extraction technique.* Journal of Biomedical Materials Research: An Official Journal of The Society for Biomaterials, The Japanese Society for Biomaterials, and The Australian Society for Biomaterials and the Korean Society for Biomaterials, 2000. **51**(3): p. 383-390.

58.   Masters, K.S., *Covalent growth factor immobilization strategies for tissue repair and regeneration.* Macromolecular bioscience, 2011. **11**(9): p. 1149-1163.

59.   Shireman, P.K. and H.P. Greisler, *Mitogenicity and release of vascular endothelial growth factor with and without heparin from fibrin glue.* Journal of vascular surgery, 2000. **31**(5): p. 936-943.

60.   Pugh, R.J., et al., *Transmembrane protein 184A is a receptor required for vascular smooth muscle cell responses to heparin.* Journal of Biological Chemistry, 2016. **291**(10): p. 5326-5341.

61.   Fritze, L.M., C.F. Reilly, and R.D. Rosenberg, *An antiproliferative heparan sulfate species produced by postconfluent smooth muscle cells.* The Journal of cell biology, 1985. **100**(4): p. 1041-1049.

62.   Clowes, A.W. and M.M. Clowes, *Kinetics of cellular proliferation after arterial injury. IV. Heparin inhibits rat smooth muscle mitogenesis and migration.* Circulation research, 1986. **58**(6): p. 839-845.

63.   Cindhuchao, N., et al., *Heparin inhibits SMC growth in the presence of human and fetal bovine serum.* Biochemical and biophysical research communications, 2003. **302**(1): p. 84-88.

64.   Antonova, L.V., et al., *Vascular endothelial growth factor improves physico-mechanical properties and enhances endothelialization of poly (3-hydroxybutyrate-co-3-hydroxyvalerate)/poly (ε-caprolactone) small-diameter vascular grafts in vivo.* Frontiers in pharmacology, 2016. **7**: p. 230.

65.   de Mel, A., et al., *Biofunctionalization of biomaterials for accelerated in situ endothelialization: a review.* Biomacromolecules, 2008. **9**(11): p. 2969-2979.

66.   Washington, K.S. and C.A. Bashur, *Delivery of Antioxidant and Anti-inflammatory Agents for Tissue Engineered Vascular Grafts.* Frontiers in pharmacology, 2017. **8**: p. 659.

67.   Strobel, H.A., et al., *Cellular self-assembly with microsphere incorporation for growth factor delivery within engineered vascular tissue rings.* Tissue Engineering Part A, 2017. **23**(3-4): p. 143-155.

68.   Gui, L., et al., *Construction of tissue-engineered small-diameter vascular grafts in fibrin scaffolds in 30 days.* Tissue Engineering Part A, 2014. **20**(9-10): p. 1499-1507.

69.   L'heureux, N., et al., *Technology insight: the evolution of tissue-engineered vascular grafts—from research to clinical practice.* Nature Reviews Cardiology, 2007. **4**(7): p. 389.

70.   Wang, G., et al., *Origin and differentiation of vascular smooth muscle cells.* The Journal of physiology, 2015. **593**(14): p. 3013-3030.

71.   Lannutti, J., et al., *Electrospinning for tissue engineering scaffolds.* Materials Science and Engineering: C, 2007. **27**(3): p. 504-509.

72.   Casscells, W., *Smooth muscle cell growth factors.* Progress in growth factor research, 1991. **3**(3): p. 177-206.

73.   Fuster, V., E.J. Topol, and E.G. Nabel, *Atherothrombosis and coronary artery disease*. 2005: Lippincott Williams & Wilkins.

74.   Chen, P.-Y., et al., *Fibroblast growth factor (FGF) signaling regulates transforming growth factor beta (TGFβ)-dependent smooth muscle cell phenotype modulation.* Scientific reports, 2016. **6**: p. 33407.

75.   Yamashita, J.K., *Expanding reprogramming to cardiovascular progenitors.* Cell stem cell, 2016. **18**(3): p. 299-301.

76.   Liu, Y., et al., *Transforming growth factor-beta1 upregulation triggers pulmonary artery smooth muscle cell proliferation and apoptosis imbalance in rats with hypoxic pulmonary hypertension via the PTEN/AKT pathways.* The international journal of biochemistry & cell biology, 2016. **77**: p. 141-154.

77.   Goumans, M.-J. and P. ten Dijke, *TGF-β signaling in control of cardiovascular function.* Cold Spring Harbor perspectives in biology, 2018. **10**(2): p. a022210.

78.   Ardila, D.C., et al., *TGFβ2 differentially modulates smooth muscle cell proliferation and migration in electrospun gelatin-fibrinogen constructs.* Biomaterials, 2015. **37**: p. 164-173.

79.   Boileau, C., et al., *TGFB2 mutations cause familial thoracic aortic aneurysms and dissections associated with mild systemic features of Marfan syndrome.* Nature genetics, 2012. **44**(8): p. 916.

80. Ramnath, N., et al., *Fibulin-4 deficiency increases TGF-β signalling in aortic smooth muscle cells due to elevated TGF-β2 levels.* Scientific reports, 2015. **5**: p. 16872.

81. Artman, M., et al., *Cardiovascular Development and Congenital Malformations: Molecular & Genetic Mechanisms.* 2008: John Wiley & Sons.

82. Azhar, M., et al., *Transforming growth factor Beta2 is required for valve remodeling during heart development.* Developmental Dynamics, 2011. **240**(9): p. 2127-2141.

83. Doetschman, T., et al., *Transforming growth factor beta signaling in adult cardiovascular diseases and repair.* Cell and tissue research, 2012. **347**(1): p. 203-223.

84. Molin, D.G., et al., *Altered apoptosis pattern during pharyngeal arch artery remodelling is associated with aortic arch malformations in Tgfβ2 knock-out mice.* Cardiovascular research, 2002. **56**(2): p. 312-322.

85. Molin, D.G., et al., *TGFb2 does not affect neural crest cell migration but is a key player in vascular remodeling during embryogenesis.* Cardiovascular Development and Congenital Malformations, 2008: p. 148.

86. Balasubramanian, P., et al., *Human cardiomyocyte interaction with electrospun fibrinogen/gelatin nanofibers for myocardial regeneration.* Journal of Biomaterials Science, Polymer Edition, 2013. **24**(14): p. 1660-1675.

87. Gallicchio, M.A., *Culture of human smooth muscle cells*, in *Atherosclerosis.* 2001, Springer. p. 137-146.

88. Gotlieb, A.I. and P. Boden, *Porcine aortic organ culture: a model to study the cellular response to vascular injury.* In vitro, 1984. **20**(7): p. 535-542.

89. Williams, M.J., et al., *Differences in the microstructure and biomechanical properties of the recurrent laryngeal nerve as a function of age and location.* Journal of biomechanical engineering, 2014. **136**(8): p. 081008.

90. Haskett, D., et al., *Progressive alterations in microstructural organization and biomechanical response in the ApoE mouse model of aneurysm.* Biomatter, 2013. **3**(3).

91. Chen, X., et al., *Second harmonic generation microscopy for quantitative analysis of collagen fibrillar structure.* Nature protocols, 2012. **7**(4): p. 654-669.

92. Lee, S.H., et al., *Proliferation and differentiation of smooth muscle cell precursors occurs simultaneously during the development of the vessel wall.* Developmental dynamics, 1997. **209**(4): p. 342-352.

93. Long, X., et al., *Smooth Muscle Calponin An Unconventional CArG-Dependent Gene That Antagonizes Neointimal Formation.* Arteriosclerosis, thrombosis, and vascular biology, 2011. **31**(10): p. 2172-2180.

94. Hughes, S. and T. Chan-Ling, *Characterization of smooth muscle cell and pericyte differentiation in the rat retina in vivo.* Investigative ophthalmology & visual science, 2004. **45**(8): p. 2795-2806.

95. El-Mezgueldi, M., *Calponin.* The international journal of biochemistry & cell biology, 1996. **28**(11): p. 1185-1189.

96. Skalli, O., et al., *Alpha-smooth muscle actin, a differentiation marker of smooth muscle cells, is present in microfilamentous bundles of pericytes.* Journal of Histochemistry & Cytochemistry, 1989. **37**(3): p. 315-321.

97. Wu, S.-C., et al., *Cell adhesion and proliferation enhancement by gelatin nanofiber scaffolds.* Journal of Bioactive and Compatible Polymers, 2011. **26**(6): p. 565-577.

98. Rungsiyanont, S., et al., *Evaluation of biomimetic scaffold of gelatin–hydroxyapatite crosslink as a novel scaffold for tissue engineering: Biocompatibility evaluation with human PDL fibroblasts, human mesenchymal stromal cells, and primary bone cells.* Journal of biomaterials applications, 2012. **27**(1): p. 47-54.

99. Rosellini, E., et al., *Preparation and characterization of alginate/gelatin blend films for cardiac tissue engineering.* Journal of Biomedical Materials Research Part A, 2009. **91**(2): p. 447-453.

100. Gardiner, E.E. and S.E. D'Souza, *A mitogenic action for fibrinogen mediated through intercellular adhesion molecule-1.* Journal of Biological Chemistry, 1997. **272**(24): p. 15474-15480.

101. Moiseeva, E.P., *Adhesion receptors of vascular smooth muscle cells and their functions.* Cardiovascular research, 2001. **52**(3): p. 372-386.

102. Sturge, J., et al., *Fibrin monomer and fibrinopeptide B act additively to increase DNA synthesis in smooth muscle cells cultured from human saphenous vein.* Journal of vascular surgery, 2001. **33**(4): p. 847-853.

103. Ishida, T. and K. Tanaka, *Effects of fibrin and fibrinogen-degradation products on the growth of rabbit aortic smooth muscle cells in culture.* Atherosclerosis, 1982. **44**(2): p. 161-174.

104. Rnjak-Kovacina, J., et al., *Tailoring the porosity and pore size of electrospun synthetic human elastin scaffolds for dermal tissue engineering.* Biomaterials, 2011. **32**(28): p. 6729-6736.

105. Lee, J.B., et al., *Highly porous electrospun nanofibers enhanced by ultrasonication for improved cellular infiltration.* Tissue Engineering Part A, 2011. **17**(21-22): p. 2695-2702.

106. Horst, M., et al., *Increased porosity of electrospun hybrid scaffolds improved bladder tissue regeneration.* Journal of Biomedical Materials Research Part A, 2014. **102**(7): p. 2116-2124.

107. Owens, G.K., *Regulation of differentiation of vascular smooth muscle cells.* Physiological reviews, 1995. **75**(3): p. 487-517.

108. Owens, G.K., M.S. Kumar, and B.R. Wamhoff, *Molecular regulation of vascular smooth muscle cell differentiation in development and disease.* Physiological reviews, 2004. **84**(3): p. 767-801.

109. Spin, J.M., L. Maegdefessel, and P.S. Tsao, *Vascular smooth muscle cell phenotypic plasticity: focus on chromatin remodelling.* Cardiovascular research, 2012. **95**(2): p. 147-155.

110. Moses, M.A., M. Klagsbrun, and Y. Shing, *The role of growth factors in vascular cell development and differentiation.* International review of cytology, 1995. **161**: p. 1-48.

111. Stegemann, J.P. and R.M. Nerem, *Phenotype modulation in vascular tissue engineering using biochemical and mechanical stimulation.* Annals of biomedical engineering, 2003. **31**(4): p. 391-402.

112. Guo, X. and S.-Y. Chen, *Transforming growth factor-β and smooth muscle differentiation.* World journal of biological chemistry, 2012. **3**(3): p. 41.

113. Kubota, K., et al., *TGF-β stimulates collagen (I) in vascular smooth muscle cells via a short element in the proximal collagen promoter.* Journal of Surgical Research, 2003. **109**(1): p. 43-50.

114. Mann, B.K., R.H. Schmedlen, and J.L. West, *Tethered-TGF-β increases extracellular matrix production of vascular smooth muscle cells.* Biomaterials, 2001. **22**(5): p. 439-444.

115. Blanchette, F., et al., *TGFbeta1 regulates gene expression of its own converting enzyme furin.* Journal of Clinical Investigation, 1997. **99**(8): p. 1974.

116. Brisset, A.C., et al., *Intimal smooth muscle cells of porcine and human coronary artery express S100A4, a marker of the rhomboid phenotype in vitro.* Circulation research, 2007. **100**(7): p. 1055-1062.

117. Burnstock, G., *Purinergic signaling and vascular cell proliferation and death.* Arteriosclerosis, thrombosis, and vascular biology, 2002. **22**(3): p. 364-373.

118.	Corrêa-Giannella, M.L., et al., *Fibronectin glycation increases IGF-I induced proliferation of human aortic smooth muscle cells.* Diabetology & metabolic syndrome, 2012. **4**.

119.	Gollasch, M., et al., *K+ currents in human coronary artery vascular smooth muscle cells.* Circulation research, 1996. **78**(4): p. 676-688.

120.	Hao, H., G. Gabbiani, and M.-L. Bochaton-Piallat, *Arterial smooth muscle cell heterogeneity implications for atherosclerosis and restenosis development.* Arteriosclerosis, thrombosis, and vascular biology, 2003. **23**(9): p. 1510-1520.

121.	Patel, S., et al., *Characteristics of coronary smooth muscle cells and adventitial fibroblasts.* Circulation, 2000. **101**(5): p. 524-532.

122.	Swindle, M., et al., *Swine as models in biomedical research and toxicology testing.* Veterinary Pathology Online, 2012. **49**(2): p. 344-356.

123.	Douglas, W.R., *Of pigs and men and research.* Space life sciences, 1972. **3**(3): p. 226-234.

124.	Keyes, J.T., et al., *Design and demonstration of a microbiaxial optomechanical device for multiscale characterization of soft biological tissues with two-photon microscopy.* Microscopy and Microanalysis, 2011. **17**(02): p. 167-175.

125.	Keyes, J.T., et al., *Adaptation of a planar microbiaxial optomechanical device for the tubular biaxial microstructural and macroscopic characterization of small vascular tissues.* Journal of biomechanical engineering, 2011. **133**(7): p. 075001.

126.	Benrashid, E., et al., *Tissue engineered vascular grafts: Origins, development, and current strategies for clinical application.* Methods, 2016. **99**: p. 13-19.

127.	Tan, A., et al., *Tissue engineering vascular grafts a fortiori: looking back and going forward.* Expert opinion on biological therapy, 2015. **15**(2): p. 231-244.

128.	Rychter, M., A. Baranowska-Korczyc, and J. Lulek, *Progress and perspectives in bioactive agent delivery via electrospun vascular grafts.* RSC Advances, 2017. **7**(51): p. 32164-32184.

129.	Han, J. and P.I. Lelkes, *Drug-Eluting Vascular Grafts*, in *Focal Controlled Drug Delivery*. 2014, Springer. p. 405-427.

130.	DeLong, S.A., J.J. Moon, and J.L. West, *Covalently immobilized gradients of bFGF on hydrogel scaffolds for directed cell migration.* Biomaterials, 2005. **26**(16): p. 3227-3234.

131.	Tallawi, M., et al., *Strategies for the chemical and biological functionalization of scaffolds for cardiac tissue engineering: a review.* Journal of the Royal Society Interface, 2015. **12**(108): p. 20150254.

132.   Reed, S. and B. Wu, *Sustained growth factor delivery in tissue engineering applications.* Annals of biomedical engineering, 2014. **42**(7): p. 1528-1536.

133.   Ham, T.R., M. Farrag, and N.D. Leipzig, *Covalent growth factor tethering to direct neural stem cell differentiation and self-organization.* Acta biomaterialia, 2017. **53**: p. 140-151.

134.   Szulcek, R., et al., *The covalently immobilized antimicrobial peptide LL37 acts as a VEGF mimic and stimulates endothelial cell proliferation.* Biochemical and biophysical research communications, 2018. **496**(3): p. 887-890.

135.   Leong, N.L., et al., *In vitro and in vivo evaluation of heparin mediated growth factor release from tissue-engineered constructs for anterior cruciate ligament reconstruction.* Journal of Orthopaedic Research, 2015. **33**(2): p. 229-236.

136.   Liu, Y., et al., *Sustained dual release of placental growth factor-2 and bone morphogenic protein-2 from heparin-based nanocomplexes for direct osteogenesis.* International journal of nanomedicine, 2016. **11**: p. 1147.

137.   Liang, Y. and K.L. Kiick, *Heparin-functionalized polymeric biomaterials in tissue engineering and drug delivery applications.* Acta biomaterialia, 2014. **10**(4): p. 1588-1600.

138.   Munj, H.R., J.J. Lannutti, and D.L. Tomasko, *Understanding drug release from PCL/gelatin electrospun blends.* Journal of Biomaterials Applications, 2017. **31**(6): p. 933-949.

139.   Wolf, M.T., et al., *Naturally derived and synthetic scaffolds for skeletal muscle reconstruction.* Advanced drug delivery reviews, 2015. **84**: p. 208-221.

140.   Goyal, R., et al., *Development of hybrid scaffolds with natural extracellular matrix deposited within synthetic polymeric fibers.* Journal of Biomedical Materials Research Part A, 2017. **105**(8): p. 2162-2170.

141.   Norouzi, M., et al., *PLGA/gelatin hybrid nanofibrous scaffolds encapsulating EGF for skin regeneration.* Journal of Biomedical Materials Research Part A, 2015. **103**(7): p. 2225-2235.

142.   Stankus, J.J., et al., *Hybrid nanofibrous scaffolds from electrospinning of a synthetic biodegradable elastomer and urinary bladder matrix.* Journal of Biomaterials Science, Polymer Edition, 2008. **19**(5): p. 635-652.

143.   Fukunishi, T., et al., *Tissue-engineered small diameter arterial vascular grafts from cell-free nanofiber PCL/chitosan scaffolds in a sheep model.* PLoS One, 2016. **11**(7): p. e0158555.

144.   Heydarkhan-Hagvall, S., et al., *Three-dimensional electrospun ECM-based hybrid scaffolds for cardiovascular tissue engineering.* Biomaterials, 2008. **29**(19): p. 2907-2914.

145. Fu, W., et al., *Electrospun gelatin/PCL and collagen/PLCL scaffolds for vascular tissue engineering.* International journal of nanomedicine, 2014. **9**: p. 2335.

146. Gautam, S., A.K. Dinda, and N.C. Mishra, *Fabrication and characterization of PCL/gelatin composite nanofibrous scaffold for tissue engineering applications by electrospinning method.* Materials Science and Engineering: C, 2013. **33**(3): p. 1228-1235.

147. Nada, A.A., et al., *Eco-friendly gelatin-based electrospun fibers to control the release of chloramphenicol.* Fibers and Polymers, 2016. **17**(12): p. 1985-1994.

148. Sohier, J., et al., *Tailored release of TGF-β1 from porous scaffolds for cartilage tissue engineering.* International journal of pharmaceutics, 2007. **332**(1-2): p. 80-89.

149. Wang, Z., et al., *Evaluation of emulsion electrospun polycaprolactone/hyaluronan/epidermal growth factor nanofibrous scaffolds for wound healing.* Journal of biomaterials applications, 2016. **30**(6): p. 686-698.

150. Wang, K., et al., *Enhanced vascularization in hybrid PCL/gelatin fibrous scaffolds with sustained release of VEGF.* BioMed research international, 2015. **2015**.

151. Rose, J.B., et al., *Gelatin-based materials in ocular tissue engineering.* Materials, 2014. **7**(4): p. 3106-3135.

152. Butler, M.F., Y.F. Ng, and P.D. Pudney, *Mechanism and kinetics of the crosslinking reaction between biopolymers containing primary amine groups and genipin.* Journal of Polymer Science Part A: Polymer Chemistry, 2003. **41**(24): p. 3941-3953.

153. Lin, H.Y., et al., *The Soluble Exoplasmic Domain of the Type II Transforming Growth Factor (TGF)-β Receptor A HETEROGENEOUSLY GLYCOSYLATED PROTEIN WITH HIGH AFFINITY AND SELECTIVITY FOR TGF-β LIGANDS.* Journal of Biological Chemistry, 1995. **270**(6): p. 2747-2754.

154. Tamimi, E., et al., *Biomechanical comparison of glutaraldehyde-crosslinked gelatin fibrinogen electrospun scaffolds to porcine coronary arteries.* Journal of biomechanical engineering, 2016. **138**(1): p. 011001.

155. Ravi, S. and E.L. Chaikof, *Biomaterials for vascular tissue engineering.* Regenerative medicine, 2010. **5**(1): p. 107-120.

156. Melchiorri, A., et al., *Contrasting biofunctionalization strategies for the enhanced endothelialization of biodegradable vascular grafts.* Biomacromolecules, 2015. **16**(2): p. 437-446.

157. Nagiah, N., et al., *Highly compliant vascular grafts with gelatin-sheathed coaxially structured nanofibers.* Langmuir, 2015. **31**(47): p. 12993-13002.

158.   Pan, Y., et al., *Small-diameter hybrid vascular grafts composed of polycaprolactone and polydioxanone fibers.* Scientific Reports, 2017. **7**(1): p. 3615.

159.   Tamimi, E., et al., *Biomechanical Comparison of Glutaraldehyde-Crosslinked Gelatin Fibrinogen Electrospun Scaffolds to Porcine Coronary Arteries.* Journal of biomechanical engineering, 2016. **138**(1): p. 011001.

160.   Weber, B., S.M. Zeisberger, and S.P. Hoerstrup, *Umbilical Cord Blood-Derived Endothelial Progenitor Cells for Cardiovascular Tissue Engineering*, in *Perinatal Stem Cells*. 2014, Springer. p. 325-336.

161.   Stroncek, J.D., et al., *Comparison of endothelial cell phenotypic markers of late-outgrowth endothelial progenitor cells isolated from patients with coronary artery disease and healthy volunteers.* Tissue Engineering Part A, 2009. **15**(11): p. 3473-3486.

162.   Cai, H., et al., *MnSOD marks cord blood late outgrowth endothelial cells and accompanies robust resistance to oxidative stress.* Biochemical and biophysical research communications, 2006. **350**(2): p. 364-369.

163.   Bompais, H., et al., *Human endothelial cells derived from circulating progenitors display specific functional properties compared with mature vessel wall endothelial cells.* Blood, 2004. **103**(7): p. 2577-2584.

164.   Schmidt, D., et al., *Umbilical cord blood derived endothelial progenitor cells for tissue engineering of vascular grafts.* The Annals of thoracic surgery, 2004. **78**(6): p. 2094-2098.

165.   Brown, M.A., et al., *Characterization of umbilical cord blood–derived late outgrowth endothelial progenitor cells exposed to laminar shear stress.* Tissue Engineering Part A, 2009. **15**(11): p. 3575-3587.

166.   Brown, M.A., et al., *Human Umbilical Cord Blood–Derived Endothelial Cells Reendothelialize Vein Grafts and Prevent Thrombosis.* Arteriosclerosis, thrombosis, and vascular biology, 2010. **30**(11): p. 2150-2155.

167.   Jung, Y., et al., *Scaffold-free, human mesenchymal stem cell-based tissue engineered blood vessels.* Scientific reports, 2015. **5**: p. 15116.

168.   Javed, M.J., et al., *Endothelial colony forming cells and mesenchymal stem cells are enriched at different gestational ages in human umbilical cord blood.* Pediatric Research, 2008. **64**(1): p. 68-73.

169.   Brown, M.E., et al., *Derivation of induced pluripotent stem cells from human peripheral blood T lymphocytes.* PloS one, 2010. **5**(6): p. e11373.

170.   Ashton, J.H., et al., *Polymeric endoaortic paving: Mechanical, thermoforming, and degradation properties of polycaprolactone/polyurethane blends for cardiovascular applications.* Acta biomaterialia, 2011. **7**(1): p. 287-294.

171.   Sasidharan, A., et al., *Simple device to determine the pressure applied by pressure clips for the treatment of earlobe keloids.* Indian Journal of Plastic Surgery, 2015. **48**(3): p. 293.

172.   Jesty, J. and D. Bluestein, *Acetylated prothrombin as a substrate in the measurement of the procoagulant activity of platelets: elimination of the feedback activation of platelets by thrombin.* Analytical biochemistry, 1999. **272**(1): p. 64-70.

173.   Merkle, V.M., et al., *Hemocompatibility of Poly (vinyl alcohol)–Gelatin Core–Shell Electrospun Nanofibers: A Scaffold for Modulating Platelet Deposition and Activation.* ACS applied materials & interfaces, 2015. **7**(15): p. 8302-8312.

174.   Merkle, V.M., et al., *Core–shell PVA/gelatin electrospun nanofibers promote human umbilical vein endothelial cell and smooth muscle cell proliferation and migration.* Acta biomaterialia, 2015. **27**: p. 77-87.

175.   Kuwahara, M., et al., *Platelet shape changes and adhesion under high shear flow.* Arteriosclerosis, thrombosis, and vascular biology, 2002. **22**(2): p. 329-334.

176.   O'Carroll, S.J., et al., *Pro-inflammatory TNFα and IL-1β differentially regulate the inflammatory phenotype of brain microvascular endothelial cells.* Journal of neuroinflammation, 2015. **12**(1): p. 131.

177.   Burrows, M.C., et al., *Hybrid scaffolds built from PET and collagen as a model for vascular graft architecture.* Macromolecular bioscience, 2012. **12**(12): p. 1660-1670.

178.   Ma, Z., et al., *Surface engineering of electrospun polyethylene terephthalate (PET) nanofibers towards development of a new material for blood vessel engineering.* Biomaterials, 2005. **26**(15): p. 2527-2536.

179.   Cassady, A.I., N.M. Hidzir, and L. Grøndahl, *Enhancing expanded poly (tetrafluoroethylene)(ePTFE) for biomaterials applications.* Journal of Applied Polymer Science, 2014. **131**(15).

180.   Takagi, H., et al., *A contemporary meta-analysis of Dacron versus polytetrafluoroethylene grafts for femoropopliteal bypass grafting.* Journal of vascular surgery, 2010. **52**(1): p. 232-236.

181.   Jeschke, M.G., et al., *Polyurethane vascular prostheses decreases neointimal formation compared with expanded polytetrafluoroethylene.* Journal of vascular surgery, 1999. **29**(1): p. 168-176.

182.   MüLLER-HüLSBECK, S., et al., *Experience on endothelial cell adhesion on vascular stents and stent-grafts: first in vitro results.* Investigative radiology, 2002. **37**(6): p. 314-320.

183.   Ren, X., et al., *Surface modification and endothelialization of biomaterials as potential scaffolds for vascular tissue engineering applications.* Chemical Society Reviews, 2015. **44**(15): p. 5680-5742.

184.   Li, Q., et al., *Functionalization of the surface of electrospun poly (epsilon-caprolactone) mats using zwitterionic poly (carboxybetaine methacrylate) and cell-specific peptide for endothelial progenitor cells capture.* Materials Science and Engineering: C, 2013. **33**(3): p. 1646-1653.

185.   Xiong, G.M., et al., *Endothelial cell thrombogenicity is reduced by ATRP-mediated grafting of gelatin onto PCL surfaces.* Journal of Materials Chemistry B, 2014. **2**(5): p. 485-493.

186.   Choi, W.S., et al., *Enhanced Patency and Endothelialization of Small-Caliber Vascular Grafts Fabricated by Coimmobilization of Heparin and Cell-Adhesive Peptides.* ACS applied materials & interfaces, 2016. **8**(7): p. 4336-4346.

187.   Huang, Y., et al., *In vitro characterization of chitosan–gelatin scaffolds for tissue engineering.* Biomaterials, 2005. **26**(36): p. 7616-7627.

188.   Wu, S.-C., et al., *Cell adhesion and proliferation enhancement by gelatin nanofiber scaffolds.* Journal of Bioactive and Compatible Polymers, 2011: p. 0883911511423563.

189.   D'Souza, S.E., M.H. Ginsberg, and E.F. Plow, *Arginyl-glycyl-aspartic acid (RGD): a cell adhesion motif.* Trends in biochemical sciences, 1991. **16**: p. 246-250.

190.   Ruoslahti, E. and M.D. Pierschbacher, *Arg-Gly-Asp: a versatile cell recognition signal.* Cell, 1986. **44**(4): p. 517-518.

191.   Widhe, M. and N.D. Shalaly, *A fibronectin mimetic motif improves integrin mediated cell biding to recombinant spider silk matrices.* Biomaterials, 2016. **74**: p. 256-266.

192.   Pierce, B.F., et al., *Viability of Human Mesenchymal Stem Cells Seeded on Crosslinked Entropy-Elastic Gelatin-Based Hydrogels.* Macromolecular bioscience, 2012. **12**(3): p. 312-321.

193.   Underwood, P.A., et al., *Evidence for the location of a binding sequence for the α2β1 integrin of endothelial cells, in the β1 subunit of laminin.* Biochemical Journal, 1995. **309**(3): p. 765-771.

194.   Saotome, T., et al., *Introduction of VEGF or RGD sequences improves revascularization properties of Bombyx mori silk fibroin produced by transgenic silkworm.* Journal of Materials Chemistry B, 2015. **3**(35): p. 7109-7116.

195.   Ingber, D.E., *Fibronectin controls capillary endothelial cell growth by modulating cell shape.* Proceedings of the National Academy of Sciences, 1990. **87**(9): p. 3579-3583.

196.   Bahou, W.F., C.L. Potter, and H. Mirza, *The VLA-2 (alpha 2 beta 1) I domain functions as a ligand-specific recognition sequence for endothelial cell attachment and spreading: molecular and functional characterization.* Blood, 1994. **84**(11): p. 3734-3741.

197.   Chen, M., et al., *Role of fiber diameter in adhesion and proliferation of NIH 3T3 fibroblast on electrospun polycaprolactone scaffolds.* Tissue Engineering, 2007. **13**(3): p. 579-587.

198.   Whited, B.M. and M.N. Rylander, *The influence of electrospun scaffold topography on endothelial cell morphology, alignment, and adhesion in response to fluid flow.* Biotechnology and bioengineering, 2014. **111**(1): p. 184-195.

199.   Adams, W.J., et al., *Functional vascular endothelium derived from human induced pluripotent stem cells.* Stem Cell Reports, 2013. **1**(2): p. 105-113.

200.   Van Rijssel, J., et al., *The Rho-GEF Trio regulates a novel pro-inflammatory pathway through the transcription factor Ets2.* Biology open, 2013. **2**(6): p. 569-579.

201.   Takahashi, M., et al., *Monocyte-endothelial cell interaction induces expression of adhesion molecules on human umbilical cord endothelial cells.* Cardiovascular research, 1996. **32**(2): p. 422-429.

202.   Blake, G.J. and P.M. Ridker, *Novel clinical markers of vascular wall inflammation.* Circulation research, 2001. **89**(9): p. 763-771.

203.   Qin, L., et al., *SOCS1 prevents graft arteriosclerosis by preserving endothelial cell function.* Journal of the American College of Cardiology, 2014. **63**(1): p. 21-29.

204.   Zou, Y., et al., *Reduced neointima hyperplasia of vein bypass grafts in intercellular adhesion molecule-1–deficient mice.* Circulation research, 2000. **86**(4): p. 434-440.

205.   Matsushita, H., et al., *eNOS Activity Is Reduced in Senescent Human Endothelial Cells Preservation by hTERT Immortalization.* Circulation research, 2001. **89**(9): p. 793-798.

206.   Tran, J., et al., *Activation of Endothelial Nitric Oxide (eNOS) Occurs through Different Membrane Domains in Endothelial Cells.* PloS one, 2016. **11**(3): p. e0151556.

207.   Ruan, T., et al., *Shear-Induced Extracellular Regulated Kinase Signaling to eNOS is Increased When Autophagy is Compromised in Endothelial Cells.* The FASEB Journal, 2015. **29**(1 Supplement): p. 956.4.

208. Li, Y., et al., *Effects of pulsatile shear stress on signaling mechanisms controlling nitric oxide production, endothelial nitric oxide synthase phosphorylation, and expression in ovine fetoplacental artery endothelial cells.* Endothelium, 2005. **12**(1-2): p. 21-39.

209. Yang, B. and V. Rizzo, *Shear stress activates eNOS at the endothelial apical surface through β1 containing integrins and caveolae.* Cellular and molecular bioengineering, 2013. **6**(3): p. 346-354.

210. Do Kang, S., et al., *Isolation of functional human endothelial cells from small volumes of umbilical cord blood.* Annals of biomedical engineering, 2013. **41**(10): p. 2181-2192.

211. Broos, K., et al., *Platelets at work in primary hemostasis.* Blood reviews, 2011. **25**(4): p. 155-167.

212. Szabo, C., *Alterations in nitric oxide production in various forms of circulatory shock.* New horizons (Baltimore, Md.), 1995. **3**(1): p. 2-32.

213. van Hinsbergh, V.W. *Endothelium—role in regulation of coagulation and inflammation.* in *Seminars in immunopathology*. 2012. Springer.

214. Cronenwett, J.L. and K.W. Johnston, *Rutherford's vascular surgery*. 2014: Elsevier Health Sciences.

215. Abou-Saleh, H., et al., *Endothelial progenitor cells bind and inhibit platelet function and thrombus formation.* Circulation, 2009. **120**(22): p. 2230-2239.

216. Shirota, T., et al., *Human endothelial progenitor cell-seeded hybrid graft: proliferative and antithrombogenic potentials in vitro and fabrication processing.* Tissue engineering, 2003. **9**(1): p. 127-136.

217. He, W., et al., *Fabrication and endothelialization of collagen-blended biodegradable polymer nanofibers: potential vascular graft for blood vessel tissue engineering.* Tissue engineering, 2005. **11**(9-10): p. 1574-1588.

218. Lee, B., et al., *Characterization and preparation of bio-tubular scaffolds for fabricating artificial vascular grafts by combining electrospinning and a co-culture system.* Macromolecular Research, 2016. **24**(2): p. 131-142.

219. Zhou, W., et al., *Electrospun scaffolds of silk fibroin and poly (lactide-co-glycolide) for endothelial cell growth.* Journal of Materials Science: Materials in Medicine, 2015. **26**(1): p. 1-14.

220. Li, Y.-S.J., J.H. Haga, and S. Chien, *Molecular basis of the effects of shear stress on vascular endothelial cells.* Journal of biomechanics, 2005. **38**(10): p. 1949-1971.

221. Sessa, W.C., *eNOS at a glance.* Journal of cell science, 2004. **117**(12): p. 2427-2429.

222.   Kolluru, G.K., et al., *Shear stress promotes nitric oxide production in endothelial cells by sub-cellular delocalization of eNOS: A basis for shear stress mediated angiogenesis.* Nitric Oxide, 2010. **22**(4): p. 304-315.

223.   Dimmeler, S., et al., *Activation of nitric oxide synthase in endothelial cells by Akt-dependent phosphorylation.* Nature, 1999. **399**(6736): p. 601-605.

224.   Uematsu, M., et al., *Regulation of endothelial cell nitric oxide synthase mRNA expression by shear stress.* American Journal of Physiology-Cell Physiology, 1995. **269**(6): p. C1371-C1378.

225.   Buga, G.M., et al., *Shear stress-induced release of nitric oxide from endothelial cells grown on beads.* Hypertension, 1991. **17**(2): p. 187-193.

226.   Hsieh, H.-J., et al., *Shear-induced endothelial mechanotransduction: the interplay between reactive oxygen species (ROS) and nitric oxide (NO) and the pathophysiological implications.* Journal of biomedical science, 2014. **21**(1): p. 1-15.

227.   Langer, R. and J. Vacanti, *Tissue Engineering.* Science, 1993. **260**: p. 920-92.

228.   Weinberg, C.B. and E. Bell, *A blood vessel model constructed from collagen and cultured vascular cells.* Science, 1986. **231**(4736): p. 397-400.

229.   L'Heureux, N., et al., *In vitro construction of a human blood vessel from cultured vascular cells: a morphologic study.* Journal of vascular surgery, 1993. **17**(3): p. 499-509.

230.   Muylaert, D.E., et al., *Environmental influences on endothelial to mesenchymal transition in developing implanted cardiovascular tissue-engineered grafts.* Tissue Engineering Part B: Reviews, 2015. **22**(1): p. 58-67.

231.   Goumans, M.-J., F. Lebrin, and G. Valdimarsdottir, *Controlling the angiogenic switch: a balance between two distinct TGF-b receptor signaling pathways.* Trends in cardiovascular medicine, 2003. **13**(7): p. 301-307.

232.   Pinto, M.T., et al., *Endothelial mesenchymal transition: comparative analysis of different induction methods.* Biological procedures online, 2016. **18**(1): p. 10.

233.   Stavropoulos-Giokas, C., D. Charron, and C. Navarrete, *Cord Blood Stem Cells Medicine*. 2014: Elsevier.

234.   Zhang, L., R. Yang, and Z.C. Han, *Transplantation of umbilical cord blood-derived endothelial progenitor cells: a promising method of therapeutic revascularisation.* European journal of haematology, 2006. **76**(1): p. 1-8.

235. Chow, T., S. Mueller, and I.M. Rogers, *Advances in Umbilical Cord Blood Therapy: Hematopoietic Stem Cell Transplantation and Beyond*, in *Advances in Stem Cell Therapy*. 2017, Springer. p. 139-168.